COMMITTEE III.1
ULTIMATE STRENGTH

COMMITTEE MANDATE

Concern for the ductile behaviour of ships and offshore structures and their structural components under ultimate conditions. Attention shall be given to the influence of fabrication imperfections and in-service damage and degradation on reserve strength. Uncertainties in strength models for design shall be highlighted.

COMMITTEE MEMBERS

Chairman: J. K. Paik
                  K. Branner
                  Y. S. Choo
                  J. Czujko
                  M. Fujikubo
                  J. M. Gordo
                  G. Parmentier
                  R. Iaccarino
                  S. O'Neil
                  I. Pasqualino
                  D. Wang
                  X. Wang
                  S. Zhang

KEY WORDS

Ultimate Strength; Ultimate Limit States; Ultimate Limit State Design; Buckling Collapse; Load-Carrying Capacity; Fabrication-Induced Initial Imperfections; In-Service Damage and Degradation; Reserve Strength; Uncertainties; Strength Model.

CONTENTS

1. INTRODUCTION

It is well recognised that limit state based approaches are much better methodologies for structural design and strength assessment than traditional working stress based approaches, the latter typically being formulated as a fraction of material such as yield strength. This is the situation because it is not possible to determine the true margin of structural safety as long as limit states remain unknown.

A limit state is defined as a condition under which a particular structural component or an entire structural system fails to perform its designated function. Four types of limit states are relevant: serviceability limit states (SLS), ultimate limit states (ULS), fatigue limit states (FLS) and accidental limit states (ALS) (Paik & Thayamballi 2003, ISO 18072-1 2007). The present Committee is concerned with ULS.

The ULS for ships and offshore structures include the failure of critical components of the structure caused by exceeding the ultimate strength (in some cases reduced by repetitive actions) by any combination of buckling, yielding, rupture or fracture, or the transformation of the structure into a mechanism associated with buckling collapse or excessive deformation. ULS typically occur under extreme actions or action effects.

To prevent ULS, the following structural design criterion is usually applied using a partial safety factor approach:

$$C_d \geq D_d ,$$

(1.a)

where $C_d = C_k / \gamma_C$ = the design value of capacity (strength), $D_d = \gamma_D D_k$ = the design value of demand (actions), C_k = the characteristic value of capacity (strength), D_k = the characteristic value of demand (actions), and γ_C, γ_D = partial safety factors of capacity or demand, respectively, in association with the uncertainties of capacity or demand, which must be greater than unity.

Equation (1.a) may be rewritten in the following form in terms of a conventional safety check.

$$\eta = \frac{C_d}{D_d} > 1 ,$$

(1.b)

where η is the measure of structural adequacy which should be greater than unity to be safe.

The characteristic value of demand in Equation (1) is determined as a form of actions or action effects under design conditions that mirror the most unfavourable situation during the design life of the target structure. The characteristic value of capacity in Equation (1) is determined based on buckling and plastic collapse or ultimate strength. It is necessary to account for various types of uncertainties arising from natural variability, the inaccuracy of procedures used for the assessment and control of actions or action effects, and variations in building procedures, which are usually formulated by either the partial safety factor format or the probabilistic format.

In this regard, it is clear that the primary tasks that need to be accomplished by the structural design criterion of Equation (1) are how to determine C_k, D_k, γ_C and γ_D. The present Committee is concerned with the determination of C_k and γ_C in conjunction with the ultimate limit state design.

Various methods are available in the literature to compute the ultimate strength of structural components or entire structural systems. Some methods are simplified but others are more sophisticated. However, all of these methods basically involve both geometric and material nonlinearities, with the former being associated with buckling and large deformation and the latter being due to plasticity. The factors that affect ultimate strength behaviour are as follows.

- Geometrical factors associated with buckling, large deflection, crushing or folding
- Material factors associated with yielding/plasticity, ductile/brittle fracture, rupture or cracking damage
- Fabrication related initial imperfections such as initial distortion, residual stress and softening
- Temperature factors such as low temperature associated with operation in cold waters or low temperature cargo, and high temperature due to fire and explosions
- Dynamic factors (strain rate sensitivity, inertia effect) associated with freak waves and impact pressure actions arising from sloshing, slamming or green water, overpressure actions arising from explosion, and impacts due to collisions, grounding or dropped objects
- Age-related deterioration such as corrosion and fatigue cracking
- Human factors relating to unusual operations in terms of ship's speed (compared to maximum permitted speed or acceleration), ship's heading, loading conditions, etc.

Any structural system consisting of various components may reach its ultimate limit state by a progressive failure of local components under extreme conditions. This means that some structural components must have already reached their ultimate strengths and entered into post-ultimate strength regimes before the system structure reached its ultimate limit state. In that case, it is necessary to characterize the post-ultimate strength behaviour of such components as well as the ultimate strength itself.

This report presents recent advances and possible future trends in ultimate strength computation methods for ship and offshore structural components and their system structures. Papers published since the ISSC 2006 Congress are mainly discussed here, but older publications are also included if they are considered to present fundamental and important findings in line with the mandate of the present Committee.

This report comprises 9 Chapters. Chapter 1 has presented the aims and scope of the Committee. Chapter 2 presents the fundamentals of the ultimate strength behaviour of structural components and system structures. Chapter 3 outlines the recent trends of regulations and international standards. Chapter 4 presents the mechanical properties of materials used to build ships and offshore structures, which are necessary to compute the ultimate strength. Chapters 5 and 6 survey recent research and developments in the ultimate strength computations of structural components and system structures, respectively. Chapter 7 presents the sources of uncertainty associated with ultimate strength models. Chapter 8 discusses the results of benchmark studies on the ultimate strength computations of stiffened steel-plate structures using nonlinear finite element analysis (FEA) methods in which the effects of various parameters of influence are investigated. Finally, Chapter 9 presents the Committee's concluding remarks and recommendations for future study.

2.   FUNDAMENTALS

2.1   *Plates*

Ship and offshore structures consist of continuous panels stiffened by stiffeners and support members. The plate panels between stiffeners and frames are the most fundamental structural components and are subjected to lateral actions due to direct action of water or cargo pressure, as well as in-plane actions caused by structural responses at the system level.

When a plate panel is subjected to compression, buckling takes place at a certain critical value of applied action and lateral deflection increases rapidly. This reduces the in-plane stiffness of the plate and produces bending stress. With the spread of yielding due to combined bending and in-plane stresses, rigidity against applied action reduces to zero, and the maximum load-carrying capacity, i.e., ultimate strength, is attained. Beyond that ultimate strength, the load-carrying capacity decreases with further increases in the lateral deflection.

The initial shape imperfection and welding residual stresses have a significant influence on the buckling collapse behaviour of the plate. The initial deflection of a rectangular plate panel produced by the fillet welding of stiffeners generally takes a thin-horse mode, and its component with the shape of the elastic buckling mode has a dominant effect on ultimate strength under thrust (Ueda & Yao 1985). Welding residual stress generally reduces the buckling and ultimate strength of plates because

the compressive residual stress is produced in the central parts of the plates.

Plate panels in ship and offshore structures are not isolated plates but a part of continuous stiffened panel. The effect of the continuity of plating thus has to be carefully considered for the evaluation of buckling and ultimate strengths. For instance, when a continuous stiffened panel is subjected to uniform lateral pressure, the plate edges are in a clamped condition, whereas when subjected to thrust the plate buckles in a simply-supported edge mode. An extent of modelling and boundary conditions that can cope with such buckling collapse behaviours must be employed.

The reduction of load-carrying capacity and resultant load shedding of a plate beyond its ultimate strength highly influence the ultimate strength of the stiffened panel to which it belongs. The post-ultimate strength behaviour of the plate, e.g., the load-shortening relationship, is influenced by many factors, such as plate slenderness, material strain-hardening and a localisation of plastic deformation due to non-uniform initial imperfections.

2.2   *Stiffened Panels*

A stiffened panel is an assembly of plating and stiffeners. It is normally designed so that the buckling of a local plate panel between stiffeners initially takes place and is then followed by overall collapse due to excessive yielding and/or stiffener failure. The primary failure modes of a stiffened panel can be categorised into the following six types (Paik & Thayamballi 2003).

- Mode I: Overall collapse after overall buckling
- Mode II: Collapse of the plating between stiffeners without their failure
- Mode III: Beam-column type collapse of a stiffener with attached plating
- Mode IV: Local buckling of stiffener web (after buckling collapse of attached plating)
- Mode V: Flexural-torsional buckling (tripping) of a stiffener
- Mode VI: Gross yielding

To estimate the ultimate strength of a stiffened panel by simplified methods, it is often necessary to accurately evaluate the post-buckling effective width of a local plate panel. The interaction between the plating and stiffener in the buckling behaviour must also be carefully considered. This interaction includes the effect of the stiffener's torsional stiffness on the buckling strength of local plate panels and that of plate bending stiffness on the lateral-torsional buckling strength of the stiffeners. The initial imperfections of plates and stiffeners have a significant influence on the ultimate strength of a stiffened panel. For stiffeners, both vertical (column type) and sideways initial distortions need to be taken into account.

Stiffened panels in ships and offshore structures are continuous structures supported by transverse frames and longitudinal girders. When a stiffener in one bay deflects

upwards, that in the adjacent bay deflects downwards to satisfy the continuity of stiffener deformation, as long as in-plane compressive actions are predominant. This effect must be considered in the buckling collapse analysis of stiffened panels by using a modelling extent that covers multiple bays with corresponding adequate boundary conditions.

The reduction of load-carrying capacity beyond the ultimate strength of a stiffened panel is generally very rapid because of the development of overall buckling deformation, which is normally accompanied by the localisation of plastic deformation either in the plate or in the stiffener. It is thus quite important to the assessment of the progressive collapse behaviour of structural systems, such as hull girder collapse, that not only the ultimate strength but also the post-ultimate strength behaviour is assessed for stiffened panels.

2.3   *Composite and Sandwich Panels*

Composite and sandwich panels have some of the same failure mechanisms as metal panels. However, as composite and sandwich panels are usually layered structures, the interface between the layers poses a special challenge when determining the ultimate strength of these panels. In the last three decades, failure caused by delamination has been of major research interest, and that type of failure will mainly be considered in the literature survey of this report.

Delamination can be defined as areas with poor or no bonding between adjacent layers. These areas are typical in layered composite structures and can be considered as interlaminar cracks that reduce the strength of the structure. Delamination normally originates from either the manufacturing process or impact damage during production, transport or service. In the manufacturing process, instabilities and imperfections of various types may result in delamination. The thermal and chemical shrinkage of composite components may also lead to delamination (Bolotin 1996). Impact damage may lead to multiple delamination, which can result in a significant reduction in strength. In addition, stress concentrations around structural discontinuities such as holes, notches, ply-drops and connections may cause the initiation and growth of delamination.

Delamination is usually the most critical type of damage that a composite and sandwich structure experiences under compressive loading (Abrate 1991, Pavier & Clarke 1995).

When a panel with delamination is subjected to compressive loading, the plies on one side of the delamination may buckle. This buckling will then introduce bending in the plies on the other side of the delamination. Hence, these remaining plies will be subjected to both bending and compressive loading, resulting in higher stresses than observed without the delamination and therefore reduced failure load (Peck & Springer 1991, Pavier & Clarke 1995). This type of buckling is known as the local buckling mode and typically occurs when the delamination is large and close to one of the surfaces. In general, however, compression-loaded panels are subjected to two buckling

modes. The other mode is known as the global buckling mode, wherein both sub-laminates buckle toward the same side of the panel. This type of buckling typically occurs when the delamination is small and deep in the laminate, as shown in Figure 1.

Local mode
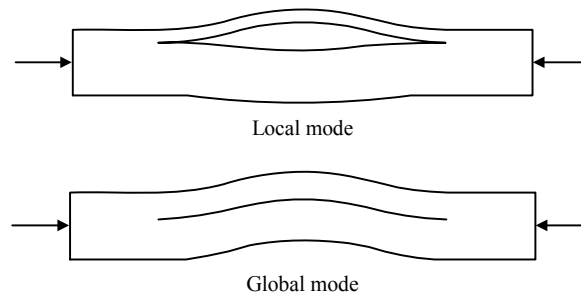
Global mode

Figure 1: Local and global modes of delamination-induced buckling, from Short *et al.* (2001)

2.4   *Tubular Joints*

Figure 2 shows the geometry of a simple tubular joint. Each joint should be considered as comprising a number of independent chord/brace intersections. Each chord/brace intersection is classified as T/Y, K or X, according to the configuration and load pattern for each load case. The following guidelines are to be used to classify tubular joints.

- For two or three brace members on one side of a chord, the classification is dependent on the equilibrium of the axial load components in the brace members. If the resultant shear on the chord member is balanced or algebraically around zero, the joint must be categorised as a K joint. If the shear balance check is not met, then the joint must be categorised (downgraded) as a T&Y joint, as shown in Figure 3. However, for braces that carry part of their load as K joints and part as Y or X joints, interpolation should be used, based on the proportion of each joint.
- For multi-brace joints with braces on either side of the chord, as shown in Figure 3, care must be taken in assigning the appropriate category. For example, a K classification would be valid if the net shear across the chord is balanced or algebraically zero. In contrast, if the loads in all of the braces are tensile, even an X classification may be too optimistic due to the increased ovalisation effect.
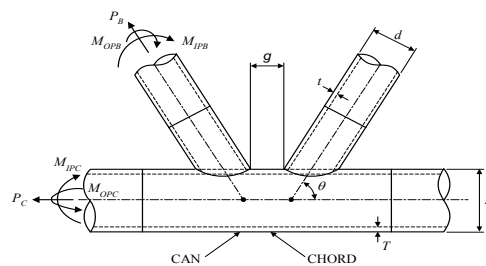
Figure 2: Geometry of tubular joints

$$0.9 \le P_1 \sin\theta/P_2 \le 1.1 \qquad 0.9 \le P_1 \sin\theta/P_2 \le 1.1 \qquad 0.9 \le P_1 \sin\theta/2P_2 \le 1.1$$

$$0.9 \le P_1 \sin\theta_1/P_3 \sin\theta_3 \le 1.1 \qquad 0.9 \le (P_1 \sin\theta_1 + P_3 \sin\theta_3)/P_2 \le 1.1$$

$$0.9 \le P_1/P_2 \le 1.1 \qquad 0.9 \le P_1 \sin\theta/P_2 \le 1.1$$
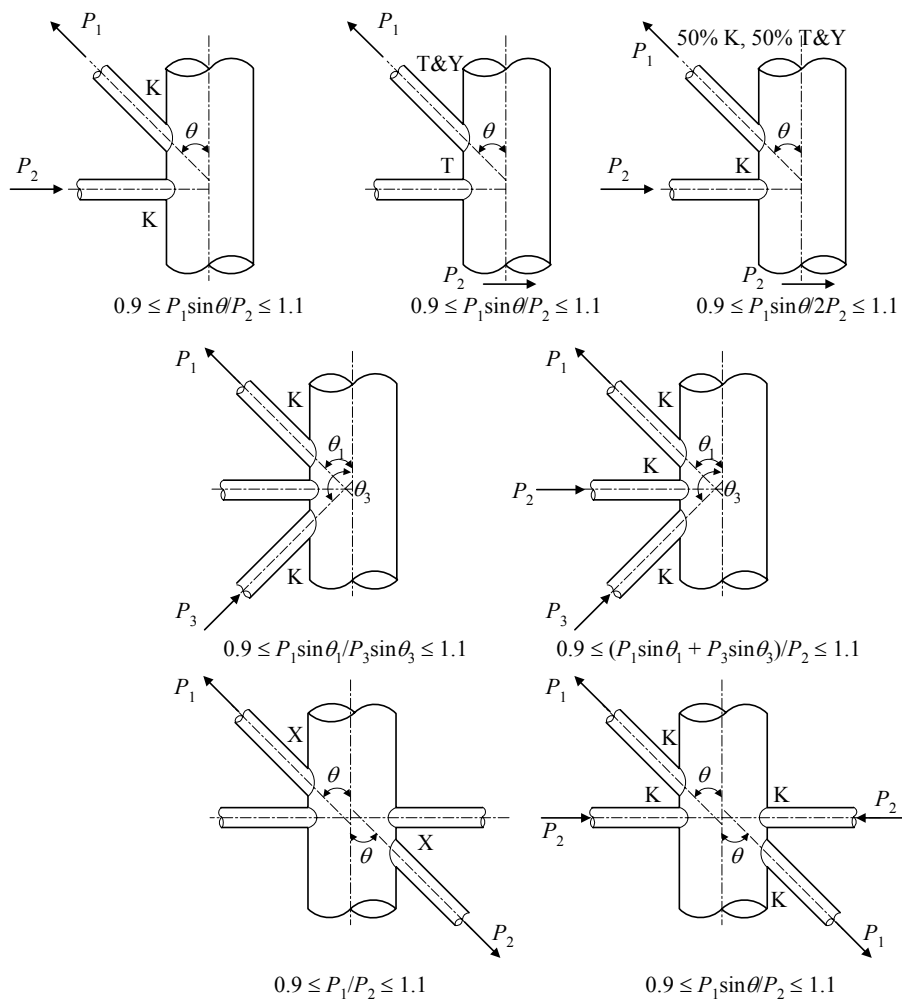
Figure 3: Examples of tubular joint categorisation

2.5   *Other Joints*

2.5.1   *Multi-planar Joints*

The interaction between out-of-plane braces can be ignored, except for overlapping braces. It is recognised that for some load cases, particularly where braces that are lying in two perpendicular planes are loaded in the opposite sense (e.g., tension and compression), as shown Figure 4, joint strength can be significantly reduced. This reduction is primarily due to the additional ovalisation occurring in the chord member. The design should account for this effect and to the application of a reduced allowable utilisation factor should be considered, especially for critical, highly stressed, non-

redundant joints. The design of multi-planar joints loaded in opposite directions should be based on suitable experimental data or nonlinear FEA. Indeed, nonlinear FEA is particularly well-suited to investigating the effects of individual parameters such as load ratio, load sequence and the interaction of out-of-plane braces.

2.5.2   Overlapping Joints

Joints with braces that overlap in plane must be checked using the formula for non-overlapping braces. However, an additional check must be performed for the region of the overlap by considering the through brace as the chord member and the overlapping brace as the brace member.

2.5.3   Grouted Joints

As shown in Figure 5, grouted joints can be classified into two types: i) those with a fully grouted chord member and ii) those with an inner steel sleeve with grout filling the annulus between the two concentric tubular members. Under axial compression, significant increases in joint strength have been recorded through test programs. Under axial tension, only modest strength enhancement has been noted, which results primarily from the reduction in chord ovalisation that occurs for the grouted specimen.
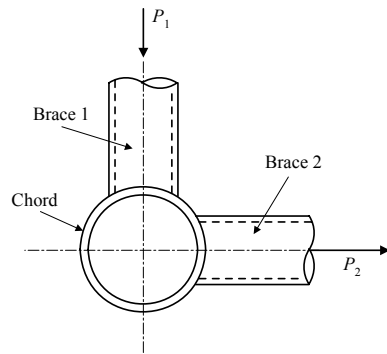
Figure 4: Multi-planar joints   Figure 5: Grouted joints
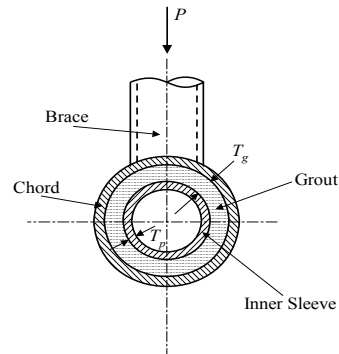
2.5.4   Ring-stiffened Joints

As in the case of grouted joints, rings substantially enhance the joint stiffness. A ring-stiffened joint should be designed based on appropriate experimental or in-service evidence. In the absence of such evidence, an appropriate analytical check must be pursued. As recommended by API RP 2A-WSD (1993), this check should be performed by cutting sections that isolate groups of members, individual members and separate elements of the joint (e.g., gussets, diaphragms, stiffeners, welds in shear and surfaces that are subjected to punching shear), and verifying that realistic, assumed stress distributions satisfy equilibrium without exceeding the allowable stress of the material (e.g., the strength of all elements is sufficient to resist the applied loading).

2.5.5   Cast Joints

Where the use of cast joints is considered, assistance from qualified specialists should be sought. This is particularly relevant for optimised cast joints where unusually demanding design criteria are proposed. Nonlinear FEA should also to be performed, giving particular consideration to the geometric and material characteristics of cast joints, including the effects of casting geometry, stress-strain relationships and casting defects. In addition, it should be recognised that the performance of cast joints beyond first yield may not be similar to that achieved in welded joints. The post-yield behaviour of cast joints should be investigated to ensure that the reserve strength and ductility against total collapse are comparable to those of welded joints.

2.6   System Structures – Ship-shaped Structures

The ultimate strength behaviour of ship-shaped structures as systems has been discussed to a large extent in past ISSC reports. Although the hull structural arrangement of and associated ultimate strength computation technologies for ship-shaped offshore structures, such as the floating production, storage offloading (FPSO) units used for offshore oil and gas development, are similar to those of trading tanker structures, there are various large differences between them as indicated in Table 1.

Table 1
Differences in the structural design of trading tankers and ship-shaped offshore units, from Paik & Thayamballi (2007)

Trading tankers	Ship-shaped offshore units
Design condition – North Atlantic wave environment	Design condition – site- and tow route-specific environments
20 to 25-year return period of wave	100-year return period of wave
Predominantly wave actions	Currents as well as wind and wave actions
Limited number of loading/offloading cycles; loading occurs in sheltered situations	More frequent loading/offloading cycles; loading occurs with relatively more environmental effects present
Limited number of loading conditions	More number and variety of loading conditions
At open sea for about 70% of the time	Offshore for 100% of the time
Weather in any direction; rough weather avoidance possible	Highly directional weather and weathervaning; rough weather avoidance not possible on site
Regular dry docking in every 5 years interval	Continuous operation usually without dry-docking
Without topsides	With topsides and associated interaction effects between hull and topsides

In Table 1, it is noted that the return period of the wave is not necessarily meant to be the life time of the structure, but there is a difference between the two. It tends that the longer the return period of the wave, the higher the design loads.

Some operational FPSO units have been converted from old very large crude carriers (VLCCs), and reductions of thickness due to corrosion should be taken into account when the ultimate strength under in-plane compressive actions is estimated. In addition, given the possibility of side collisions with supply vessels, small damages should be considered when estimating the ultimate strength of panels. As FPSO units are rarely removed from oil fields and structural repairs must be undertaken during operations, such knowledge of the damage severity is useful.

2.7   System Structures – Other Types of Offshore Structures

Offshore structures that deserve the special attention of designers are rigid risers and pipelines. Given their working loads, the collapse behaviour of such structures is mainly related to their capacity under external pressure and axial bending. The ultimate strength under external pressure is the collapse pressure, an instability failure that is strongly dependent on the pipe diameter to thickness ratio, the initial out-of-roundness (ovality) and the material yield stress. The residual stress due to fabrication processes can also affect the collapse pressure, but its influence is of less importance and normally not considered in formulations. The ultimate strength under pure bending is defined by the maximum bending moment or the critical curvature, which depends on the pipe moment of inertia and the yield stress. The material strain hardening can also affect the limit bending moment.

The design of submarine pipelines for deep waters is critically affected by the collapse pressure, as these are static structures resting on the sea floor. Otherwise, due to the laying process (reeling, J-lay or S-lay), a combination of bending and pressure may occur at the sag-bend region near the sea floor.

Rigid risers are dynamically loaded structures. Their design is based on global and local analyses. The local failure is normally determined by the ultimate strength under combined pressure and bending loads. Some combination of external pressure and axial tension may occur near the sea surface because of the large weight of the structure. Nevertheless, design according to the combined pressure-bending capacity normally leads to stiff structures. Flexible composite pipes are frequently used for riser applications, but their ultimate strength is considered only as a parameter for qualification tests.

Afterward, the ultimate strength can be represented by the pressure-curvature (P-K) failure envelope or P-K diagram, as given in Figure 6, normalised by the pipe collapse pressure (Pco) and the critical curvature (Kcr). This type of diagram can be obtained numerically or from the recommended rules. It can be used for the design of rigid pipelines and risers, provided that suitable safety factors obtained from a reliability study are employed.
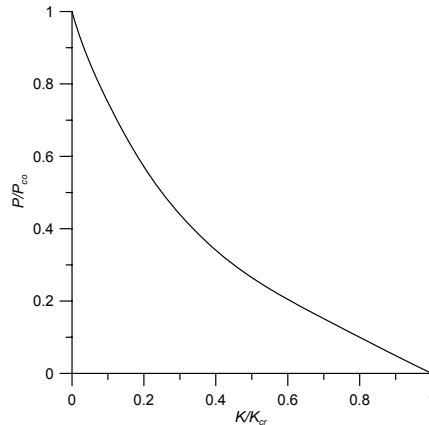
Figure 6: Sample of the pressure-curvature failure envelope for pipes

Other offshore structures that currently are seeing an increasing interest are wind turbine structures. They consist of a rotor and a nacelle that is supported by a tower and a foundation, as shown in Figure 7. For offshore wind turbines, five different foundation concepts are generally considered, dependent on water depth and environmental conditions. These are monotower structures, tripod structures, jacket structures, gravity structures and floating structures. The foundations are similar to what is found in the off-shore oil and gas sector, and the ultimate strength can be treated in the same manner.

The three-bladed concept, usually referred to as the Danish concept, for the wind turbine rotor is the most commonly used for modern wind power plants. The blades are long and slender structures and the outer contour is governed by aerodynamic considerations. A more thorough description of wind turbines can be found in the guidelines of DNV/Risø (2002).

The design of the wind turbine blade is a compromise between aerodynamic and structural considerations. Aerodynamic considerations usually dominate the design for the outer two thirds of the blade, whereas structural considerations are more important for the design of the inner one third of the blade. Structurally, the blade is typically hollow, with the outer geometry formed by two shells. One or more structural webs are fitted to join the two shells together and transfer shear loads.
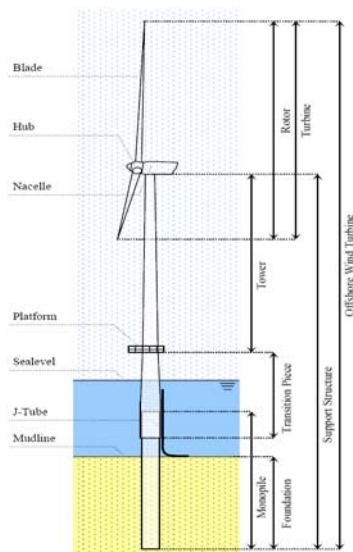
Figure 7: Definition of offshore wind turbine components, from De Vries *et al*. (2007)
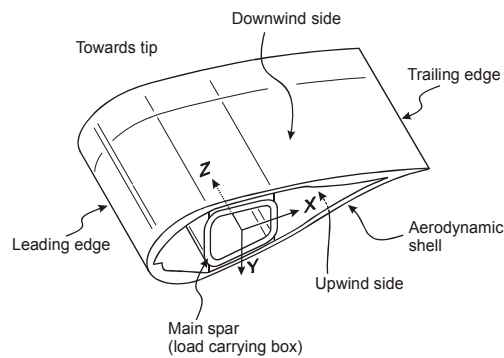
Figure 8: Blade structure

Some designs are constructed with a load-carrying box girder (main spar) supporting the outer shell. The box girder gives the blade sufficient strength and stiffness, both globally and locally. Globally, the blade should be sufficiently stiff so that it does not collide with the tower under all types of loading. Locally, the webs, together with the stiffness of the outer shell, ensure that the aerodynamic profile is maintained. The materials used are highly advanced composites that have high strength- and stiffness-to-weight ratios. The webs usually extend from the root of the blade to a position close to the tip, and the load carrying flange of the box girder is generally of single-skin construction. The webs are usually quite thin sandwich structures and their main purpose is to take the shear loads on the blade. However, nonlinear effects at high loading result in higher loading on these webs, which may result in a lower than expected ultimate strength of the whole blade when the design is based on linear calculations. Figure 8 shows a typical structural layout for a wind turbine blade with a load carrying girder. In the prediction of the ultimate strength of wind turbine blades, it is important to take nonlinear effects into account, such as buckling and the so-called 'Brazier effect' (see Brazier 1926).

3.   MARITIME REGULATIONS, INTERNATIONAL STANDARDS AND BEST PRACTICES

3.1   *General*

The three major movements in maritime industries that were discussed in previous ISSC committee reports on ultimate strength are reviewed in this chapter together with examples of best practices to highlight the engineering analysis and full-scale testing philosophy of other industries. This may facilitate development of a common approach within maritime industries to ultimate strength assessment by FEA and full scale testing methods. One aspect of the committee mandate is to highlight uncertainties in strength models for design. Currently, however, there is no common approach to this subject, and no requirement to find one under existing maritime regulations.

The development of maritime regulations in the future will benefit from a common approach to uncertainty analysis, which will also support the development of International Maritime Organisation (IMO) goal-based standards. In addition, this will increase confidence levels during the design and through-life operation of ships and offshore structures. A consistent approach by designers, regulators, builders and repairers is needed to ensure that the operators of ships and offshore structures benefit from robust designs that are fit-for purpose and able to withstand harsh operating conditions throughout their service lives. In this respect, shipping in particular has a different approach to other industries in that the hardware is not tested in the harsh environmental conditions in which it will be required to operate before it receives a seaworthiness certificate.

Comparisons made with the aviation and space industries show that they have much more stringent safety regimes, particularly with regard to full scale testing prior to achieving airworthiness or flight approval. Shipping has many variations in structural design, which is a major reason for the lack of a thorough design and testing programme for each ship put into service. Although the size of large ships and offshore structures means that environmental tests to ensure the ability to withstand typical worst-case operating conditions is not feasible, efforts have to be made in the development of accurate and realistic modelling of these environments for standardised ship and offshore structural designs, together with representative model testing in suitable test facilities. The results of these models have to be cross-checked with data feedback from continuous monitoring during service life. This will lead to further improvements and better understanding of uncertainties, and increased confidence levels with model predictions that are closer to real operating conditions. For additional information on international standards and regulations, the reader is referred to Mansour & Liu (2008).

3.2 Maritime Regulations

At the highest level in the marine regulatory world, the IMO has established the Goal-Based New Ship Construction Standards (GBS) as highlighted by the 16th ISSC Committee III.1 on Ultimate Strength. It has always been recognised that the best way to improve safety at sea is by developing international regulations that are followed by all shipping nations. Flag states and classification societies are responsible for the majority of the classification of new ships and ships in service, to ensure that initial

design rules and regulations are complied with and maintained throughout their operational lives, by regular periodical, intermediate and special surveys, and occasional surveys after accidents such as collision and grounding.

An important regulation that has entered into force in the last 10 years is the International Safety Management (ISM) Code. Not only are flag states and classification societies responsible for the hardware standards, they also provide certification of company/operator and shipboard safety management systems. However, the owner/operator and ship's crew are responsible for the correct maintenance and operation of the ship on a daily basis. Ship crews are often faced with difficult decisions and at times the safety margins can be exceeded, e.g., in determining the ship's speed in heavy weather, or when loading operations exceed the approved loading manual requirements. In addition, some owners/operators do not maintain internal structures adequately in older ships, and corrosion margins can be exceeded between survey periods, etc.

These human factors must be taken into account as part of ultimate strength assessment in the future design of ships. The associated uncertainties need to be understood and allowed for in the design loads and safety factors applied. There is, however, currently no research into the human element and its contribution to ultimate strength assessment.

In this light, progress made by the European Commission (EC) and the European Maritime Safety Agency (EMSA) should be highlighted. The EMSA was established in 2002 (under Regulation (EC) Nº 1406/2002 of 27 June 2002) in the wake of the Erika and Prestige oil tanker accidents, and it is one of the key European Union (EU) level initiatives aimed at improving the situation within Europe. The EMSA's main objective is to provide technical and scientific assistance to the EC and its Member States in the proper development and implementation of EU legislation on maritime safety, pollution by ships and security on board ships. One of the EMSA's most important supporting tasks is to improve cooperation with, and between, Member States in all key areas. In addition, it has operational tasks in oil pollution preparedness, detection and response.

As a body of the EU, the EMSA sits at the heart of its maritime safety network and collaborates with many industry stakeholders and public bodies, in close cooperation with the EC.

The current EMSA ship safety standards work programme is concentrating on the following subjects.

- Evaluation of the lessons learned from operational experience with double hull oil tankers
- Condition assessment scheme for tankers
- IACS common structural rules for bulk carriers and oil tankers
- Goal-based standards for ship design and construction

Ultimate strength will be addressed in the safety standards developed, and the committee recommends that close attention be paid to those standards, particularly if the approach is different than that currently required by IACS Common Structural Rules and/or ISO 18072-1 (2007).

3.2.1 Goal-based Standards

The last committee highlighted the development of IMO goal-based standards. At that time, the IMO had concluded that it was necessary to identify the fundamental standards to which new ships must comply, but it had only stated what had to be achieved, and had left classification societies, ship designers, naval architects, marine engineers and ship builders the freedom to decide how best to employ their professional skills to comply with the required standards. Unfortunately, this committee is not able to report any further progress on that subject. There is no international legislation or guidance on how to achieve the new standards, and research in this area has yet to be published. It will be important for the next committee to follow developments in this area, as there is a wide scope for interpreting the current standards, which could have a major influence on ultimate strength assessment and how it will be performed.

3.2.2 Common Structural Rules

Since the last committee meeting, the IACS Common Structural Rules (CSR) for Oil Tankers and Bulk Carriers were unanimously adopted by the IACS Council for implementation on 1 April 2006. This was a major change in the direction of the IACS, and new ships are now under construction and entering operation based on these rules. It is too early to have gained sufficient experience from the new CSR, but future committees should take care to review operational feedback on the performance of ships that have been classed according to them and what lessons can be learned with respect to ultimate strength.

The IACS has now implemented the CSR maintenance programme, IACS Procedural Requirement No. 32, via the IACS CSR Knowledge Centre (KC). PR 32 requires each IACS member to implement internal procedures to ensure that the CSR are maintained and updated as improvements are made via the knowledge centre, which is also responsible for the calibration and validation of the various software tools used by different societies to ensure consistent results are obtained during application. Once an IACS member's bulk carrier or oil tanker has been built according to the CSR, it will have a specific 'CSR' class notation.

The current work programmes are available on the IACS website. One of the current hull-panel work programmes is to cross check the requirements of the FEA of CSR for bulk carriers and oil tankers (the PT/FEA cross check) and cross check the prescriptive requirements of CSR for the same (the PT/Rules cross check), thus providing

confidence in the consistent implementation of the requirements of FEA and prescriptive rules. The results of these cross checks should be available for future committee work and may have an impact on ultimate strength assessment. Revisions and amendments to the current IACS CSR and new CSR for new ship types should be taken into consideration during future committee work.

It is interesting to compare the ultimate strength performance of ship structures designed by pre-CSR versus CSR methods. In this regard, a series of the ultimate strength investigations have been performed for AFRAMAX class tankers (Paik 2007c, Paik *et al.* 2007), for 300k tankers (Paik *et al.* 2008b), and for 170k bulk carriers (Paik *et al.* 2008c).

3.2.3   *International Standards*

As noted by the previous technical committee, the International Organisation for Standardisation (ISO) has now published ISO 18072-1 (2007): Ships and marine technology – Ship structures – Part 1 – General requirements for their limit state assessment. The current working group for ship structures is TC 8/SC 8/WG3, which is currently working on ISO/DIS 18072-2: Ships and marine technology – Ship structures – Part 2 – Requirements for their ultimate limit state assessment.

Another related standard that may be further developed for ships and offshore jack-up platforms is ISO 16587 (2005): Mechanical vibration and shock – Performance parameters for condition monitoring of structures. This is currently applicable to offshore platforms only, and future application to ships will be a valuable standard. The standard describes the performance parameters for assessing the condition of structures, including types of measurement, factors for setting acceptable performance limits, data acquisition parameters for constructing uniform databases, and internationally accepted measurement guidance (e.g., terminology, transducer calibration, transducer mounting and approved transfer function techniques). The procedures relate to the in-service monitoring of structures, and include all components and sub-assemblies that are necessary for the functioning of the structure as a complete entity. The monitoring is intended to be ongoing through the lifecycle of the structure, which will be very valuable for obtaining real-time information in the future.

Other published ISO standards are ISO/TR 11069 (1995): Aluminium structures – Materials and design – Ultimate limit state under static loading, and ISO 19901 (2004): Petroleum and natural gas industries – Specific requirements for offshore structures – Part 2: Seismic design procedures and criteria.

Another important development in the engineering analysis community is the publication of the 'Guide for verification and validation in computational solid mechanics' published by the American Society of Mechanical Engineers as ASME V&V 10-2006 (2006). Although only a guide, it indicates that a standard may well be developed and issued in the future, and it is a very comprehensive and valuable

contribution to the subject of finite element method (FEM) verification and validation.

3.3   *Best Practices for Ultimate Strength Analyses*

Great emphasis is now placed on numerical modelling and engineering analysis in the design of ships and offshore structures, but less is placed on full-scale testing to measure the actual values of stresses and loads, acceleration, forces, etc., particularly during operation and in real-life harsh conditions. Due to the very large size of some ships, and the fact there is no standardisation of ship types, the shipping industry is in a difficult position compared to the aviation, space and automotive industries, where crash testing, full scale fatigue testing, demonstration in service of hundreds of actual flying hours, etc. are needed before safety approval is given, especially for new aircraft types. Sea trials provide limited information on ships, which are not tested in harsh environmental conditions. Hence, it will be useful to look at other possibilities that could add value to the shipping industry in terms of engineering analysis, simulation modelling, benchmarking and full scale testing.

3.3.1   *NAFEMS*

At the 15th ISSC, Committee II.1 made reference to the National Agency for Finite Element Methods and Standards (NAFEMS) FENET project. The website for this project is no longer available, but the results can still be found at www.nafems.org by using the search term 'FENET'. NAFEMS was founded as a special interest group in the UK during 1983 with the specific objective of promoting the safe and reliable use of finite element (FE) and related technology. At that time, the engineering community was primarily concerned with the accuracy of stress analysis codes, which were predominantly based on the FEM. The initial efforts concentrated on developing standard benchmarks against which codes could be tested. NAFEMS published the results of these benchmarks for a variety of codes and the software industry quickly responded by adopting these tests as a method of improving and verifying the accuracy of codes. Today, most major vendors routinely use the NAFEMS benchmarks as part of their ongoing quality control process. Engineers rely on computer modelling and simulation methods and tools as vital components of the product development process.

As these methods develop at an ever-increasing pace, the need for an independent, international authority on the use of this technology has never been more apparent. NAFEMS is the only worldwide independent association dedicated to this technology. To promote best practise, certification to NAFEMS QSS 001 – Engineering Simulation – Quality Management Systems – Requirements (which are based on ISO 9001) could be valuable to the users of FEA tools. To facilitate knowledge sharing, NAFEMS organises world congresses, national events and seminars, publishes a magazine entitled Benchmark, issues many publications to promote best practise, and is also involved in industry projects.

An important NAFEMS project to highlight is SAFESA (SAFE Structural Analysis).

This was the result of a major initiative undertaken by 5 UK organisations with the support of the UK Department of Trade and Industry. The basis of the SAFESA approach is to formalise the structural qualification process to minimise the opportunity for error. The approach involves the identification, quantification and treatment of errors, which are identified by their sources and progressively reduced to acceptable levels by suitable treatment. The SAFESA Management Guidelines is one of a series of documents describing the SAFESA approach to structural qualification supported by FEA. This document provides detailed information in the quality chain to recognised international standards. One chapter is particularly interesting with respect to the treatment of uncertainties and error. The document concludes with a 'SAFESA error treatment procedure', and details are available at www.nafems.org.

Other NAFEMS interest areas are FEM validation, updating and uncertainty quantification for linear and non-linear models. Membership of NAFEMS is one way of developing best practice and learning lessons from other industries, and facilitating knowledge transfer between industries.

3.3.2   Full-scale Testing

An example of full scale testing whereby designs have to be tested prior to launch approval is the space industry. The European Space Agency (ESA) has been established since the 1960s, and space applications have played an important role in reliable telecommunication and satellite services for ships and offshore structures in daily operations (particularly under extreme weather conditions, given the need for accurate and valid weather reports) and communication systems for emergencies. Such information services are likely to increase in the future, in terms of both quantity and quality of the data and tools.

The qualification of a spacecraft for flight includes a 100% environmental test in dedicated test facilities. A typical satellite has to withstand high levels of acoustic noise and vibrations during launch, and once in space is then subject to radiation, high and low temperatures and thermal cycles. Consequently, it is normal practice to use a prototype model and/or a structural model in a full scale test campaign with dummy instruments to assess the structure during vibration tests, shock tests and thermal tests, and to review its electromagnetic compatibility. It will then return for qualification as a flight model with all flight instruments fitted and be fully tested again.

The ESA has its own engineering, quality and safety standards, and it would benefit future committee work in promoting best practice to look at how these approach the ultimate strength aspects of engineering structures, to determine where improvements can be made and lessons learned from an industry where the mass of the structure is very critical and material thickness is kept to the minimum while maintaining the necessary strength to prevent buckling. Space engineering standards have been developed to include requirements for operational environment, thermal control, mechanical structures, fracture control and full scale testing.

International symposiums are held in the space industry to cover subjects other than ultimate strength that can be of relevance to the works of other ISSC committees. For instance, the mechanical testing papers given at the 6th International Symposium on Environmental Testing for Space Programmes held in 2007 included one on 'Methods for validation of strength and stability under environmental factors for rocket and space equipment by testing at special shock stands' and another on 'Virtual testing simulation tools for a new electro-dynamic shaker'. Permission would be needed from the ESA to publish such research papers, and this could also provide a platform for the transfer of knowledge between the two industries. It was not a requirement of the current committee to review research work in other industries, but we should stress again that doing so would be a way of fostering common engineering approaches to often similar problems, learning lessons from each other and preventing one industry from making the same mistakes as others that have since put solutions in place.

4.   MATERIALS USED FOR SHIPS AND OFFSHORE STRUCTURES

This chapter presents the mechanical properties of the materials that are typically used in design of ships and offshore structures, including offshore wind turbines. Some of the latest findings in the literature are reviewed and grouped after the type of material used.

In the majority of cases, ultimate strength is determined in complex structures that are subjected to compression loads, where either 'shape instability' or material 'failure' can occur, both contributing to the collapse of the structure. Instability phenomena play a fundamental role in accelerating the achievement of large strain values and, consequently, the failure of material. In this context, a simple 'elastic-perfectly plastic' constitutive law of material can be accepted, leading to reasonably conservative results. However, for cases in which instability phenomena are less significant, a correct evaluation of the ultimate strength cannot be obtained without using realistic models of the material properties.

4.1   Steel

4.1.1   Current Procedure and Data for Steel Materials

For ship structural materials such as steel and aluminium alloys, the constitutive laws available in the literature in terms of stress-strain relationship curves are generally obtained using ASTM tensile coupon test programs, where the shape and the size of samples are prescribed. In the context of ship structures, the dimensions of the required test samples are not very small (the effective 'extensometer' length is about 50 mm), and the quantities that are directly measured (load and elongation) and evaluated (strain and stress) by the test must be considered as averaged values referring to the initial length and initial sectional area of the samples: see Figure 9. Stress and strain values obtained in this way are known as 'engineering stress' and 'engineering strain'. A typical engineering stress-strain relationship is presented in Figure 10.

According to the engineering values in Figure 10, it is possible to make the following considerations.

- Part 'A-B' of the curve represents the linear elastic region that can be characterised by Young's modulus and Poisson's ratio; in this zone the specimen experiences uniform strain and sectional contraction along its length;
- Point 'B' represents the onset of yielding; after this point the specimen experiences significant plastic deformations, although it still has a 'uniform' strain distribution and a uniform sectional 'contraction'; in fact, the whole of 'A-C' is known as the 'field of uniform strain';
- Point 'C' represents the onset of necking: i.e., deformations tend to be localised within a small region of the specimen, which experiences large strain values and a significant cross-section reduction; this region experiences a fully tri-axial stress field; and
- Point 'D' represents the failure of the specimen.
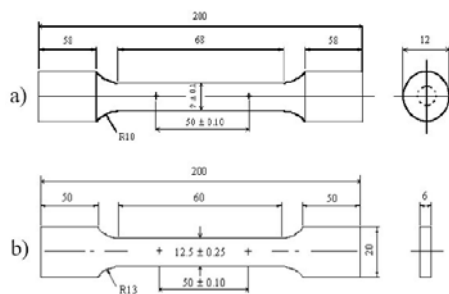
Figure 9: Shapes and dimensions of typical ASTM test samples: (a) cylindrical and (b) sheet, from Cabezas & Celentano (2002)
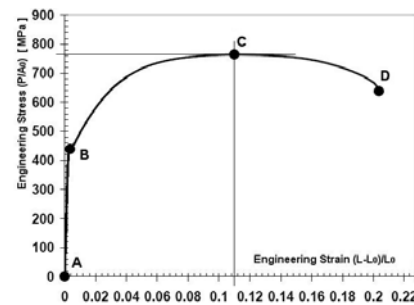
Figure 10: Analysis of a SAE 1045 steel tension specimen: averaged experimental stress-strain curve – engineering values, from Cabezas & Celentano (2002)

4.1.2   *Engineering and True Data Formulations*

According to the previous description, we can define the engineering stress-strain values as follows.

Engineering strain: $\varepsilon_E = (L - L_0) / L_0$ (2)

Engineering stress: $\sigma_E = P/A_0$,   (3)

where, L_0 = the initial 'extensometer' length of the specimen, L = the actual 'extensometer' length of the specimen, P = the actual applied load and A_0 = the initial sectional area of the specimen.

Material models based on engineering data are, however, not suitable for analysis where strain values greater than 1% are reached. The first step in improving the model is the introduction of the 'true' stress-strain values. True strain can be considered as the

sum of 'incremental' variations of strain obtained during an incremental load application, i.e.,

$$\varepsilon_T = (L_1 - L_0) / L_0 + (L_2 - L_1) / L_1 + \cdots\cdots + (L_n - L_{n-1}) / L_{n-1}, \text{ i.e., } \varepsilon_T = \int dL/L = \ln(1+\varepsilon_E).$$
(4)

Imposing no volume variation by dv = 0, it is possible to account for the reduction of the cross-section area to obtain the true stress values, which results in

$$\sigma_T = \sigma_E(1+\varepsilon_E).$$
(5)

An immediate feedback on the different response of the two formulations (engineering and true) can be easily obtained considering the following two cases: a specimen that is elongated up to double its initial length, L = 2 L_0, and a specimen that is ideally compressed to reach a final length equal to zero, L = 0. Hence,

• Engineering strain is 1.0 for L = 2 L_0 and -1.0 for L = 0,
• True strain is 0.7 for L = 2 L_0 and -∞ for L = 0.

According to Equations (4) and (5), the true stress-strain curve can be obtained from the engineering data, improving the material model in the part 'B-C' of the curve. In particular, for the case in Figure 10, the engineering data for point 'C' are ε_E = 0.15 and σ_E = 760 MPa, whereas the corresponding true values are $\varepsilon_T \cong 0.14$ and $\sigma_T \cong 874$ MPa. After point 'C', the onset of necking deeply modifies the response of the specimens, and further considerations and approaches are necessary to achieve a reasonable material model to be used in numerical simulations.

4.1.3   Material Behaviour after Necking

Point 'C' identifies the maximum load capability of the material specimen, the maximum engineering stress (σ_E = P/A_0) and the onset of necking. After this point, the true stress (σ_T) still increases, because the decrease of the section area is greater than the decrease of the load (Mirone 2004). Within the region of necking, stress and strain lose their uniaxial properties assuming a more complex tri-axial state, as shown in Figure 11, so that it is convenient to make reference to equivalent stress and equivalent strain, according to the von Mises formulation. Referring to Figure 11, the following quantities can be defined.

ε_N	Considère strain, i.e., the onset of necking
$\varepsilon_{eq} = \varepsilon_z = \varepsilon_{zAvg} = 2\ln(a_0/a)$	
$\sigma_{zAvg} = \sigma_T$	Average axial stress, equal to the true stress, i.e., F/A
$\sigma_z(r)$:	Axial stress distribution in the necking section
$\sigma_r(r)$ $\sigma_\theta(r)$:	Radial and tangential stress distribution in the necking section
$\sigma_{eq}(r)$:	Equivalent stress, according to von Mises
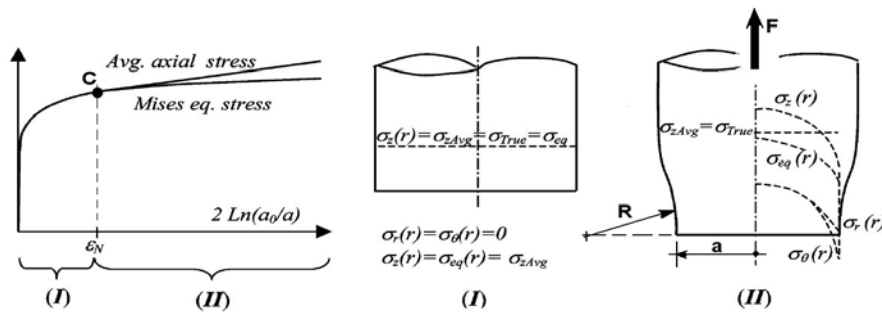
Figure 11: Stress distribution in necked area

Several models have been set up for describing the material behaviour in this particular condition. One of the first approaches still currently used is that of Bridgman (1952), which provides an 'analytical' correlation between the equivalent stress σ_{eq} and the axial averaged stress σ_{zAvg}, i.e., true stress:

$$\sigma_{eq} = k\sigma_{zAvg}, \qquad\qquad \text{where: } k = [(1+2R/a)\ln(1+a/2R)]^{-1}$$
'a' and 'R' according to Figure 11.

More recently, further efforts have been dedicated to this topic based on the extensive use of non-linear FEA, such as in the work of La Rosa *et al*. (2003). Their paper deals with the numerical simulation of tensile tests to evaluate the correlation between σeqAvg and σzAvg in several ductile materials. Of the 14 materials considered, the results for spheroidal steel, stainless steel, mild steel and aluminium alloy are reported in Figure 12. As can be seen, the dependence on the material is almost negligible. Another example of traction test simulation is provided by Cabezas & Celentano (2002), who started with engineering stress-strain data relevant to SAE 1045 steel to develop a complete post-necking characterisation of the material, as shown in Figure 13. The figure indicates that the onset of necking (point 'C') is not more easily recognisable, which is different from the engineering curve in Figure 10.
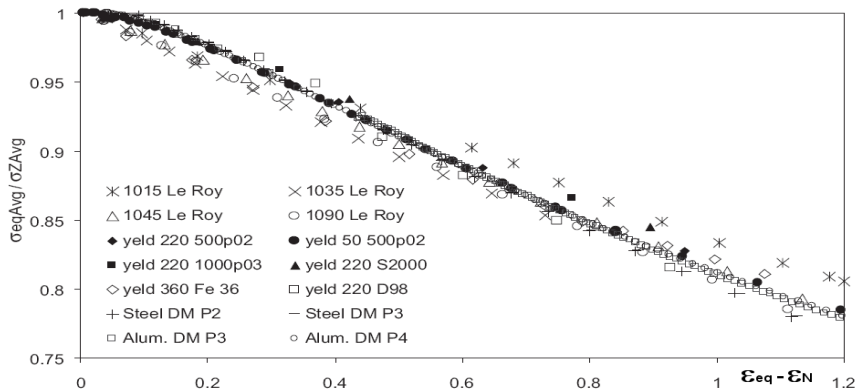
Figure 12: $\sigma_{eqAvg}/\sigma_{zAvg}$ ratio versus post-necking strain, from La Rosa *et al*. (2003)
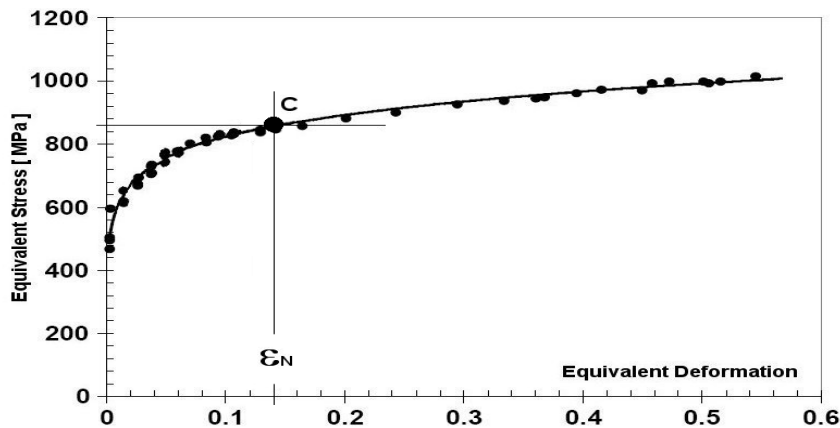
Figure 13: Analysis of a SAE 1045 steel tension specimen. True equivalent values,
from Cabezas & Celentano (2002)

An interesting and useful collection of material behaviours is reported by Doege *et al*.
(1986). Their textbook contains a well-organised collection of stress/strain curves
(equivalent true values) for approximately 150 different metallic alloys, as functions of
both temperature and deformation velocity.

4.1.4   Mechanical Properties of Steel Materials

The most common steels used in ship and offshore structures are identified by
classification societies based on their minimum yield stress level, R_{eH} (N/mm^2), as
normal strength steels, R_{eH} = 235 N/mm^2, and higher strength steels, R_{eH} = 315, 355,
390 N/mm^2. Normal steels are subdivided into grades A, B, D and E according to their
impact properties evaluated at +20, 0, -20 and -40 °C, respectively. The same criteria
are used for high strength steels, which are subdivided into the grades AH, DH, EH and
FH, followed by the values of the minimum yield stress level. Minimum property
requirements are given in Tables 2 and 3.

Classification societies provide minimum requirements for the mechanical properties of
steels. Very interesting in this context is the investigation reported by Bollero *et al*.
(2002), in which the stochastic characterisation of the yield stress is performed by
means of detailed data made available by several steel manufacturers. In particular, data
on steel plates of grade 32 (nominal yield stress of 315 MPa) and thickness in the range
of 12 to 20 mm are considered in the analysis as the most typical for shipbuilding
applications. Figure 14 shows the results obtained in the form of a normalised
histogram compared with a Gaussian distribution featuring the same average and the
standard deviation values of 405 MPa and 24 MPa, respectively. For the case
considered, the probability associated with yield stresses that were lower than the
nominal value was less than 10^{-4}.

Table 2
Mild steel, grades and relevant properties

Steel grade	Yield stress ReH [N/mm^2] MIN	Tensile strength Rm [N/mm^2]	El. % MIN	Average impact energy (J) – Minimum requirements KVL longitudinal – KVT transverse – t = thickness (mm)						
				Test temp. °C	T ≤ 50		50 < t ≤ 70		70 < t ≤ 100	
					KVL	KVT	KVL	KVT	KVL	KVT
A	235	400/520	22	+20	-	-	34	24	41	41
B	235	400/520	22	0	27	20	34	24	41	41
D	235	400/520	22	-20	27	20	34	24	41	41
E	235	400/520	22	-40	27	20	34	24	41	41

Table 3
High strength steel, grades and relevant properties

Steel grade	Yield stress ReH [N/mm^2] MIN	Tensile strength Rm [N/mm^2]	El. % MIN	Average impact energy (J) – Minimum requirements KVL longitudinal – KVT transverse – t = thickness(mm)						
				Test temp. °C	T ≤ 50		50 < t ≤ 70		70 < t ≤ 100	
					KVL	KVT	KVL	KVT	KVL	KVT
AH32	315	440/570	22	+20	31	22	38	26	46	31
DH32				0	31	22	38	26	46	31
EH32				-20	31	22	38	26	46	31
FH32				-40	31	22	38	26	46	31
AH36	355	490/630	21	+20	34	24	41	27	50	34
DH36				0	34	24	41	27	50	34
EH36				-20	34	24	41	27	50	34
FH36				-40	34	24	41	27	50	34
AH40	390	510/660	20	+20	39	26	46	31	55	37
DH40				0	39	26	46	31	55	37
EH40				-20	39	26	46	31	55	37
FH40				-40	39	26	46	31	55	37

4.2   Aluminium Alloys

Aluminium is a non-magnetic material with low mechanical resistance, depending on the impurities contained within it and the plastic deformation to which it is subjected. The maximum values of tensile strength in aluminium range from 80 MPa in the annealed condition to 150 MPa in the strain hardened condition after plastic deformation. In addition, aluminium has a low specific weight (approximately 1/3 of steel) and an excellent formability. It can easily be forged, rolled in thin sheets and extruded in profiles with complex sections; such behaviours allow to the adoption of design solutions (type and geometry of structural elements, joint details) that are quite different from typical steel structures. In addition, pure aluminium is also particularly resistant to corrosion in marine environments.

The excellent mechanical characteristics of aluminium (and its alloys) in terms of

resistance and ductility are essentially due to the face-centred cubic metallurgical structure that it has in common with austenitic structures, but unlike those structures its mechanical properties are not deeply influenced by low temperatures. Other aluminium properties are an elevated reactivity with oxygen that gives a highly refractory oxide (Al_2O_3), elevated thermal and electrical conductivities, a thermal expansion coefficient approximately double that of steel and a melting point temperature of about 660 °C. As aluminium alloys do not manifest a well defined/localised 'yielding point', the yield stress is substituted by the value of stress that leads to a permanent deformation of 0.2% ($R_{P0,2}$).
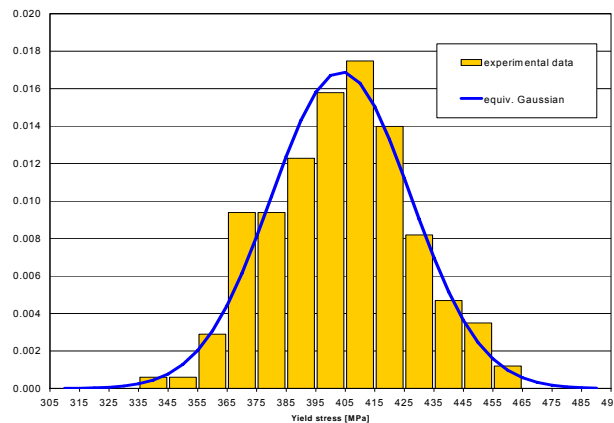
Figure 14: Experimental probability density function for the yield stress, from Bollero *et al*. (2002)

4.2.1 *Hardening and Chemical Composition of Wrought Aluminium Alloys*

There are 8 series of industrial aluminium alloys, with the properties shown in Table 4. They are divided into the following categories.

- Strain hardening alloys, the 1000's, 3000's, 5000's and 8000's series, the mechanical properties of which are deeply influenced by production processes (i.e.: rolling or extrusion) and by intermediate or final annealing
- Age hardening alloys, the 2000's, 6000's and 7000's series, the final mechanical properties of which are the result of specific thermal processes

Despite their excellent mechanical properties, alloys in the 2000's series with copper and 7000's series with zinc (with or without copper) cannot be used in marine applications without adopting special protection because of their low corrosion resistance. The 7000's series alloys without copper can be arc welded. However the high sensitivity of the heat affected zone to exfoliating corrosion demands very strict precautions for marine applications. The aluminium alloys most commonly used in marine applications belong to the 5000's and 6000's series, which have been selected for their mechanical properties, their ease of assembly by welding and their excellent

corrosion resistance in marine environments. According to the ease with which they are processed, 5000's series alloys are most often used in rolled elements, whereas both 6000's and 5000's series alloys are used in extrusions, depending on the shape complexity of the section.

4.2.2 *Mechanical Properties of Aluminium Alloys*

The great demand for aluminium structures in both high-speed vessels and for the upper decks of large cruise vessels has led to an increasing interest in adapting the ULS design techniques developed and currently used for steel structures. The adaptation of ULS techniques to aluminium alloys needs to account for the different elastic-plastic behaviour of the material after the proportional limit and also for the reduced strength region or the heat-affected zone (HAZ) due to the fusion weld processes, which is normally neglected in steel structures. For the two 5000's and 6000's marine alloy series, the HAZ can extend up to 30 mm from the weld centreline and the reduction in proof strength in this region can be 30-50%. Figures 15 and 16 present the typical distributions of strength (hardness) across the weld for 5000's and 6000's series, and Figure 17 shows the stress-strain curves (basic and weld) for the same materials.

Table 4
Aluminium, grades and relevant properties

| Hardening type	Series	Additional basic Elements	Content (% of weight)	Possible additives	Ultimate tensile strength Rm (MPa)
Strain hardening	1000	None	–	Cu	50 - 150
	3000	Manganese	0.5 – 1.5	Mg, Cu	100 - 260
	5000	Magnesium	0.5 – 4.5	Mn, Cr	100 - 400
	8000	Iron/silicon	0.3 – 1/0.6 - 2		130 - 190
Age hardening	6000	Magnesium/silicon	0.5-1.5/0.5-1.5	Cu, Cr	150 - 310
	2000	Copper	2 – 6	Si, Mg	300 - 450
	7000	Zinc/magnesium	4 – 8/1 – 3	Cu	320- 350(no Cu) 430 - 600 (+ Cu)
	8000	Silicon	2 – 13.5	Mg, Cu	130 - 190
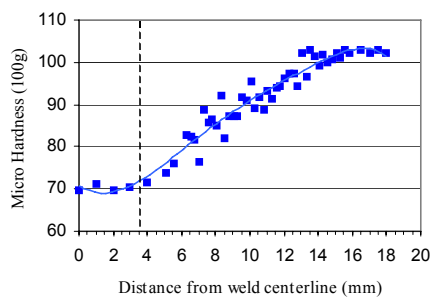
Figure 15: Hardness measurements of a 6mm butt-welded 5383 aluminium alloy
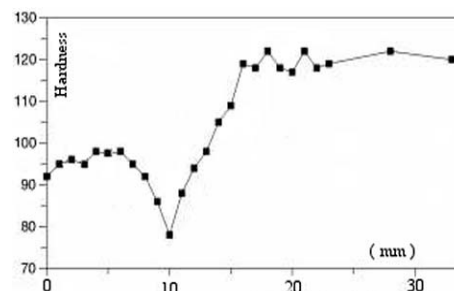

Figure 16: Material strength across weld of 6000's series

Although steel structures can be successfully schematised by assuming homogeneous material properties, at least within well-identified parts of the hull, this assumption cannot be adopted for welded aluminium structures. Proper uses of extrusions and friction stir-welding can significantly contribute to reducing the softened zone, but at the present time it is not possible to avoid all fusion welds in the hull, such as welds on transverse frames and welds between blocks.

While these under-matched zones can be accounted for in the traditional allowable working stress design by adjusting the allowable stress of the structure, or assuming that the entire structure was made with the worst material (leading to a conservative but consistent design), the limit-state approach requires the set-up of appropriate models to integrate the local material properties (e.g., in the softened zone) with the overall failure modes of the entire structural members.
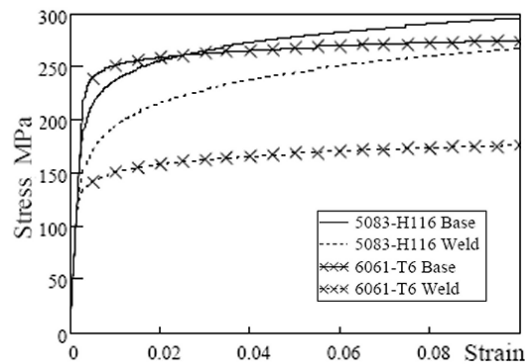
Figure 17: Typical tress-strain curves for 5000's and 6000's series, from Collette (2007)

A particular response effect due to the softened zone is that the plastic flow of the structure is essentially concentrated in it, which can cause ductile failure even when the average global strain of the hull is still quite low. Hence, the global failure response of the hull can appear similar to a brittle fracture, although it remains a ductile concentrated failure. For this reason the tensile failure, often not considered in the case of steel, becomes important for aluminium structures.

In this context, Collette (2007) provided an interesting investigation of the influence of the HAZ on the ultimate limit state of both welded samples and more complex structural elements. The analysis was based on the adoption of two different models for evaluating the residual strength of welded samples: i.e., the simpler 'series model' and the more complex 3D model of Satoh & Toyoda (1970). Collette (2007) also dealt with the evaluation of the global limit state of a quite large structure (squared box girder, 3×3 m squared section), subjected to bending load. The results provide significant evidence of the need to improve the limit state model for the aluminium weld.

Paik *et al*. (2005a) discussed refined ULS methods for aluminium multi-hull vessels,

based on the MAESTRO and ALPS codes. Their work was based on extensive and interesting investigations (theoretic, numeric and experimental) carried out on the collapse mechanism of a wide range of aluminium structural element types, taking into account the softening effects in the HAZ, the initial welding distortions and the residual stresses. The effects of repetitive load cycles on the initial stresses were also studied by proper experimental model tests. This paper provides useful, semi-empirical, closed form design formulations for evaluating the ULS of stiffened and unstiffened panels, including both the HAZ and initial imperfections.

Paik *et al.* (2006) reported other important results in the field of aluminium ULS in an effort to obtain a relevant design database of the statistics of the initial imperfections occurring during the welding of aluminium stiffened plate structures, because the initial imperfections due to welds can significantly reduce the load-carrying capacity of those structures. A large number of single and multi-bay aluminium stiffened plate structures were analysed. The material of the plating and the stiffeners varied, with 5083-H116 (rolled), 5383-H116 (rolled), 5383-H112 (extruded) and 6082-T6 (extruded) aluminium alloys used. The dimensions and types of structures also varied, encompassing different kinds of stiffeners, different plate thicknesses, different dimensions and different numbers of frame bays. Fabrication induced initial imperfections were considered to be of six basic types: the initial distortion of plating (between stiffeners), column-type initial distortion of stiffeners, sideways initial distortion of stiffeners, residual stresses of plating, residual stresses of stiffener web and material softening in the HAZ. All of these imperfections were directly measured on the realised prototype structures and statistically characterised.

Sielski (2007, 2008) reviewed the research needs in relation to aluminium structures. Concerning ultimate strength, the important areas needing investigation are the effect of transverse welds and the HAZ on the ultimate longitudinal strength, ultimate strength under combined loads, the effect of initial imperfections and simplified methods for predicting the load-shortening curves of stiffened panels for hull-girder collapse analysis.

4.3 *Composites and Sandwich Core Materials*

Composite and sandwich materials are usually used in structures when light weight and high performance is required. The operational parameters of and conditions for these structures often lead to the following material requirements focused on stiffness, density and long fatigue life:

- High material stiffness is needed to maintain optimal structural shape;
- Low density is needed to reduce inertia forces; and
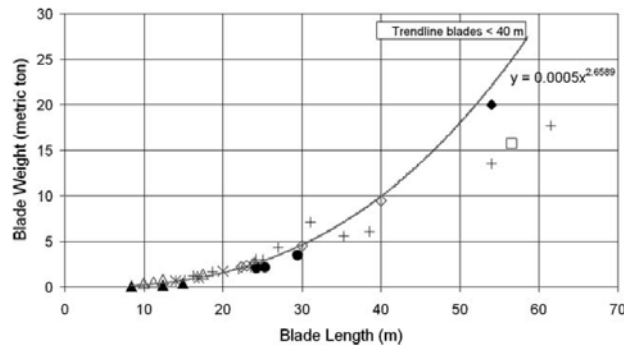- Long-fatigue life is needed to reduce material degradation.

Figure 18: Development in wind turbine blade weight versus length. Symbols indicate different manufacturers and processing technologies, from Brøndsted *et al.* (2005)

This is particularly true for wind turbine blades, where high material stiffness is needed to maintain the aerodynamic shape of each blade and prevent the blades from colliding with the tower under high wind conditions. The optimal design of wind turbine blades is a complex and multifaceted task that requires the optimisation of properties, performance and economy. Brøndsted *et al.* (2005) illustrated the combined result of the design process and the materials in the form of blade weight as a function of blade length, as presented in Figure 18. The lower end of the curve represents relatively short blades of 12-15m in length, as were common during the early years of the wind turbine industry in the 1980s. The points represent blades of increasing length, as developed until the present. An empirical curve is shown for those points representing blades with lengths below 40m, giving a power law with an exponent of approximately 2.66; this is lower than expected for a simple up-scaling of the design on a volume basis (exponent 3), but is higher than up-scaling of only two dimensions (length and thickness, exponent 2). This rather low exponent is a good indication of the high quality of the design process. Three recent and very long blades of 54 to 61.5m, from LM Glasfiber (2004), plotted in Figure 18, show the further improvement in the design process by the points being below the extrapolated empirical curve. However, it should be noted that these designs might be based on different wind load classifications and improved operational control algorithms in newer wind turbines will also reduce the loading.

In terms of material strength, i.e., resistance against long-time fatigue loads and ultimate loads, it is important to consider material fracture toughness. Ashby (1992) presented diagrams for the toughness in relation to density. The merit index for high fracture toughness and low density shows that candidate materials are woods and composites, which not surprisingly are the most commonly used materials for wind turbine blades.

The mechanical behaviour of composite materials is influenced by a variety of parameters. The homogeneity and quality of the materials manufactured are essential. Defects such as wrinkles, misalignment and porosities formed during the manufacturing process can lead to failure mechanisms such as fibre fracture, interface

cracking and matrix cracking, which are sources of micro-buckling, trans-laminar crack growth and delamination. These failure mechanisms have essential influences on the resulting properties, and it is the obtainable material quality that sets the limits for the mechanical properties and their variations. From a basic materials approach, the mechanical properties are controlled by the damage initiation and evolution.

4.3.1   Tensile Properties

According to Brøndsted *et al.* (2005), the tensile testing of composite materials is performed using well-established techniques and is governed by standards, where the ASTM D3039 (2000) and ISO 527 (1997) are the most well documented and widely used. Making between five and ten tests on small specimens usually generates the static strength data of the materials, e.g., modulus, Poisson's ratio, strength and strain properties. The standards deal with tensile testing of both unidirectional and multidirectional fibre composites.

4.3.2   Compressive Properties

Compression strength is the most critical static property of many composite materials. The compression strength of unidirectional carbon fibre epoxy is about 60% of the static tensile strength according to Brøndsted *et al.* (2005). Basically, failures in such materials come from the micro-buckling of the fibres, and several papers have taken a micromechanical approach to solving this problem. Fleck (1997) presented the main mechanics of compressive failure, whereby from a stability point of view the fibre alignment must be within ±1° to avoid micro-buckling and instability.

Because the main fibre direction in the flanges of wind turbine blades is almost entirely unidirectional, compressive strength has become the main topic for optimising the manufacture of unidirectional materials. To document these properties, many attempts have been made to develop the most reliable test methods. The compression test of unidirectional composites is probably the most debatable type of testing. In a compression test, the critical factor appears to be instability. This establishes the requirements for the test set-up and alignment of the test fixture. Early suggestions were to use supported test fixtures, such as the Celanese fixture and the IITRI test fixture (Lamothe & Nunes 1983) as adopted in ASTM D3410 (1995), and the Boeing fixture defined by ASTM D695 (2002), which suggests the need to use a supporting jig for thick specimens. Several other techniques of anti-buckling support have been suggested, but the results have been contradictory.

Adams & Welsh (1997) suggested a combined loading compression test method where the load transfer to the test specimen is controlled end loading and shear loading introduced from the sides of the specimens. In addition, Adams (2002) discussed the use of tabbed and untabbed compression specimens, but neither of these test techniques has provided convincing results, especially in relation to unidirectional carbon fibre composites.

ISO 14126 (1999) is a compression testing standard that takes into account the bending during the test and gives a maximum bending ratio for accepting the test results. To further reduce the bending and to gain better control of the end-to-shear load ratio, the Risø National Laboratory for Sustainable Energy, Technical University of Denmark developed a new concept of the combined compression test fixture, as described by Brøndsted *et al.* (2005). This concept of performing compression testing appears to be very successful. Bending is almost avoided, and it has been possible to obtain compression strengths of carbon-epoxy composites that are 30-40% higher than those measured earlier. The OPTIMAT project has shown that even for glass/epoxy, the compression strengths measured are 20% higher when using a combined loading fixture compared with those using a short-gauge-length free specimen.

4.3.3   Shear Properties

The knowledge of the shear properties of composites is also of vital importance when modelling structural behaviour. According to Brøndsted *et al.* (2005), the shear modulus is most successfully measured by the V-notch beam method published by Iosipescu (1967) and standardised in ASTM D5379 (1998). However, when measuring laminate shear properties, the ±45° tensile test can be used, as standardised in ISO 14129 (1998) or ASTM D3518 (2001). Interlaminar shear is measured by the rail shear test, ASTM D3846 (1994), or by the short beam bending test, ILSS ASTM D2344 (1995), although the latter is not suitable for measuring design data and is mainly used in production control and data comparison.

4.3.4   Other Database of Material Properties

During the past two decades, valuable experience has been obtained in different national and international research programmes. In three European projects, from 1986 to 1996, research focused on the mechanical behaviour of wind turbine blades and their materials. Static properties and the high cycle fatigue behaviour of glass-polyester and glass-epoxy materials were measured. Test techniques were developed and design curves based on constant load amplitude tests and on variable amplitude tests using stochastic load histories were established. The results from these projects were collected in books edited by Kensche (1996) & Mayer (1996). De Smet & Bach (1994) collected the data into the FACT database.

Supported by the Sandia National Laboratories, Montana State University has worked intensively since 1989 on characterising composite materials for wind turbines. The results from this programme are collected in the large DOE/MSU database, first presented by Mandell & Samborsky (1997). Since 2001, that database has been updated annually.

European activities have continued in the recently completed, OPTIMAT project (http://www.wmc.eu/optimatblades.php), under the 5th EU framework programme (van

Wingerde *et al*. 2003). This project aimed to provide accurate design recommendations for the optimised use of materials within wind turbine blades and to achieve improved reliability. The project investigated the structural behaviour of the composite material (glass-epoxy) under the unique combination of conditions experienced by blades such as variable amplitude loading, complex multiaxial stress states, extreme environmental conditions, thick laminates and their possible interactions (Smits *et al*. 2004a, 2004b).

5.   STRUCTURAL COMPONENTS

5.1   Plates

Plate elements in a continuous plate structure can deflect for various reasons, such as lateral pressure actions, buckling under in-plane actions and initial weld imperfections. A concept of equivalent flat plate, i.e., without lateral deflection but with reduced plate effectiveness, gives an efficient procedure for computing the behaviour of a plate accompanied by deflection. Paik (2008b) review the recent advances in plate effectiveness evaluation in terms of the effective breath associated with the shear-lag effect, the effective width associated with buckling in compression, and the effective shear modulus for a plate under edge shear, including formulations of the effective width for the post-ultimate strength regime. Belenkiy *et al*. (2007) made a review on the effective breadth of the flange plating of the primary support members in double skin ship structures.

Regarding unstiffened plates surrounded by support members under combined biaxial thrust and lateral pressure, Paik *et al*. (2008d) performed a series of benchmark studies on the methods for ultimate limit state assessment. ANSYS/FEA, DNV/PULS, ALPS/ULSAP and IACS/CSR are taken as the candidate methods. The results indicate that the ultimate strength behaviour of a plate is significantly affected by parameters such as the initial deflection shape and boundary conditions of the plate, as well as loading conditions. DNV/PULS and ALPS/ULSAP are assessment methods in terms of computational efforts and the resulting accuracy, compared to more refined nonlinear FEA. Fujikubo *et al*. (2005b) developed a simplified method of estimating the ultimate strength of a continuous plate, which is typical in ship bottom plating, subjected to combined transverse thrust and lateral pressure. The effects of rotational restraints caused by lateral pressure actions along support members and a change in the collapse mode from a simply supported mode to a clamped mode with an increase in lateral pressure are explicitly taken into account. The proposed formulae give accurate predictions of ultimate strength in comparison to FEA results. Luis *et al*. (2008) studied the effect of dimple-type initial deflections on the ultimate strength performance of plates. Wang & Huang (2009) studied the elasto-plastic buckling behaviour of rectangular plates under biaxial loadings. Steen *et al*. (2008) formulated the elastic postbuckling stiffness of rectangular plates under biaxial compression.

Hong & Amdahl (2007) investigated the resistance of laterally patch loaded plates. The

plastic yield line theory was adopted with consideration of the influence of membrane-force effects during finite deformations. A new plastic collapse mechanism, called the 'double-diamond' pattern, is introduced to give a better estimate of collapse mode and strength than the conventional 'roof-top' mechanism shown in Figure 19. Through a series of comparisons with FEA results, the proposed formulation gave a very accurate prediction of the plate resistance when finite, permanent deformation is accepted, which may be the case for a plate subjected to abnormal ice actions and collisions. The required plate thickness according to the IACS unified requirement for polar ships is in good agreement with that obtained from the proposed formula when no permanent deformation is allowed.

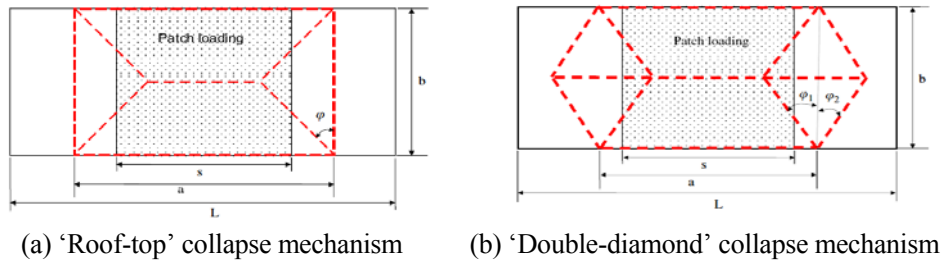(a) 'Roof-top' collapse mechanism   (b) 'Double-diamond' collapse mechanism

Figure 19: Plastic collapse mechanism for laterally patch loaded plates

Samuelides *et al.* (2007) investigated the applicability of analytical methods based on plastic analysis for the prediction of the permanent deflections of steel plates under dynamic lateral pressure loads and the simulation using FE codes. These methods are applied to predict the deformations of steel plates, measured in the blast load tests reported in the literature. The range of applicability of analytical methods and the appropriate procedures for FE simulation are discussed.

Perforated plates are used in ships and offshore structures to make a way of access or to lighten the structure. As the perforations reduce the ultimate strength of the plates, their effect needs to be investigated where it is likely to be significant. Paik (2007f) proposed the closed-form empirical formulae of the ultimate strength of perforated plates under edge shear loading based on FEA results, and also those of the ultimate strength interaction relationship for combined biaxial compression and edge shear loadings (Paik 2008a). The ultimate interaction relationships of perforated plates under combined loads differ from those of perfect plates without cutouts. Kim *et al.* (2008) performed axial compression tests on a total of 90 perforated plates and 9 stiffened panels with openings. The motivation lay in the evaluation that the current design practice for perforated plates was not relevant for relatively large opening sizes and/or large plate thickness. Based on the test results and the nonlinear FEA results, new design formulae of buckling and ultimate strengths were derived. Harada & Fujikubo (2005) investigated the ultimate strength of a girder web stiffened by two equidistant vertical or horizontal stiffeners with a cutout in the central local plate panel. They found that the ultimate strength of a stiffened web with cutout was higher than that of a

simply-supported isolated plate with cutout because of the restraint from the adjacent non-perforated plate panels. A set of closed-form empirical formulae of buckling and ultimate strengths was proposed based on FEA results. Ishibashi *et al.* (2006) developed an ISUM plate element to simulate the buckling/plastic collapse behaviour of a girder web with a cutout. They considered the effect of perforation by removing the corresponding area from the region of the stiffness integration of the element.

5.2   *Stiffened and Corrugated Panels*

Continuous efforts have been devoted to the ultimate strength assessment of stiffened flat panels with a view to obtaining a better understanding of buckling/plastic collapse behaviour and the factors that influence it, and to develop improved methods for prediction of the ultimate strength of stiffened panels and systems in terms of both accuracy and efficiency.

Badran *et al.* (2007) studied the buckling strength of stiffened panels with Y shaped stiffeners. Loskin *et al.* (2008) derived a buckling strength design formula for grillages. Paik (2007g) corrected a significant amount of experimental and numerical data on the ultimate strength of longitudinally stiffened panels under uniaxial compression, and used it to identify the uncertainty in the ultimate strength predictions of existing simplified formulations. A large scatter was observed in the predictions and its possible sources were discussed from several viewpoints including the collapse modes involved, effective width of the plating and initial imperfections. The collected data are considered to be quite useful for future benchmark studies related to the ultimate strength of stiffened panels. Paik *et al.* (2008e) performed a benchmark study on the ultimate limit state assessment of stiffened plate structures under combined biaxial compression and lateral pressure actions by taking IACS/CSR, ANSYS/FEA, DNV/PULS and ALPS/ULSAP as the candidate methods. The object structure, the bottom part of an AFRAMAX-class double-hull oil tanker structure, is taken as a target structure in the benchmark study in this committee report.

Fujikubo *et al.* (2005a) developed a set of design formulae to estimate the ultimate strength of a continuous stiffened panel subjected to combined transverse thrust and lateral pressure, extending their basic model for continuous unstiffened plates (Fujikubo *et al.* 2005b). The effect of the stiffener's torsional stiffness on the elastic buckling strength of a local plate panel was introduced, and the overall collapse of stiffeners under lateral pressure was included as a possible failure mode. Through a comparison with FEA results, the proposed formulae were proven to give a good prediction of the ultimate strength of continuous stiffened panels. Brubak *et al.* (2007) developed a semi-analytical method for the buckling strength analysis of plates with an arbitrary stiffener arrangement under in-plane loadings. The buckling strength limit was predicted using a simplified displacement magnification method based on elastic critical strength and von Mises yield criterion for the membrane stress as the strength limit. This method allowed for a very efficient analysis of buckling strength, and the results were on the conservative side compared to the ultimate strength limit obtained by the fully nonlinear FEM.

Zhang *et al*. (2008) presented work carried out on the ultimate shear strength of ship structures. A simple formula for assessment of the ultimate shear strength of plates and stiffened panels in intact and damaged situations was developed. The proposed formula was verified against results from ABAQUS non-linear finite element software and a large number of published results. Application of the proposed method to the side shell structure of a double hull oil tanker was carried out and the results were found to compare favourably with results from ABAQUS. The method was also applied to collision damaged side shell structures.

Karvinen & Pegg (2006) proposed a simplified method for the nonlinear failure analysis of stiffened panels. A component failure load was determined using a detailed nonlinear FE analysis, and then a linear course-meshed FE model of the same component was analysed to ascertain the linear stress distribution corresponding to the failure load. The resulting failure stresses were employed as criteria for course-meshed larger structural models. This approach was effective for estimating initial failure loads. Simple closed-form analytical formulas for the buckling loads of compressively loaded orthotropic composite and isotropic plates braced by longitudinal stiffeners were derived by Mittelstedt (2008), together with the closed-form expressions for the minimum bending stiffness EImin required for the stiffeners.

Gordo & Guedes Soares (2008a,b) performed axial compression tests on stiffened steel panels with different combinations of mechanical material properties and geometric configurations for the stiffeners, including the use of 'U'-shaped stiffeners. The effectiveness of high tensile steel S690 was also considered. All test modes were designed so that they had a similar squash load. The hybrid material panels showed better performance than the full S690 panels because they had a higher sectional area and inertia moment, leading to lower column slenderness and higher critical stress. The authors suggested the need for further study on the normalising stress to be used for the design of hybrid panels.

Curved plates or stiffened panels are often used in ships and ship-shaped offshore structures, such as in bilge circle parts and deck plating with cambers. Compared to flat stiffened panels, however, ultimate strength design formulations for these plates and panels are not readily available. Cho *et al*. (2007) performed axial compression tests and nonlinear FE analyses on six curved stiffened panels representing the bilge strakes of container ships. From the comparison and parametric studies, they concluded that further research is needed into the rational inclusion of curvature effects in the ultimate strength formulation. Moon *et al*. (2009) presents the results of the theoretical and finite element analyses of the lateral-torsional buckling of I-girders with corrugated webs under uniform bending.

Because of their high bending and shear stiffness and relatively low fabrication cost, corrugated panels have a wide range of applications, e.g., internal bulkheads in the cargo region of bulk carriers and tankers, and load carrying members in living quarters in offshore structures. It has been recognised that the buckling failure modes of a corrugated panel can be categorised at three levels: (1) local face/web plate buckling, (2) column buckling of unit corrugation, and (3) entire corrugation buckling. Sun & Spencer (2005) provided the technical background for ABS recommendations for the

strength assessment of each failure mode by including the model uncertainty obtained through a comparison with extensive laboratory tests and FEA results.

Kippenes et al. (2007) developed a semi-analytical method for assessing the ultimate capacity of corrugated panels and showed good agreement between the predicted strengths and the FEA results. They also showed that the local deflection of the corrugation due to lateral pressure has little effect on overall capacity, whereas the end restraint effect of the surrounding structure is of great importance to the initial buckling and progressive failure mechanism. Alinia & Mossavi (2009) studied local buckling of longitudinally stiffened web plates under interactive shear and bending. Brubak & Hellesland (2008) presented strength criteria in semi-analytical, large deflection analysis of stiffened panels under local and global bending.

5.3   *Composite and Sandwich Panels*

As described in Section 2.3, delamination is usually the most critical type of imperfection or damage that composite and sandwich structures experience under compressive loading. Goldfeld (2009) presented a formulation in linear bifurcation analysis of laminated shells.

To understand the effect of delamination on the compressive behaviour of laminated composite materials, compression tests have been conducted on various composite and sandwich panels. Short *et al.* (2001) tested glass-fibre-reinforced plastic (GRP) test specimens containing artificial delaminations of various size and depths. Good agreement between the FE predictions and experimental measurements were found for the whole range of delamination geometries tested. FE and simple closed-form models were also developed for delaminated panels with isotropic properties. This enabled a study of the effect of delamination geometry on compressive failure without the complicating effects of orthotropic material properties. A buckling mode map, allowing the buckling mode to be predicted for any combination of delamination size and through thickness position was developed and is shown in Figure 20. The results of this study can be used to derive a graph of non-dimensional failure load versus non-dimensional failure stress, as shown in Figure 21.
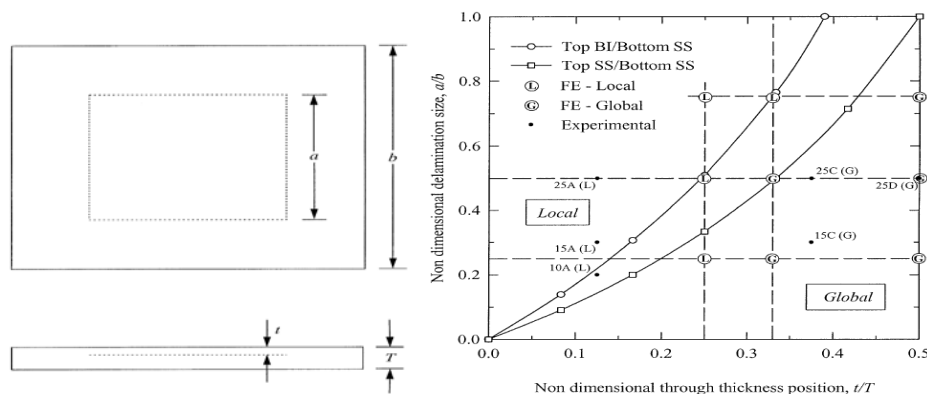

Figure 20: Buckling-driven delamination mode map for various delamination sizes and through thickness positions, from Short *et al.* (2001)
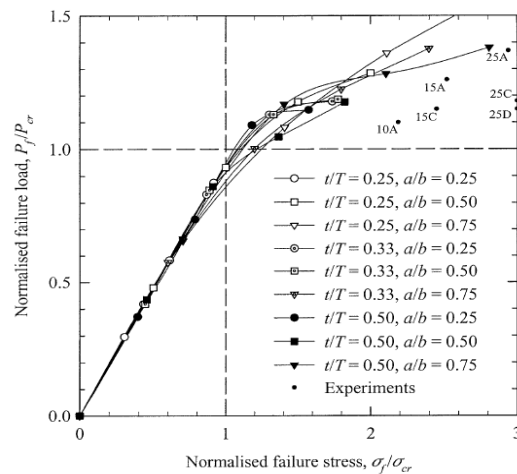
Figure 21: Normalised compressive failure stress versus normalised failure load, from
Short *et al*. (2001)

Nilsson *et al*. (2001) conducted a numerical and experimental investigation of buckling
driven delamination and growth of the debonded area. Carbon fibre/epoxy panels with
implanted artificial delamination were tested. The average maximum load for the
delaminated panels was approximately 10% lower than the maximum load for the
undelaminated panels. The maximum load was found to be almost unaffected by
delamination depth. Both the tests and the numerical analyses showed a strong
interaction between delamination growth and global buckling load for all delamination
depths. Delamination growth initiated at or slightly below global buckling in all
specimens. In all of the tests, the delaminations grew more or less symmetrically and
perpendicular to the direction of the load. At the global buckling load, crack growth
parameters increased drastically with the applied load. The authors thus concluded that
structures which may contain delaminations should not be allowed to buckle globally.

Short *et al*. (2002) studied the effect of curvature on delamination in laminates. Tests
on flat and curved delaminated GFRP specimens showed the failure load for flat
specimens to be the same as, or higher than, that for curved specimens, depending on
the size and through thickness position of the delamination. Tests on the curved
laminates demonstrated an asymmetry of failure load with the through thickness
position of the delamination. A delamination near the convex side gave a greater
strength reduction than a delamination near the concave side, where both delaminations
were at the same depth.

Much work has addressed the problem of modelling the onset of
delamination/debonding in composite structures and the consequent propagation.
Davies *et al*. (2006) developed a new interface element that has a monotonic
(exponential) force/displacement law. This enabled them to use elements considerably
larger than the small process zone. The simple benchmarks used show that the interface
element initiates and propagates correctly, without needing an initial flaw.
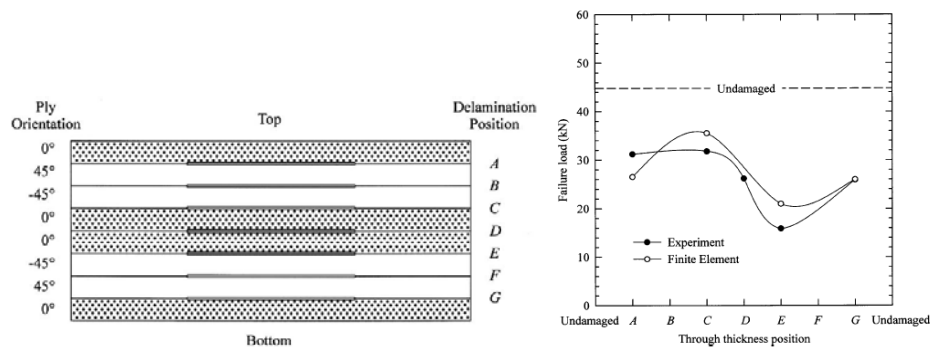
Figure 22: Comparison of experimental and FE predicted failure loads for specimens containing two delaminations in the C and x positions, from Wang *et al*. (2005)

Multiple delaminations cause greater strength reductions than single delaminations. As damage resulting from impacts may consist of multiple delaminations, it is of interest to understand the mechanism of strength reduction for such laminates. Wang *et al*. (2005) studied flat glass fibre reinforced plastic specimens containing a single or two embedded delaminations. They found that that the maximum reduction in strength for multiple delaminations occurs when the delaminations split the laminate into sub-laminates of similar thickness, as shown in Figure 22. Shufrin *et al*. (2008) presented a semi-analytical approach to determine the buckling strength of generally supported laminated plates under a general combination of inplane shear, compression, and tensile actions.

5.4   *Tubular Members and Joints*

The behaviour and strength of tubular members have been investigated by various researchers, with particular attention on strengthening through in-filling of concrete in the thin-walled steel tubes. The behaviour of tubular members under different loading conditions have been reported by Han *et al*. (2006, 2007), Bambach *et al*. (2008) and Yu *et al*. (2008). Graham (2007) applied the nonlinear finite element method to the prediction of the collapse strength of ring-stiffened cylinders under hydrostatic loading.

As a result of active research and developments in tubular joints, as highlighted by Wardenier & Choo (2006) and Vegte *et al*. (2008b), new recommendations in API RP 2A (Pecknold *et al*. 2007) and IIW (IIW 2008, Wardenier *et al*. 2008a, Zhao *et al*. 2008) have been proposed. The development of the AISC (Packer *et al*. 2008) and CIDECT (Wardenier *et al*. 2008b) design guides have benefited significantly from the systematic research conducted by the international members of IIW XV-E, including the papers by Vegte *et al*. (2007a, b, 2008a, b).

For overlapped joints, the strength enhancement over simple joints has been investigated by Wardenier (2007) and Qian *et al*. (2007).   Gho & Yang (2008) reported the study on completely overlapped joints, which may be useful for selected

applications.

Thick-walled joints are increasing used in Jack-up platforms and cast steel nodes in composite bridges in Germany and Switzerland to minimise environmental loadings and enhance fatigue lives. Design recommendations have benefited from recent results published by researchers in National University of Singapore (Choo *et al*. 2006, Qian *et al*., 2007, 2008) and Karlsruhe University (Puthli 2008).

The behaviour of grouted joints subjected to in-plane bending moment has been investigated and reported by Choo *et al*. (2007a, b). Significant joint strength enhancement and stress reduction around the brace-chord intersection have been observed.

In certain applications, high strength steel is increasingly used. The Eurocode EN 1993-1-12.2007 (2007) considered high strength steel up to 700 MPa, and Fleischer *et al*. (2008) reported results on the static strength of such joints.

5.5 *Effect of Dynamic/Impact Pressure Actions*

The structural components of ships and offshore structures are likely to be subjected to many types of dynamic or impact actions. Some of these actions arise during accidents, such as explosions, grounding and collisions. There are also other dynamic actions acting on the service condition of marine structures, such as those arising from sloshing, slamming or green water, and they are likely to cause damage to structural components.

Jones (2006) reviewed some of the recent developments in the dynamic inelastic behaviour of structures. During a high velocity impact of a structure on a nearly incompressible fluid, impact pressure actions with high-pressure peaks occur. Shipbuilding companies have carried out several studies to model slamming using FEM software with added mass techniques to represent fluid effects. In the added mass method, the inertia effects of the fluid are not taken into account and are only valid when the deadrise angle is small.

Aquelet *et al*. (2006) presented a prediction of the local high-pressure load on a rigid wedge impacting a free surface. Paik & Shin (2006) developed closed-form design formulations for predicting the structural damage of ship stiffened panels under impact pressure loads such as sloshing, slamming and green water. Existing formulations of permanent panel deflection developed under quasi-static pressure loading condition in the literature were expanded to account for the dynamic effects that are associated with the impact pressure actions. The validity of the proposed method was confirmed by comparison with the present LS-DYNA numerical simulations for ship stiffened panels and experimental results where available.

Qin & Batra (2008) developed a hydroelastic model based on a {3,2}-order sandwich composite panel theory and Wagner's water impact theory for investigating the fluid-

structure interaction in the slamming process. The sandwich panel theory incorporated the transverse shear and the transverse normal deformations of the core, whereas the face sheets were modelled with the Kirchhoff plate theory. The structural model was validated with the general-purpose FE code ABAQUS. The hydrodynamic model, based on Wagner's theory, considered the hull's elastic deformations. A numerical procedure to solve the nonlinear system of governing equations, from which both the fluid and the structure's deformations could be simultaneously computed, was developed and verified. The hydroelastic effects on the hull's deformations and the unsteady slamming load were delineated. This work advances the state of the art of analysing hydroelastic deformations of composite hulls subjected to slamming impact.

Rabczuk *et al*. (2007) developed a simplified method for explaining the effects of fluid-structure interaction in sandwich structures that are subjected to dynamic underwater loads. The method provides quite accurate predictions of the impulse on submerged structures for a large range of loads and core yield strengths. It is a simple model with two lumped masses, one of which is subjected to an incident wave and the other to represent the core. This enables phenomena such as the buckling of the components of the core to be taken into account and is simple enough to be used as a design tool. Comparisons with calculations of complete fluid-structure models in the study showed very good agreement.

Thin walled structures subjected to pulse compressive loading can lose stability when the critical amplitude for pulse loading is achieved. Kubiak (2007) proposed a new criterion for critical amplitude of pulse loading leading to the buckling of structures. The local, global and interactive dynamic buckling was analysed. The proposed criterion is a modification of the quasi-bifurcation criterion formulated by Kleiber *et al*. (1987). The results obtained using the proposed criterion were compared with other well-known criteria, the Volmir (V) and Budiansky-Hutchinson (B-H) criteria. Rushton *et al*. (2008) studies the failure mechanism of steel pipes under a very high rate of loading arising from the detonation of a high explosive.

5.6   *Effect of Fabrication-induced Initial Imperfections*

Welding can induce the following six types of initial imperfections in metal structures.

- Initial distortion of the plating between the stiffeners, w_{opl}
- Column-type initial distortion of the stiffener, w_{oc}
- Sideways initial distortion of the stiffener, w_{os}
- Residual stress in the plating between the stiffeners, σ_{rc}^{p} (compressive) or σ_{rt}^{p} (tensile)
- Residual stress in the stiffener web, σ_{rc}^{s} (compressive) or σ_{rt}^{s} (tensile)
- Softening in the HAZ

For welded steel structures, the first five types of initial imperfections are of primary concern, although the softening phenomenon in the HAZ is usually insignificant and

thus ignored in terms of ultimate strength performance. However, the effect of the softened zone is significant for aluminium structures fabricated by fusion welding, in addition to the first five types of initial imperfections. The properties in the softened zone are often formulated in association with the reduced yield strength and breadth of this zone. These weld-induced initial imperfections reduce the ultimate strength performance of structures in a sensitive manner, and must be dealt with as important parameters of influence in structural design and strength assessment.

For steel stiffened plate structures fabricated via fusion welding, the following has often been utilised in the shipbuilding industry as a representative value of fabrication-induced initial imperfections.

$$w_{opl} = \begin{cases} 0.025\beta^2 & \text{for the slight level} \\ 0.1\beta^2 & \text{for the average level} \\ 0.3\beta^2 & \text{for the severe level} \end{cases} , \quad \sigma_{rcx}^p = \begin{cases} -0.05\sigma_Y & \text{for the slight level} \\ -0.15\sigma_Y & \text{for the average level} \\ -0.3\sigma_Y & \text{for the severe level} \end{cases} ,$$

$$w_{oc} = w_{os} = 0.0015a ,$$

where $\beta = (b/t)\sqrt{\sigma_Y/E}$, b = plate breadth between stiffeners, t = plate thickness, σ_Y = material yield strength, E = Young's modulus, a = panel length. It is interesting to note that the average level of w_{opl} for steel plate elements is sometimes defined by classification societies as $w_{opl} = b/200$.

Paik *et al.* (2006) suggested the following initial imperfections for aluminium stiffened plate structures fabricated by fusion welding, while it was found that friction stir welding can mitigate the initial imperfections to some extent (Paik 2009).

$$w_{opl} = \begin{cases} 0.018\beta^2 t & \text{for the slight level} \\ 0.096\beta^2 t & \text{for the average level} \\ 0.252\beta^2 t & \text{for the severe level} \end{cases} , \quad w_{oc} = \begin{cases} 0.00016a & \text{for the slight level} \\ 0.0018a & \text{for the average level} \\ 0.0056a & \text{for the severe level} \end{cases} ,$$

$$w_{os} = \begin{cases} 0.00019a & \text{for the slight level} \\ 0.001a & \text{for the average level} \\ 0.0024a & \text{for the severe level} \end{cases} , \quad \sigma_{rcx} = \begin{cases} -0.110\sigma_{Yp} & \text{for the slight level} \\ -0.161\sigma_{Yp} & \text{for the average level} \\ -0.216\sigma_{Yp} & \text{for the severe level} \end{cases} ,$$

$$\frac{\sigma_{YHAZ}}{\sigma_Y} = \begin{cases} 0.906 & \text{for the slight level} \\ 0.777 & \text{for the average level} \\ 0.437 & \text{for the severe level} \end{cases} \quad b_{HAZ} = b_t = \begin{cases} 11.3\,\text{mm} & \text{for the slight level} \\ 23.1\,\text{mm} & \text{for the average level} \\ 29.9\,\text{mm} & \text{for the severe level} \end{cases} .$$
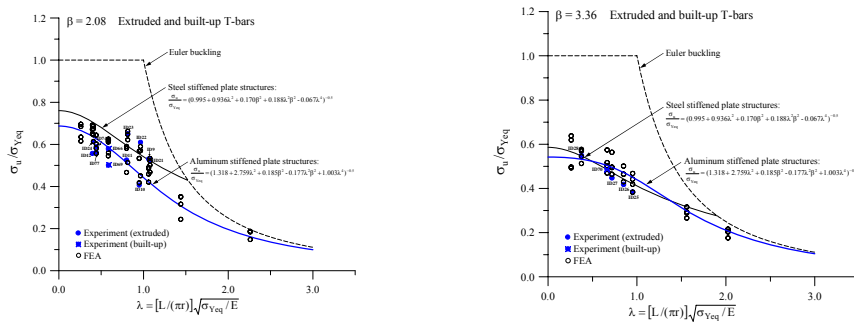
Figure 23: Accuracy of the closed-form empirical ultimate strength formula for aluminium stiffened plate structures with flat bars, from Paik *et al*. (2008a)
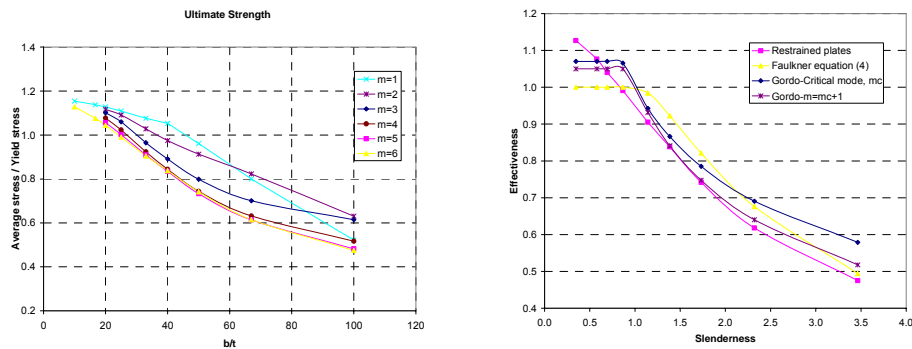
Figure 24: Ultimate strength of plates made of mild steel and comparison with other formulas, from Gordo (2008) (m=buckling half wave number, 'slenderness'=$\frac{b}{t}\sqrt{\frac{\sigma_Y}{E}}$, b=plate breadth, t=plate thickness, σ_Y=yield stress, E=elastic modulus)

The effects of initial imperfections may be much more dramatic in compression, because the structure may become weaker and the degradation of ultimate strength due to premature buckling may reach high values. Masaoka & Mansour (2008) presented simple design equations to account for the effect of imperfections on compressive strength of stiffened plates. Mukherjee & Yao (2006) investigated the influence of residual stress distribution on the collapse behaviour and strength of stiffened panels by FEA considering experimentally measured residual stress distributions in rolled and built-up tee-bar stiffeners. The residual stress in the flange of the rolled tee-bar section is compressive, whereas that of built-up section tensile. This results in lower compressive ultimate strength of the former section.

The effects of residual stresses and imperfections may be reduced by introducing alternative joining processes. Murphy *et al*. (2007) characterised the effects of friction stir welding assembly methods on stiffened panel static strength performance. They characterised the degradation of strength due to the use of advanced joint techniques and concluded that collapse behaviour is less sensitive to these processes than initial

panel buckling behaviour.

The effect of fabrication-induced initial imperfections on aluminium structures was analysed in a series of experiments performed by Paik *et al*. (2008a), and the collapse characteristics of aluminium stiffened plate structures used for marine applications was investigated (Paik 2007a). The tests results were compared with those of FE models, taking into account initial distortions as shown in Figure 23 (Paik 2007a, b, Paik *et al*. 2008a). Fabrication-related initial imperfections were considered to significantly affect the ultimate limit state behaviour, and thus it is of vital importance to identify the features of initial imperfections prior to computations. The study led to the development of a statistical database of fabrication related initial imperfections on welded aluminium stiffened plate structures (Paik *et al*. 2006, Paik 2007b). In addition, the residual stresses were measured in the plate and stiffener and compared with traditional models. The initial imperfections for welded aluminium structures were classified in three levels where the ratio wopl/$\beta 2t$ was 0.018, 0.096 and 0.252 for slight, average and severe levels of plating imperfections. Similar classifications were introduced for different types of stiffener imperfections that may serve as reference for the FE modelling of aluminium stiffened panels. The study also quantified a degradation in the mechanical properties of the aluminium in the HAZ of the order of 25% for the yield stress. The compressive residual stresses varied from 8% for slight level to 22% for severe level imperfection. Specific formulas were proposed for aluminium structures, as presented in the Figure 24.

Gordo (2008) investigated the effect of the shape and amplitude of distortions in restrained unstiffened plates under longitudinal compression, as shown in Figure 24. Restrained plates do not allow the linear displacement of the lateral edges but they can rotate freely. Gordo concluded that the shape is more important than the amplitude of imperfections for this type of plate. The minimum ultimate strength was obtained for a wave length of the imperfections equal to the plate's width. Design formulas were proposed for restrained plates with different modes of imperfection.

Khedmati & Rastani (2006) analysed three different stiffener-to-plate welding procedures, i.e. continuous, chain intermittent and staggered intermittent fillet welding using ADINA, and evaluated the impact of such procedures on the ultimate strength associated with the different failure mechanisms.

The continuity of ship plating allows different patterns of initial welding distortion in adjacent plates. Luis *et al*. (2006) showed that using a single plate can be conservative or unconservative, depending on the plate slenderness and shape of initial deflections. They concluded that for design purposes it would generally be enough to consider assemblies of three adjacent plates, as the results for five plate assemblies were not very different.

5.7   Effect of In-service Degradation

In-service degradation of the behaviour of structural components mainly results from corrosion, denting and cracking, and affects the static and fatigue strength of the components (Paik & Melchers 2008).

5.7.1   Corroded Plates

Teixeira & Guedes Soares (2008) investigated the collapse strength of plates with nonuniform corrosion by nonlinear FEA, where the corrosion pattern was represented by random fields to simulate the present practice of thickness measurement patterns. Paik *et al*. (2004) concentrated on the effect of pit corrosion on the ultimate shear strength of plate elements. A design formula was derived from the regression analysis of FE results that may be applied in the reliability assessment of pit corroded plates. Nakai *et al*. (2006) performed nonlinear FEA of plates with various distributions of pitting corrosion of a circular cone shape and discussed their effects on the ultimate strength of the plates under inplane compression and bending.

Ok *et al*. (2007a, b) studied more than 200 plates with corrosion in different locations to assess the effects of localised pitting corrosion on the ultimate strength of unstiffened plates. The length, breadth and depth of pit corrosion had weakening effects on the ultimate strength of the plates. The most deteriorating effect on strength was found to occur when corrosion spread transversely on both edges of the plate. Formulae to predict the ultimate strength of locally corroded plates under uniaxial in-plane compression were proposed based on the artificial neural network method. Guo *et al*. (2008) presented a semi-probabilistic approach to asses the time-varying ultimate strength of aging tanker's deck plates considering corrosion wastage.

Smith & MacKay (2005) presented an extension to Kendrick's method to evaluate the overall elastoplastic response and collapse pressure of ring-stiffened cylinders that accounted for non-uniform properties in the circumferential direction. This was shown to be an efficient way of estimating the effect of localised thinning on the overall collapse pressure.

5.7.2   Dented Plates

In-service damages are also accumulated throughout a ship's life due to overloading or accidents, and may change or even 'shakedown' the production related imperfections. Such typical damages are those in the inner bottom plating due to heavy grab operations and in the shell plating due to slamming or ice pressure. These damages are characterised by one sided residual deflections over adjacent panels accompanied by residual stresses. Nikolov (2007, 2008) calculated the residual stress pattern resulting from the damage of the plating and evaluated the ultimate strength of such plates under longitudinal or transverse loading. He concluded that the methods used in the IACS Common Rules for Bulk Carriers, generally overestimate the ultimate strength, and that the residual stresses due to damage have a great influence on the ultimate strength of damage plating. He also found that anti-symmetric damage of adjacent plates is the

most unfavourable shape of damage in terms of the ultimate strength. The amplitude of local damage is not as important to the plate's strength.

Witkowska & Guedes Soares (2008) conducted a similar study and concluded that stiffened panels present quite good performance while subjected to the local damage, but depending on geometrical characteristics a problem of stiffener deformations may occur, lowering the ultimate strength. The position of the dimple imperfection on the panel is an important factor, reducing the collapse strength and inducing a more violent collapse (Guedes Soares 2007).

Paik (2005) concentrated on the effect of indentation on the ultimate shear strength of plate elements. He derived a design formula from the regression analysis of FE results which can be applied on the establishment of the damage tolerance design of steel plated structures with local denting. Gavrylenko (2007) presented results from a joint theoretical and experimental investigation of the buckling of cylindrical shells containing localised dent damage, based on a new numerical method for the evaluation of the load carrying capacity of shells.

5.7.3   Cracked plates

Paik and his colleagues concentrated on the effect of cracking on the strength of plate elements (Paik *et al.* 2005b, Paik 2008c) and stiffened panels (Paik & Kumar 2006) in tension or compression. Theoretical models for predicting the ultimate strength of the cracked plates and stiffened panels under axial compression or tension were presented based on FE analysis. A design formula was derived from the regression analysis of FE results that can be applied in the reliability assessment of cracked plates. Alinia *et al.* (2007) investigated the effect of relative crack length on the buckling capacity of shear panels, developing a procedure for the modelling and analysis of shear panels containing central or edge cracks using the FEM.

5.8   Effects of Accident-induced Damages

5.8.1   Numerical and Analytical Approaches

Zhang & Suzuki (2006) studied the effect of several parameters on the crashworthiness of a single-hull bottom structure due to raking, using LS-DYNA code. Balden & Nurick (2005) described the numerical simulation results of experimental studies that had been conducted in 1991. The experiment investigated deformation and post-failure response of a plate subjected to blast loading. The FE code ABAQUS was used to simulate the structural response of the respective blast structures, whereas the hydro-dynamic code AUTODYN was used to characterise the localised blast pressure, time and spatial history. The simulations showed satisfactory correlation with the experiments for energy input, large inelastic deformations and post-failure motion. Alsos & Amdahl (2007) presented integrated local and global grounding analyses of ships considering the effects of tidal changes. Hong & Amdahl (2008a,b) studies a

theoretical model for the crushing of web girders under localized in-plane loads arising from collision and grounding.

Park & Cho (2006) performed a numerical study and comparison with experimental data. Practical yet accurate formulae were proposed to predict the structural damage of rectangular unstiffened and stiffened plates under explosion loads. Regression analyses of the parametric study results were performed to derive design formulae, which produced linear relationships between the residual damages of plates and an impact parameter. These formulae were compared with existing formulae and were found to be more accurate. Yamada & Pedersen (2008) carried out a benchmark study of procedures for analysis of axial crushing of bulbous bows. Methods based on intersection unit elements such as L-, T- and X-type elements as well as methods based on plate unit elements were used in the analysis by a comparison with experimental results obtained from large-scale bulbous bow test models.
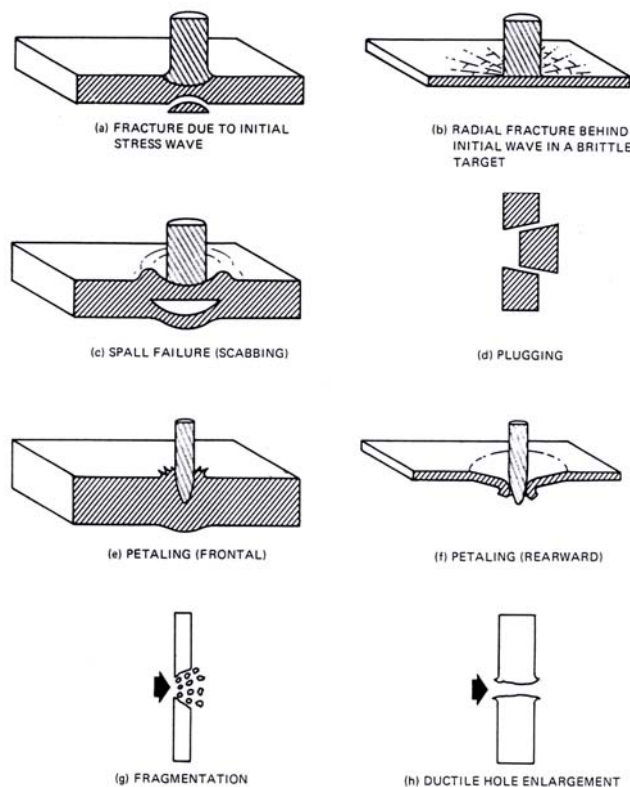

Figure 25: The mechanisms of perforation by ballistic impacts, from Backman & Goldsmith (1978)

Deformation and perforation of ship structures under dropped objects or ballistic impacts are of interest. The plate perforation involves a very complex mechanical

issues depending on material and geometric properties of the target and the characteristics of the striker including impact velocity and its shape, size, mass, etc. The ballistic perforation on plates include fracture due to initial stress, wave, fracture in the radial direction, spalling, scabbing, plugging, frontal or rearward petaling or fragmentation in the case of brittle targets or hole enlargement in the case of ductile targets as shown in Figure 25 (Backman & Goldsmith 1978). Paik & Won (2007) studied the deformation and perforation of ship structures under ballistic impacts.

Zheng *et al*. (2007) studied the damage of side structures due to ship-ship collisions. Another interesting study concerning structural response to underwater explosion was carried out by Rajendran *et al*. (2006). The design of ship plates against underwater explosion is a mandatory requirement of warship construction. Although non-contact underwater explosions of small intensity induce dynamic stresses that die with time, moderate intensity causes permanent or inelastic deformation, and severe intensity leads to rupture. The intensity of an explosion increases with the explosive charge quantity, and decreases with standoff. Therefore, a range of combinations of explosive charge quantity and standoff distance may deliver the same amount of shock energy to the plate. However, the energy-coupling factor between a shock wave and the plate is the maximum only for a specific configuration of explosion. This leads to the so-called effective shock factor, which forms the basis for assessing elastic–plastic behaviour in the plating. Permanent plate deformation was predicted by analytical and empirical methods in this study. Contact explosion damage was predicted as a function of target material parameters and explosive parameters with an energy-coupling factor. Design guidelines were determined for ship plates that are subjected to underwater explosion.

5.8.2   *Experimental Investigation*

Though experimental approach is the most expensive one, it is the only way to check the accuracy of proposed analytical and numerical solutions. Schleyer & Langdon (2005) presented the results of experimental, analytical and numerical studies on the responses of ¼ scale stainless steel blast wall panels and connection systems. The panel design was based on a deep trough trapezoidal profile with welded angle connections at the top and bottom and free sides. The loading applied to the panel was a triangular pulse pressure representative of a gas explosion overpressure. The aim was to investigate the influence of the connection detail on the overall performance of the panel/connection system under pulse pressure loading and to develop appropriate analytical and numerical models for correlation with the test results. Part I of the study reported on the experimental investigations, and the analytical modelling considerations were examined in Part II. FEA, with ABAQUS, was used to simulate the blast wall panel behaviour and was discussed in Part III (Schleyer *et al*. 2006, Schleyer & Langdon 2006). Large permanent plastic deformations were produced in the panels without rupture, and localised buckling developed at the centre of the corrugations. This work highlights the importance of correctly modelling the support details and the variation in strength with blast direction (the blast wall panels being stronger in the design direction). As a result of modelling the supports and including

membrane action, the modelling approaches predict a design capacity that is 39% higher than the current design guidance predicts.

Schleyer *et al*. (2007) published the results from an experimental investigation of blast wall panels under shock pressure loading, and Schleyer and his colleagues (Schleyer *et al*. 2006, Schleyer & Langdon (2006) studied nonlinear FEM computations. A series of field tests was carried out on ¼ scale stainless-steel blast panels. The panel design was based on a deep trough trapezoidal profile, with welded angle connections at the top and bottom and free sides. The loading applied to the test panel was a shocked pressure pulse representative of the positive phase of the air blast loading that arises from a high-explosive charge. The aim of this work was (1) to show the effect of panel response on the reflected blast loading and (2) to investigate the influence of the connection detail on the overall performance of the panel/connection system under shocked pressure loading. The data were also used to develop appropriate analytical and numerical models for correlation with the test results. Large permanent plastic deformations were produced in the panel without rupture. The work showed that the connection detail can significantly influence the response and blast resistance of the panel to extreme pressure loading. The results highlighted the conservative nature of the design guidance for blast wall design, which limits deflections to 1/40th of the height of the blast wall. This in turn should lead to a more economical design. The results also showed that further test work is required to confirm whether the panel response has any appreciable effect on the pressure loading.

6.   SYSTEM STRUCTURES

6.1   Ship-shaped Structures

Ship-shaped structures have been widely analysed for design and research due to the development of several software packages able to deal with complex structural systems. Different methods have been compared during the last years, from computationally heavy FEMs to fast approximate methods.

Moan (2004) demonstrated the many opportunities that exist for developing new structures and operational procedures when rational methods are used to handle new technology, as well as the corresponding needs for research and development. The study calls for particular attention to be given to current trends and expected future changes regarding the design and fabrication of marine structures. Amlashi & Moan (2008) presented nonlinear finite element modelling and analysis of the ultimate strength of a bulk carrier hull girder under alternate hold loading condition.

FPSOs have been widely used for the development of offshore oil and gas fields because of their many attractive features. They are mostly ship shaped, and either converted from existing tankers or purpose built. The hull structural scantling design of tankers may be generally applicable to FPSOs. Wang *et al*. (2008) considered that the

determination of ultimate hull girder strength by complete non-linear analysis could be complicated and time consuming, and thus introduced different methodologies for the assessment of hull girder ultimate strength. They presented numerical calculations of that ultimate strength based on six different FPSO designs, analysing their results in terms of differences, and drew conclusions based on reliable methodologies for the assessment of hull girder ultimate strength in FPSOs.

Ozguc *et al*. (2006a,b) applied progressive collapse analysis to analyse the hull girder ultimate strength of a typical bulk carrier under combined bending moment. An interaction between vertical and horizontal bending was presented and compared with previous results. It was confirmed that interaction is not symmetric due to the difference between the hogging and sagging ultimate bending moment.

The same type of approach was used by Chen & Guedes Soares (2008) to estimate the ultimate strength collapse of ships made of composite materials. The load-average strain curve derived from a progressive failure nonlinear FEA was used to represent the behaviour of each stiffened composite panel that formed a hull cross section.

Using a software system that integrated nonlinear FEA, the idealised structural unit method, the simplified method and the analytical method, Qi & Cui (2006a) conducted a comparative study of the ultimate hull girder strength of a 300,000dwt double hull tanker, and also compared the results with the single step procedure of CSR for double hull tankers (JTP CSR).

Following the recent research into the loss of the Capesize bulk carrier M.V. Derbyshire, Paik *et al*. (20089) investigated the possibility of sinking being initiated by the failure of hull structures rather than by other loss scenarios such as hatch cover failure subsequent to water ingress into the cargo holds. They concluded that the M.V. Derbyshire could have sunk due to hull girder collapse with or even without unintended water ingress into cargo holds. In other studies, they compared the ultimate limit state performance of an AFRAMAX-class hypothetical double hull oil tanker structure designed using the IACS CSR method with the same-class/type tanker structure designed using the IACS pre-CSR method (Paik 2007c, Paik *et al*. 2008f). Comparison of the results with FEA and ALPS/ULSAP was also presented.

The reserve strength of damaged ships against bending moments has attracted the attention of several researchers, who have dealt with different type of ships. Huilong *et al*. (2008) used the Smith method to analyse damaged warships. They investigated the effect of parameters such as the size of holes caused by weapons, the yielding stress of the material and the thickness of the plating. Sun & Wang (2005a,b) systematised the procedure for evaluating the progressive collapse of a hull girder, presenting a formulation for the stress strain curves of the stiffened elements.

Gordo & Guedes Soares (2004, 2007, 2008c) presented experimental results for box girders under pure bending. They presented the moment curvature curves allowing for

the analysis of elastic-plastic behaviour until collapse, the evaluation of the ultimate bending moment and post collapse behaviour. The residual stress relief during loading and unloading path was also analysed, and the results are compared with those of a test on a similar box girder made of very high tensile steel. Also presented was a method to estimate the residual stress level of the structure, taking into consideration stress relief during initial cycling loading.

6.2   *Other Marine Structures*

This section focuses on off-shore wind turbines, specifically the ultimate strength of the rotor blades. Few publications on the FE modelling, structural analysis and ultimate strength of wind turbine blades are available in the literature. Most published research has used quite coarse mesh FE analysis of the entire wind turbine blade.

Kong *et al*. (2005) predict strains, global deflections and Eigen frequencies and compare their predictions with experimental results. They find that linear analysis give good predictions, which suggests that for design purposes the examined non-linear effects are not significant for this particular design, where the strain level is also low (less than 1000 $\mu\varepsilon$).

Jensen *et al*. (2005) reported a comparison between FE analysis and full-scale testing. In this study, the blade was loaded to catastrophic failure and strong non-linearities were found even at lower loads. The Brazier effect dominated the inner part of the blade. The relative deflection of the cap was measured and compared with the results of linear and non-linear FE analysis: see Figure 26. It was thus recommended that non-linear global FEA be used in the design process. Measurements supported by FE-results showed that debonding of the outer skin was the initial failure mechanism followed by delamination, which led to collapse. When the skin debond reached a certain size, the buckling strength of the load carrying laminate became critical and final collapse occurred.

Branner *et al*. (2008) tested the load carrying box girder for a similar blade and studied the effect of sandwich core properties on ultimate strength of the box girder. They compared the experimental transverse (vertical or 90º) strains for both faces of the sandwich web with both linear and non-linear FEA, see Figure 27. The strains were measured on the upper part of the web towards the leading edge, where the failure was observed. The longitudinal strains caused by bending of the box girder led to associated strains in the transverse direction due to the Poisson's ratio effect. The transverse strains were positive (tension) in the shear webs of the upper part of the box girder where the bending caused compression and the transverse strains were negative (compression) in the lower part.

Initially, the Poisson's ratio results in a linear increasing transverse strain with load, as shown in Figure 27. However, as the load increases, the strains become non-linear with respect to applied load and the graphs deflect towards compressive strains. The

difference between the linear and the non-linear results is, at least in part, caused by the Brazier effect. The crushing pressure flattens the cross-section and introduces compressive strains into the shear webs. However, this crushing pressure varies with the square of the applied load, resulting in the noted deviation from linear responses. The flattening of the cross-section will probably initiate buckling, which then accelerates the failure. Other non-linear phenomena, such as changes in geometry and loading configuration (which follows the geometry in the non-linear analysis), will also contribute to the observed non-linearities. For further discussion of this, see Jensen (2008).
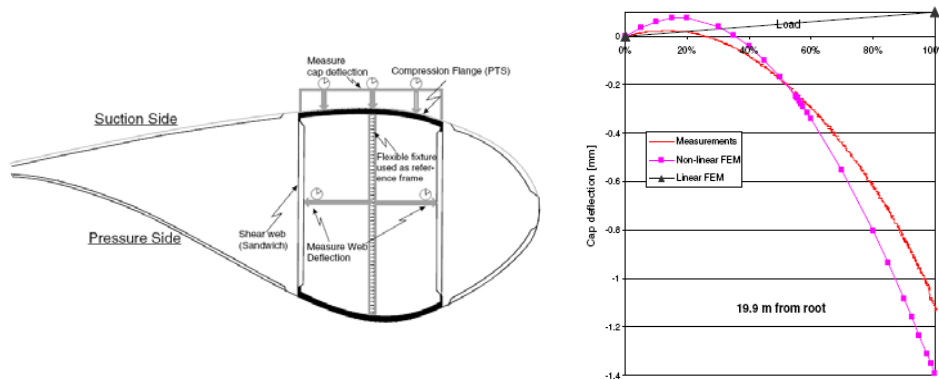
Figure 26: Relative deflection of the cap measured and compared with the results of linear and non-linear FE analysis, from Jensen *et al*. (2005)
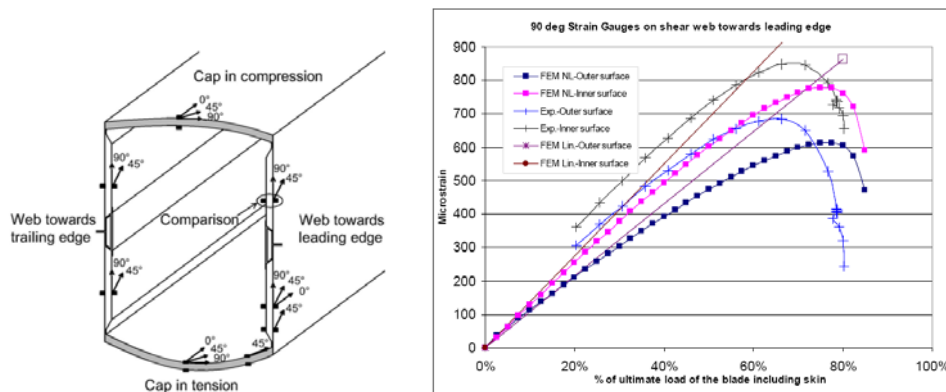
Figure 27: Comparison of FE-results and measurements for back to back strain gauges on upper web part, from Branner *et al*. (2008)

Branner *et al*. (2008) also found that the corner stiffness greatly influence the overall non-linear behaviour of the box girder as the webs take a much greater part in the overall deformation of the cross section when the corners are stiff. From the stiff corner models it can be seen that the core density has somewhat of an influence on the ultimate strength, whereas the soft corner models show that the core density has almost

no influence on the ultimate strength. Branner (2006) earlier conducted an experimental study of the ultimate strength of a box girder, in which the shear webs initiated failure.

Overgaard & Lund (2005) conducted another blade collapse study, performing geometrically nonlinear and linear pre-buckling analyses to predict the failure of the blade due to local buckling on the suction side of the airfoil. The imperfection sensitivity of the blade was evaluated by imposing the strain gauge measurement for the full-scale experiment as an imperfection pattern. Figure 28 displays the response of the obtained imperfection amplitude where the 23% amplitude model fits the best of the evaluated models. It can be seen that the imposed imperfection pattern is directly proportional to the longitudinal strain measured by the strain gauges. An important discovery here is that the buckling shape is unaffected by the presence of imperfections, but the local strain at the maximum geometric imperfection amplitude is linearly dependent on the imperfection amplitude. The epic centre of the buckling shape mode is at the core and flange material transition, but the structural collapse is at the geometric imperfection amplitude.
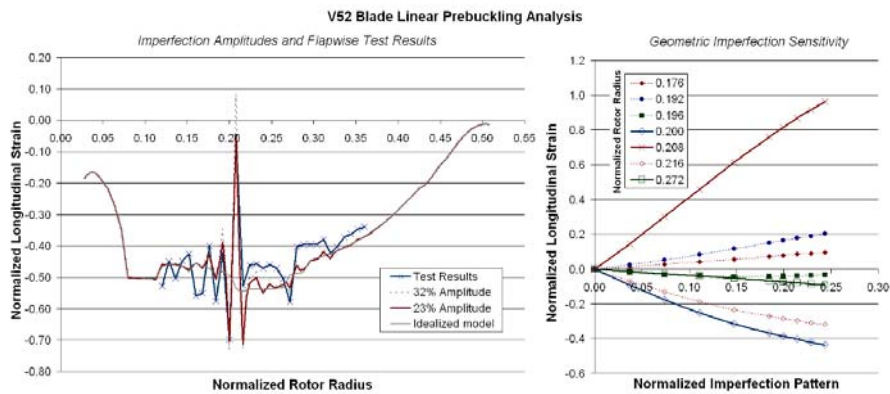
Figure 28: Response of the obtained imperfection amplitude compared with test results, from Overgaard & Lund (2005)

Kühlmeier (2007) also worked with the buckling of wind turbine blades in his Ph.D. thesis. Kuhlmeier *et al*. (2005) earlier built a 9m long airfoil blade section, designed to fail in buckling, and tested it destructively in a four-point bending configuration. They found that a linear buckling analysis will over-predict the ultimate strength of the blade, with the strength of that over-prediction depending on the size of the imperfections present in the blade and the sensitivity of the structure to the imperfections. They suggested that a bifurcation buckling analysis with a knockdown factor applied on the buckling load would give a good estimate of the blade's ultimate strength. The value of the knockdown factor would depend on the size of the imperfections as well as the imperfection sensitivity. For the 9m blade section, a factor of 1.25 could be used to assess the ultimate strength of the blade.

Berggreen *et al*. (2007) studied the advantages of applying a sandwich construction as

opposed to traditional single skin composites in the flanges of a load carrying box girder for a very large 180 m wind turbine rotor. Their results indicated that buckling is the governing criterion for the single skin design. Introducing a sandwich construction in the flange was found to result in a more globally flexible structure, making tower clearance the critical criterion. A significant weight reduction by more than 20% and an increased buckling capacity was obtained with the sandwich construction as opposed to traditional single skin composites.

Overgaard & Lund (2007a,b) compared the results from a full-scale blade test until failure with FE analysis using a mixed-mode bilinear cohesive element for numerical simulation. The mixed-mode cohesive element formulation was an indirect use of linear elastic fracture mechanics in a damage mechanics framework. Constitutive softening models are associated with severe solution difficulties, and therefore an efficient and robust solution strategy for dealing with large three-dimensional structures was needed and implemented. The studies showed that it is possible to predict the structural behaviour of a wind turbine blade based on nonlinear fracture mechanics in a geometrically nonlinear framework: i.e. to account for buckling and delamination interaction, as shown in Figure 29. Overgaard and Lund used the implemented numerical schemes to compare the numerical damage predictions for a wind turbine blade with a flap-wise static test result. The results displayed strong geometric and material instability interactions, which indeed caused a progressive collapse of the wind turbine blade as seen in the full-scale experiment. The critical buckling load of the blade triggered locally originated delamination at the corner and in middle of the flange at the point of inflection of the buckling pattern. These were ultimately the starting points of the progressive chain of events that lead to a structural collapse of the complete wind turbine blade.
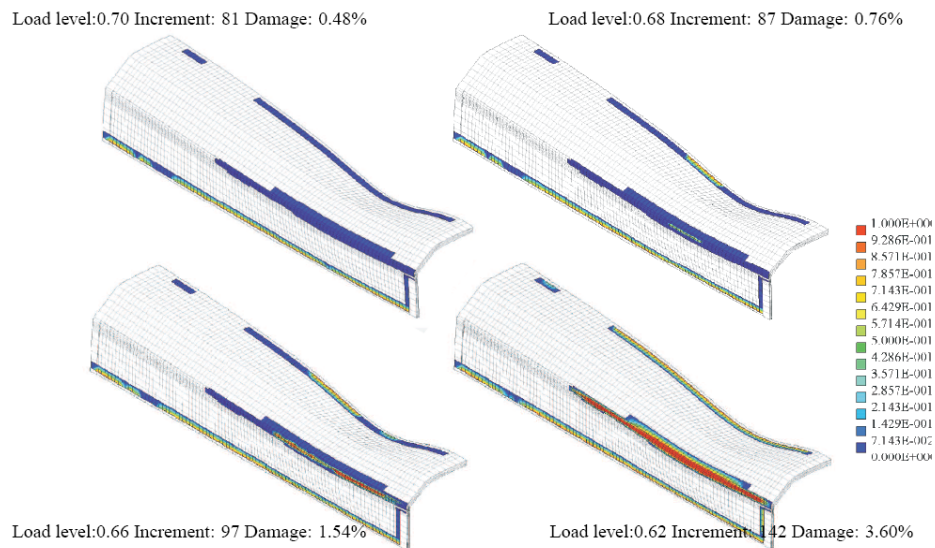

Figure 29: Sequential damage propagation, from Overgaard & Lund (2007a)

6.3   *Effect of Fabrication-induced Initial Imperfections*

Estefen *et al*. (2007) analysed the design of the new generation of semi-submersible platforms for offshore oil and gas production based on column square cross-sectional area. Studying a segment of the column structural arrangement between robust transverse frames to analyse the failure behaviour of the stiffened panels, they integrated the results to track the progressive failure of the whole column. They also carried out numerical and experimental simulations for small scale isolated panels to perform a correlation study to adjust the numerical model for further use in more complex numerical simulations of the structural failure of the column arrangement. The influence of real measured imperfections and idealised imperfections on the ultimate strength were compared.

Vhanmane & Bhattacharya (2008) applied to six benchmark cases a methodology that explicitly included the effect of initial imperfections and residual stresses on the stress strain curves of the stiffened elements. The results were compared with published results using different approaches.

6.4   *Effect of Accident-induced Damage*

An accident is an unexpected, undesirable event that often results in structural damage or harm to people. Common accidents on system structures are collisions, grounding, fire and explosions. Proper procedures for predicting the response of marine structures to extreme loads during accidents are important aspects of ship and offshore structure design.

6.4.1   *Collisions and Grounding*

Paik (2007d,e) developed practical FEM techniques to simulate the crashworthiness of ships in collisions or grounding. Approaches to defining the relevant FE mesh size, material stress-strain relationship and critical fracture strain were addressed and the dynamic effects related to dynamic yield strength, dynamic fracture strain, inertia and friction were dealt with so that the crushing and rupture behaviour in collisions and grounding could be analysed efficiently and accurately. Benchmark studies on material tensile coupon test specimens and a perforated plate under axial tension were undertaken for the simulation of fracture behaviour. Applications to the existing test structural models, which involved both crushing and fracture behaviour, were shown in comparison with the experimental results and the corresponding FE simulations to confirm the validity of the proposed methods.

Ships carrying liquid cargo are sometimes struck by other vessels, and any consequent outflow of crude oil causes very serious damage to the environment. Zhang & Suzuki (2007) presented a numerical simulation of a collision between a container ship and a double-hull very large crude carrier (DH VLCC). Three different numerical simulation

methods were adopted to model fluid-structure interaction in liquid-filled cargo tank, namely the arbitrary Lagrangian-Eulerian FE model, the Lagrangian FE model and the linear sloshing model. The numerical simulation results revealed that the fluid-structure interaction of a liquid cargo-filled tank has a significant effect on the motion and structural response of the struck cargo tank. Compared with the calculation results of the ALE FEM, the linear sloshing model underestimates the influence of the fluid-structure interaction of the liquid cargo tank whereas the Lagrangian-Eulerian FE model may be considered as a practical method for engineering applications as it provides more reasonable results with a relatively low computational time.

Moan (2007) summarized the methods for predicting accidental damage and the survival of the damaged structure. Although nonlinear FEMs generally need to be applied, he concluded that simplified methods, such as those based on plastic mechanisms, developed and calibrated using more refined methods, may limit the computational effort required, allowing them to become especially applicable to risk analysis scenarios.

6.4.2   *Explosions*

Internal loading from an accidental or deliberate impulsive shock can produce the tearing or dishing of a ship's structural arrangement. The problem is particularly worthy of attention due to the confinement of the air blast (closed-domain) and the complexity of the geometry. Pahos *et al*. (2008) investigated this aspect, modelling a cargo hold in the parallel middle body of a Capesize Bulk Carrier in an attempt to gain an introspective look at the response of the steel structure. A typical hold structure is composed of a mixture of plate arrangements such as stiffened square plates at the side, corrugated panels forming the bulkheads, and a series of inclined plates at the hopper and topside tanks. Each plate responds in its own unique manner due to its incident angle in respect of the impeding impulsive wave. Using the results from the fluid/structure interaction, Pahos *et al*. investigated the resultant levels of structural damage by carrying out explicit FEA for the transient loading.

Gong & Lam (2006) analysed the attenuation of floating structure response to an underwater shock. An explicit FE approach interfaced with the boundary element method was used for the shockfluid-structure interaction. The bulk cavitation induced by an underwater shock near the free surface was considered, and two types of floating structural configurations were modelled: a two-layered panel and a sandwich panel, both of which were extracted from typical floating hulls, with the former corresponding to a single hull with coating material and the latter to a double hull with different material fillings. Their effective structural damping and stiffness were formulated and incorporated in the fluid-structure-coupled equations, which related the structure response to fluid impulsive loading and were solved using the coupled explicit FE and boundary element codes. The cavitation phenomenon near the free surface was captured via the presented computational procedure. The attenuation effects of the floating structure response to the underwater explosion were also examined. From the

results obtained, insights were gained into the improvement of floating structures to enhance their resistance to underwater shock.

Lai (2007) investigated a time-domain FEM/DAA coupling procedure to predict the transient dynamic response of a submerged sphere shell with an opening subjected to an underwater explosion. The elastic-plastic material behaviour of the transient fluid-structure interaction related to the structural response equation was presented. The transient responses of structures to different charge distances were also examined. The effects of standoff distance on the pressure time history of the shell to underwater explosion (3001b TNT) were presented. Additionally, the transient dynamic responses to underwater explosion shockwaves in the sea and the air were compared.

Liang & Tai (2006) investigated the shock responses of a ship hull that had been subjected to a non-contact underwater explosion. They developed a procedure that coupled the nonlinear FEM with the doubly asymptotic approximation method, and which considered the effects of transient dynamic, geometrical nonlinear, elastoplastic material behaviour and fluid-structure interaction. This work addressed the problem of the transient responses of a 2000-ton patrol-boat subjected to an underwater explosion. KSF = 0.8 was adopted to describe the shock severity. Additionally, the shock loading history along the keel, the acceleration, the velocity and the displacement time histories were presented. Furthermore, the study elucidated the plastic zone spread phenomena and deformed diagram of the ship. Such information on the transient responses of ships to underwater shock is useful in designing ship hulls to enhance their resistance to underwater shock damage.

Hong & Amdahl (2008a) proposed a theoretical model of structural damage for crushed bottom longitudinal girder strength during accidents. They used plastic methods of analysis to establish the basic folding mechanism. Proposing a simplified analytical expression for the energy dissipation associated with bending and membrane energy, they found good agreement between the simplified method and simulations using LS-DINA code in most of the cases.

7.   UNCERTAINTIES IN ULTIMATE STRENGTH MODELS

7.1   *General*

The uncertainties in ultimate strength models include those in environmental conditions, operating conditions, design variations, constructions, materials, load modelling and structural modelling (Mansour & Liu 2008). Uncertainties in demand modelling can include those in:

- Still-water bending moments
- Wave environments including wave heights and wave periods
- Ship speed, headings

- Determinations of dynamic wave loads acting on the structures

Uncertainties in capacity response modelling may include those in:

- Material properties
- Scantlings
- Construction, i.e., geometric imperfections and welding induced residual stress
- Structural defects, e.g., corrosion wastage, fatigue cracks and minor damages
- Calculation methods for determining ultimate strength

7.2   *Uncertainties in Actions (Demand)*

Still-water loads are forces that result from the action of the ship's self-weight, including equipment, cargo and buoyancy, and they vary from one load condition to another. Ivanov & Wang (2007) presented an approximate analytical method for calculating still water shear forces and bending moments, the ship's trim and the radii of the gyration of gravity and buoyancy forces in the early design stages. Moan *et al.* (2005) studied wave environment effects on wave induced loads. A detailed review of the uncertainties in wave environments and wave loads will not be conducted here, but can be found in the reports of ISSC committees I.1– Environment and I.2 – Loads.

7.3   *Uncertainties in Strength (Capacity)*

Uncertainties in structural ultimate strength have to be considered at different stages of a ship's life. Design ultimate strength is supposed to predict the actual strength of a ship when the extreme load occurs, provided that standard maintenance has been carried out during the ship's life. As Boon (2007) showed, the main strength uncertainties deal with the limitation of the design predicting model. Moreover, variability in material mechanical characteristics depending on the steel maker's available product and previous structural damage may affect the actual ultimate strength. Different components have been analysed, including hull girders.

7.3.1   *Model Uncertainties*

The determination of hull girder strength model uncertainty has been investigated by many authors, generally with the aim of providing data for an ultimate strength reliability analysis model. Some study results are summarised in Table 5. In addition to the model, the main sources of variation influencing hull girder ultimate strength are FEM mesh refining, thickness and yield stress. The uncertainty models of these parameters have been analysed as shown in Table 6.

Analysing the uncertainties of hull girder ultimate strength remains rather informal. No full scale experiments have been carried out and uncertainty results are estimated from numerical models. However, numerical models should be assessed with experimental results. This has been done for stiffened plates, comparing FEM and experimental

results as presented in Table 7.

A stiffened panel is already a complex structure and more factors are involved in global ultimate strength uncertainties. Plate analysis allows a better control of parameters governing the uncertainties. The ultimate strength of plates has been analysed with different finite element methods and different buckling modes, as presented in Table 8. When controlling the defect shape, the uncertainties for various plate aspect ratios, given the buckling mode, are presented in Table 9.

Table 5
Ultimate strength reliability models

Parameter	Case	Mean	COV	Source
Capacity calculation Global strength uncertainty		1.05	0.1	Horte *et al.* (2007)
	FEM1	0.900	0.144	Qi & Cui (2006b)
	FEM2	0.887	0.083	Qi & Cui (2006b)
	Paik	0.895	0.108	Qi & Cui (2006b)
	EPM1	0.894	0.118	Qi & Cui (2006b)
	EPM2	0.898	0.109	Qi & Cui (2006b)
	DH VLCC Hog – Sag	-	0.054–0112	Ozguc *et al.* (2006a,b)
	SH VLCC	-	0.051–0.049	Ozguc *et al.* (2006a,b)
	Container Ship		0.077–0.145	Ozguc *et al.* (2006a,b)
	Bulk Carrier		0.043–0.050	Ozguc *et al.* (2006a,b)
	Energy Concentration ISSC		0.054–0.064	Toderan *et al.* (2006)
	Energy Concentration Case A		0.055–0.068	Toderan *et al.* (2006)
	Energy Concentration Case B		0.110–0.119	Toderan *et al.* (2006)
		1.0	0.10	Khan *et al.* (2006)

Table 6
ModelLing of uncertainties

Effect	Variable	Mean	COV	Source
Nonlinear FEM	Meshing $\dfrac{\sigma_{fmesh}}{\sigma_{rmesh}}$	0.952–0.924		Harada & Shigemi (2007)
Thickness		1.0 1.0	0.04 0.006	Harada & Shigemi (2007) Toderan *et al.* (2006)
Yield stress		1.1	0.06	Harada & Shigemi (2007)

Curved shells and pipes have also been considered, and the uncertainties related to their boundary conditions are summarised in Table 10. In terms of accidental loads, some experimental studies have been carried out (e.g., Paik & Seo 2007), but no reference design approaches have been fully recognised and it is difficult to infer the relevant uncertainties.

Parunov *et al.* (2007) carried out hull girder reliability analyses with respect to ultimate bending moments of new type oil tankers that differ from traditional oil tankers designed by classification society rules. The new type oil tankers are designed using direct hydrodynamic analysis to determine design vertical bending moments instead of

adopting IACS rule values. One of the most interesting conclusions from the study is that the annual hull-girder reliability of the new type oil tanker is increased considerably compared to the conventional oil tanker. Sensitivity and parametric studies were also performed with regard to random variables representing modelling uncertainties.

Table 7
Comparison between FEA and experiments

Parameter		Mean	COV	Comment	Source
Shear Strength	$\dfrac{\sigma_{analytical}}{\sigma_{FEA}}$	1.0	0.06	Depending of slenderness	Zhang & Kumar (2007), Zhang *et al.* (2008)
Compressive strength aluminium stiffened panel	$\dfrac{\sigma_{analytical}}{\sigma_{FEA\ or\ Exp}}$	0.97	0.101	Aluminium stiffened panels with T bar	Paik (2007a), Paik *et al.* (2008a)
Compressive strength aluminium stiffened panel	$\dfrac{\sigma_{analytical}}{\sigma_{FEA\ or\ Exp}}$	0.98	0.114	Aluminium stiffened panels with flat bar	Paik (2007a), Paik *et al.* (2008a)
Compressive strength aluminium stiffened panel	$\dfrac{\sigma_{analytical}}{\sigma_{FEA\ or\ Exp}}$	0.97	0.106	Aluminium stiffened panels with T and flat bar	Paik (2007a), Paik *et al.* (2008a)

Table 8
Uncertainties of Ultimate strength due to plate initial shape

Parameter	Case	Mean σ_u / σ_Y	COV	Source
Plate imperfection shape	Case 1	0.729	0.016	Guedes Soares *et al.* (2005)
	Case 2	0.881	0.005	
	Case 3	0.687	0.008	
	Case 4	0.756	0.007	

Table 9
Uncertainties of Ultimate Strength due to control of plate initial shape

Parameter	Case	Mean σ_u / σ_Y	COV	Source
Plate imperfection shape	Case 1	0.714	0.00300	Guedes Soares *et al.* (2005)
	Case 2	0.709	0.01019	
	Case 3	0.719	0.00876	
	Case 4	0.709	0.01505	
	Case 5	0.678	0.01943	
	Case 6	0.705	0.01749	
	Case 7	0.713	0.03770	

Table 10
Uncertainties of Ultimate Strength of pipes due to boundary condition

Parameter		Mean	COV	Comment	Source
Cylindrical shell and equivalent barrel	$\dfrac{\text{Numerical}}{\text{Experimental}}$	1.0-1.04	0.08	Mean depending on the yield stress assumption	Blachut & Smith (2008)

7.3.2   Other Sources of Uncertainty

Other sources of uncertainty related to material mechanical characteristics and dimensional margins. Concerning the material as rolled, the true yield stress and ultimate strength are not accurately known at the design stage, as only a minimum value is required for yield stress and a range for ultimate strength. Given process and test approval, it is unlikely that the mechanical characteristics will be below the minimum required, so the yield stress and ultimate strength of material are well modelled with a Weibull minimum 3 parameter law as the minimum corresponding to the required value (Boutillier *et al.* 2008). Another source of uncertainty is due to the strain hardening effect not being explicitly taken into account (La Rosa *et al.* 2003, Manevich 2007).

In the same way, excluding gross errors, thickness is well controlled during fabrication, and can be considered as deterministic in as built condition. When considering in-service condition, degradation has to be taken into account, with the first source of uncertainty being the ageing effect. For steel ships, ageing mainly involves corrosion with a loss of thickness after the end of the coating, life as indicated in Table 11.

Although, corrosion phase sequence, including coating degradation, seems to have been generally considered, its relationship with abovementioned analyses and statistical models remains unclear. This is particularly true of unexpected structural strength reduction, due to the crack effect, accidental deformation or local collapses. Paik & Kumar (2006) considered the effect of cracking damage, and Khan & Das (2008) considered accident condition. These analyses were based on specific scenarios and are probably not representative of world fleet conditions. Recent contributions were also made by Paik & Melchers (2008).

Table 11
Uncertainties of corrosion in aged ships

Parameter		Mean	COV	Comment	Source
Corrosion loss (mm) 20 years		2.11 1.34 1.38	0.59 0.50 0.35		Gudze & Melcher (2006)

Corrosion loss (mm) 1 year	Coating life 5 years	0.0463	0.7583	All data	Paik & Frieze (2001), Paik (2004), Paik *et al.* (2003a,b)
	Coating life 7 years	0.0549	0.7596		
	Coating life 10 years	0.0684	0.7897		
	Coating life 5 years	0.1481	0.1428	95% above band	
	Coating life 7 years	0.1777	0.1316		
	Coating life 10 years	0.1926	0.3630		

8. NONLINEAR FINITE ELEMENT METHOD COMPUTATIONS: ULTIMATE STRENGTH CHARACTERISTICS OF STEEL STIFFENED PLATE STRUCTURES

8.1 General

To validate the FEM as a suitable tool for assessing the ultimate strength of plated structures and also to investigate the ultimate strength characteristics, a series of nonlinear finite element method computations were carried out with varying various parameters of influence. A detailed description of the object structure was elaborated by Jeom Paik (Pusan National University) and later published (Paik *et al.* 2008e). Each participant in the benchmark study was free to choose FEM software and instructed to carry out simulations independently. Many commercial and national institutions, listed in Table 12, were involved in the study. Table 13 lists the parameters of influence dealt with in the benchmark study.

8.2 Description of the Computations

The structure considered in the benchmark study is a section of a steel stiffened panel, which is a component of a ship hull. Dimensions of the panel are described in Figure 30. The geometry of the panel includes initial imperfections, described in terms of trigonometric functions and certain amplitudes. Imperfections are applied separately to stiffeners, plates between stiffeners (local modes) and to the entire panel as a whole (global mode).These are presented in Figures 31 and 32.

Table 12
Institutions involved in conduct of benchmark study for steel stiffened panels

Participant			FEM software
Xiaozhi Wang	American Bureau of Shipping (ABS)	USA	ANSYS
Guy Parmentier	Bureau Veritas	France	ABAQUS

Raffaele Iaccarino	Cetena S.P.A.	Italy	MSC/MARC
Jose Manuel Gordo	Instituto Superior Tecnico (IST)	Portugal	ANSYS
Ilson Paranhos Pasqualino	Laboratório de Tecnologia Submarina (LTS)	Brazil	ANSYS
Shengming Zhang	Lloyd's Register	UK	ABAQUS
Jurek Czujko	Nowatec AS	Norway	LS-DYNA
Masahiko Fujikubo	Osaka University	Japan	ABAQUS
Jeom Kee Paik	Pusan National University	Korea	ANSYS

Table 13
Parameters of Influence dealt with in the benchmark study

Parameter	Participants	Section
Type of boundary conditions	All	0
Effects of lateral pressure	All	0
Mesh density and size	Instituto Superior Tecnico, Osaka University, Nowatec AS	8.3.4
Material hardening	Cetena S.P.A.	8.3.5
Form of geometrical imperfections	Instituto Superior Tecnico	0
Welding induced geometrical imperfections	Nowatec AS	0
Effects of residual stresses	Lloyd's Register, Nowatec AS	8.3.8
Effect of cracking damage	Bureau Veritas	8.3.10

Two cases of boundary conditions are taken into account – longitudinal edges are simply supported or clamped in the first and the second case respectively. The longitudinal edges are those parallel to the stiffeners. Boundary conditions are described in detail in Figure 33. In addition to two cases of boundary conditions, eight load cases are considered. A load case includes in-plane loads σx and σy, which are or are not combined with lateral pressure (see Figure 34). For simplicity, the steel material of the panel is modelled as an elastic-plastic with no hardening, thus all of the material parameters needed to describe the material properties are as follows:

- Young's modulus, E = 205800 MPa
- Poison's ratio, ν = 0.3
- Yield strength, σ_Y = 315 MPa
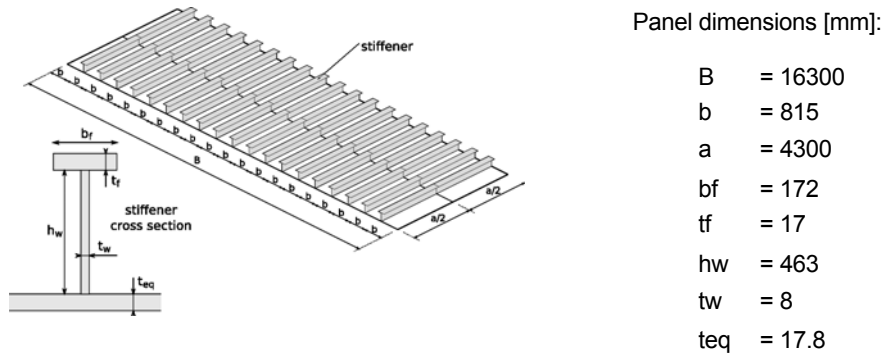- Material density, ρ = 7.8 × 10-9 t/mm^3

Panel dimensions [mm]:

B	= 16300
b	= 815
a	= 4300
bf	= 172
tf	= 17
hw	= 463
tw	= 8
teq	= 17.8

Figure 30: Dimensions of the stiffened panel

woc = a/1000   wos = a/1000
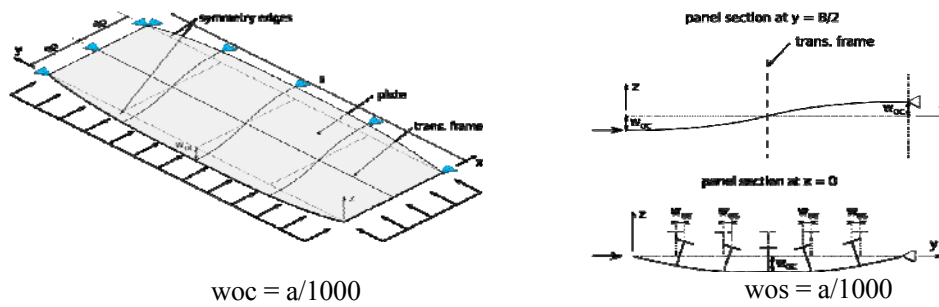
Figure 31: Global mode (column type) of initial imperfections

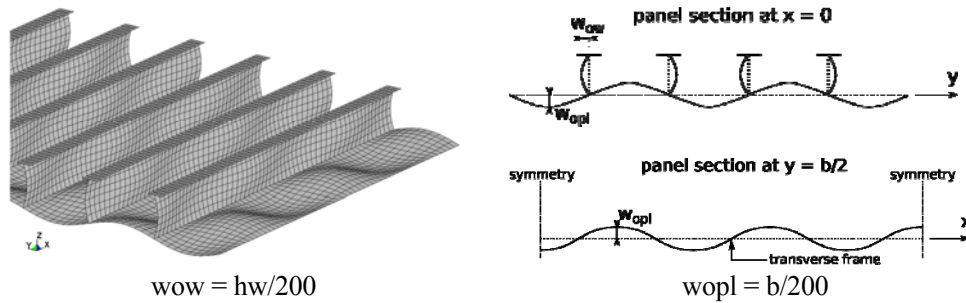wow = hw/200   wopl = b/200

Figure 32: Local mode of imperfections

8.3   *Computational Results and Discussions*

The structural response of the panel was measured in terms of load ratios and global strains εx and εy calculated as follows:

- Load ratio x = σ_x/σ_Y
- Load ratio y = σ_y/σ_Y
- Global strain x = u_x/a

• Global strain y = u$_y$/B

where σ_x and σ_y are loads as described in Figure 34, panel dimensions a and B are described in Figure 30 and ux and uy are changes in panel length in the x and y direction respectively. It is clear that the value of load ratios is between 0 and 1. A load ratio equal to 1 means that the panel is damaged due to plastic flow, whereas values lower than 1 mean that the panel has undergone buckling.

8.3.1   Consistency of Results

The ultimate strengths of the panel for each load and boundary condition case expressed in terms of load ratios are presented in Table 14. This table indicates the values of ultimate strength averaged from all participants, as well as the deviance of maximum and minimum results from the average. Comparisons of load ratio-global strain relations obtained by all benchmark study participants for all load cases with simply supported longitudinal edges are presented in Figure 35.
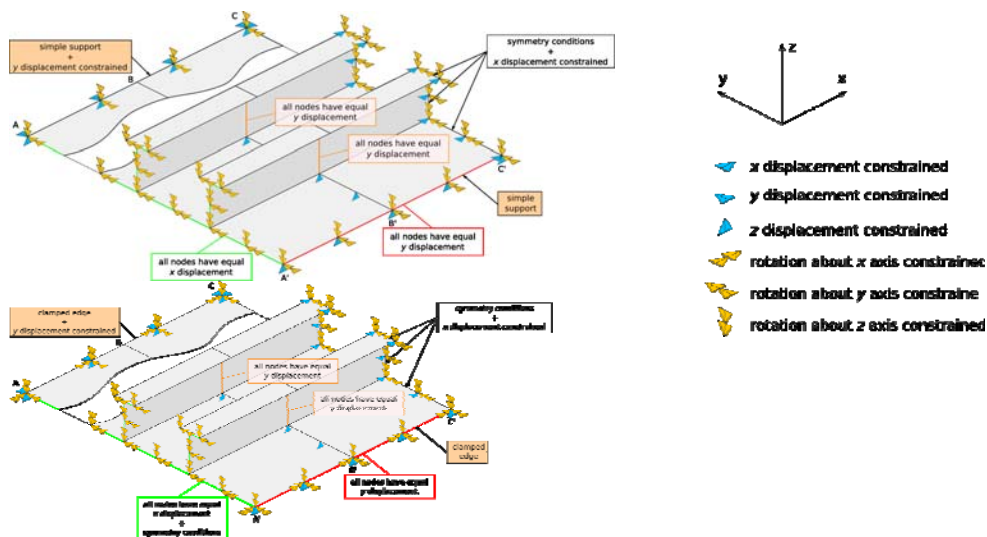

Figure 33: Two cases of boundary conditions – longitudinal edges simply supported (upper figure) or clamped (lower figure)

Intuitively, panel strength is much higher in cases of compression along stiffeners than in the perpendicular direction, because stiffeners then contribute to panel stiffness in bending. In cases of compression across stiffeners, the panel's structural response is linear only in a very small range of loads. As the load magnitude increases the panel stiffness drops down gradually, which quickly leads to buckling.

The remarkable fact is that the differences between maximal and average results, as well as between minimal and average (see Table 14), are very small and exceed 10% in only one case. The best coincidence of results can be observed for cases with

predominant longitudinal compression (along stiffeners) – not only the ultimate strength but also the stiffness of the panel obtained by the different participants is almost the same (see Figure 35).

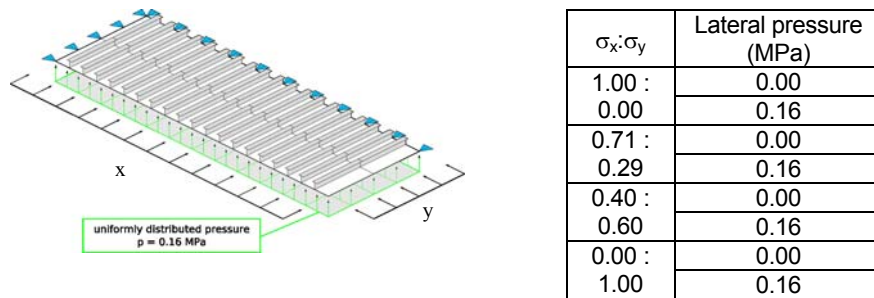| $\sigma_x : \sigma_y$	Lateral pressure (MPa)
1.00 :	0.00
0.00	0.16
0.71 :	0.00
0.29	0.16
0.40 :	0.00
0.60	0.16
0.00 :	0.00
1.00	0.16

Figure 34: Load cases considered in the benchmark study

Table 14
Results of the benchmark study for all cases of load and boundary conditions
(Results reported in this table are averaged from values obtained by all participants IN the study. Deviances of the maximal and minimal result are reported for each case.)

| $\sigma x : \sigma_y$	Lateral pressure (MPa)	Boundary condition	Ultimate strength		Difference	
			σ_{xu}/σ_Y	σ_{yu}/σ_Y	Minimum	Maximum
1.00 : 0.00	0.00	simple	0.8180	0.0000	-1.7%	+2.6%
		clamped	0.8243	0.0000	-1.8%	+2.4%
	0.16	simple	0.7506	0.0000	-1.3%	+2.7%
		clamped	0.7538	0.0000	-0.8%	+1.9%
0.79 : 0.21	0.00	simple	0.7768	0.2065	-2.5%	+4.0%
		clamped	0.7849	0.2086	-2.7%	+3.6%
	0.16	simple	0.7145	0.1899	-2.2%	+4.4%
		clamped	0.7187	0.1911	-2.0%	+4.5%
0.40 : 0.60	0.00	simple	0.2225	0.3337	-2.0%	+7.8%
		clamped	0.2266	0.3400	-3.0%	+7.2%
	0.16	simple	0.2120	0.3180	-8.3%	+13.1%
		clamped	0.2178	0.3266	-2.8%	+5.6%
0.00 : 1.00	0.00	simple	0.0000	0.3476	-1.5%	+5.2%
		clamped	0.0000	0.3550	-2.6%	+6.2%
	0.16	simple	0.0000	0.3250	-8.7%	+4.9%
		clamped	0.0000	0.3388	-2.6%	+6.7%
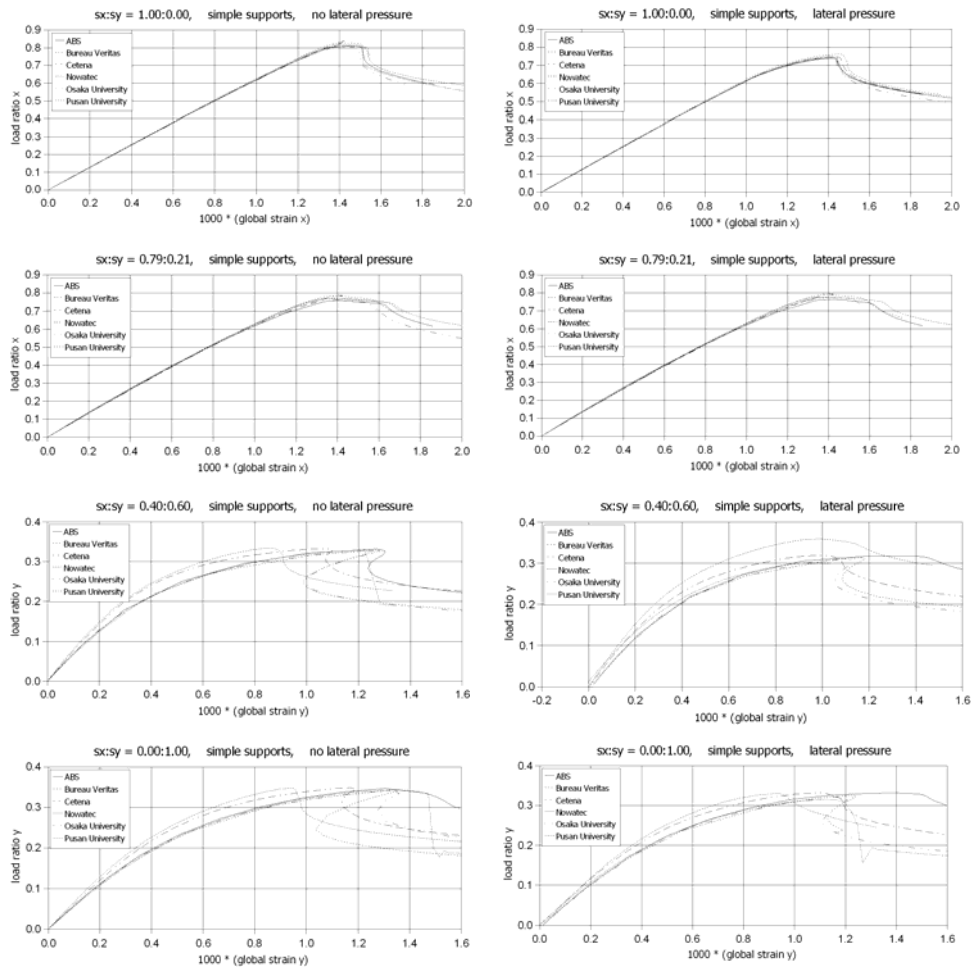
Figure 35: Relations between load ratio and global strain for all cases with longitudinal edges simply supported. (Results obtained by different participants of the study are presented to show differences in obtained solutions)
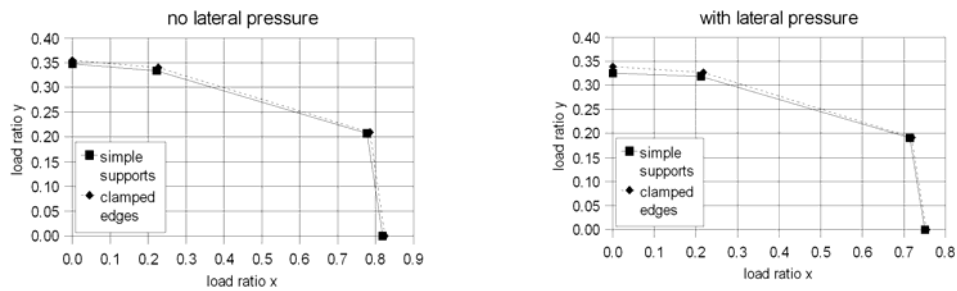
Figure 36: Influence of boundary conditions on panel strength

In cases with compression perpendicular to the stiffeners, clear differences in structural stiffness are visible in Figure 35; however, the values of ultimate strength are still in very good agreement. The presented results prove that FEA is a reliable and mature method for the assessment of the ultimate strength of plated structures. The results obtained by different analysts are consistent and seem to be software independent. Differences arise due to different modelling techniques rather than the use of a specific FEA solver, but are small enough to allow the assessment of structural strength with reasonable accuracy.

8.3.2   Effect of Boundary Conditions

Two boundary conditions were considered in the benchmark study – the panel edges parallel to the stiffeners (longitudinal edges) were either simply supported or clamped. Figure 36 presents a comparison of ultimate strength for both boundary conditions. Apparently, the boundary conditions on longitudinal edges have only a minor influence on panel strength, but when the edges are clamped the panel strength increases slightly.

8.3.3   Effect of Lateral Pressure

The benchmark results indicate that lateral pressure is a significant parameter in the design and modelling of stiffened panels, and clearly affects safe range of in-plane loads. Lateral pressure of 16 bars resulted in a drop of ultimate strength by 5-10%: see Figure 37. This imposes bending in stiffeners and increased membrane forces in the plate. Thus, the drop in strength is greater when the longitudinal in-plane load (along stiffeners) is predominant, because in this case panel strength depends more on the stiffeners.
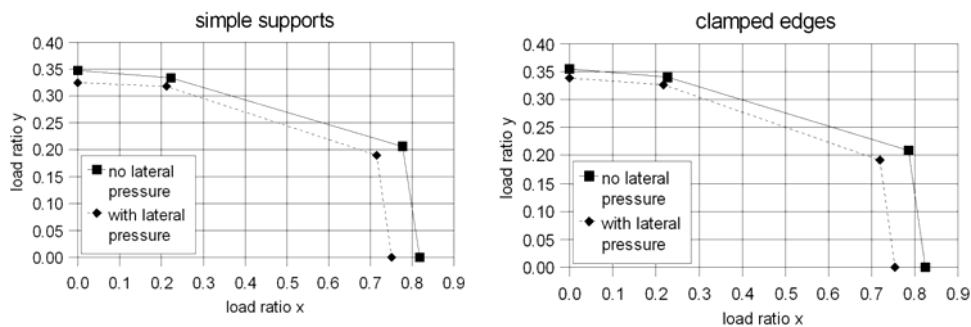

Figure 37: Influence of lateral pressure on panel strength

8.3.4   Effect of Mesh Density

The dependence of results on mesh density was studied by the Instituto Superior Tecnico. Two models were analysed, the first one with a coarse mesh (size to thickness ratio for shell elements equal to 10) and the other with a fine mesh (size to thickness equal to 5). Additionally, two shell element types were used – Ansys 43 element with

four nodes and Ansys 281 element with eight nodes. The results are presented in Figure 38. The plots show that mesh refinement changed the results only for the four-node element, whereas the eight-node element gave the same results for both coarse and fine mesh. This occurred because the eight-node element uses quadratic shape functions and is thus generally more accurate and does not require as fine a mesh as the four-node element. Hence, mesh convergence study should be carried out to make sure that the mesh is fine enough. One should always remember that the shell element mesh should be fine enough to properly describe the model shape (also after deformation) but at all times must satisfy requirements considering the element size to thickness ratio (usually at least 5).

An additional study was performed by Osaka University to investigate the influence of model size on result accuracy. In addition to the model considered in previous chapters (the one-bay model), two new models were used: a larger two-bay model, and a smaller stiffener space model, as shown in Figure 39. A comparison of the results is presented in Table 15 (values of ultimate strength) and Figure 40 (relations of load ratio to global strain).
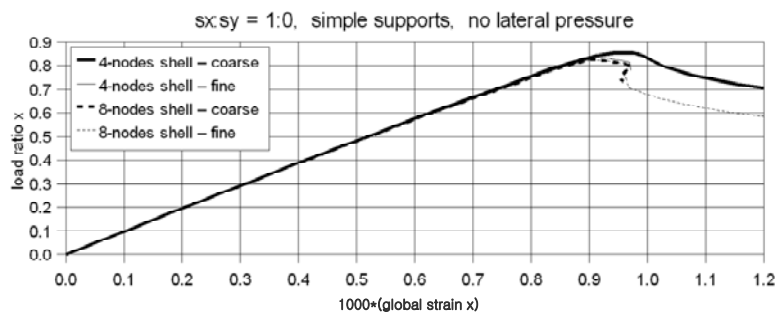

Figure 38: Comparison of results for models with different densities of mesh and element formulations Influence of Model Size
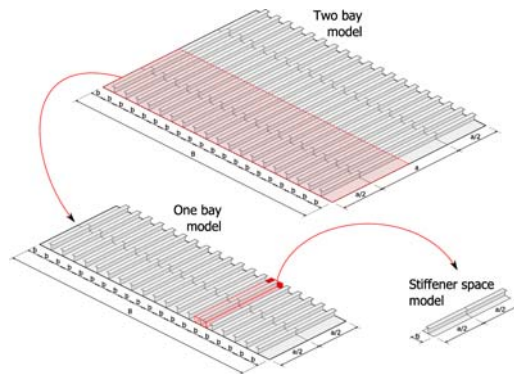

Figure 39: Explanation of two-bay model, one-bay model and stiffener space model. The one- bay model was used to carry out basic benchmark analyses as a reference model. The two-bay and stiffener space models were used to perform additional studies

The general conclusion is that ultimate strength can be assessed with good accuracy

using smaller models containing only one stiffener. However, in cases with compression across the stiffeners a completely different post-buckling behaviour was obtained – the stiffener space model did not exhibit snap-back phenomena because the whole panel and a small section have different collapse modes. In the whole panel, plastic deformation is localised in one local plate panel and unloading takes place in the rest of the panel.

When considering a small section of the panel, the distribution of plastic deformation is more uniform. This difference in the behaviour of models of different sizes indicates that one should use simplified models with caution and precede them with a testing phase. In some cases, different behaviour may produce much larger differences in ultimate strength than in the present study. The larger, two-bay model gives excellent coincidence with the reference, one-bay model in the pre-buckling phase and displays a greater decrease of strength after buckling.

Table 15
Results of ultimate strength for models of different sizes

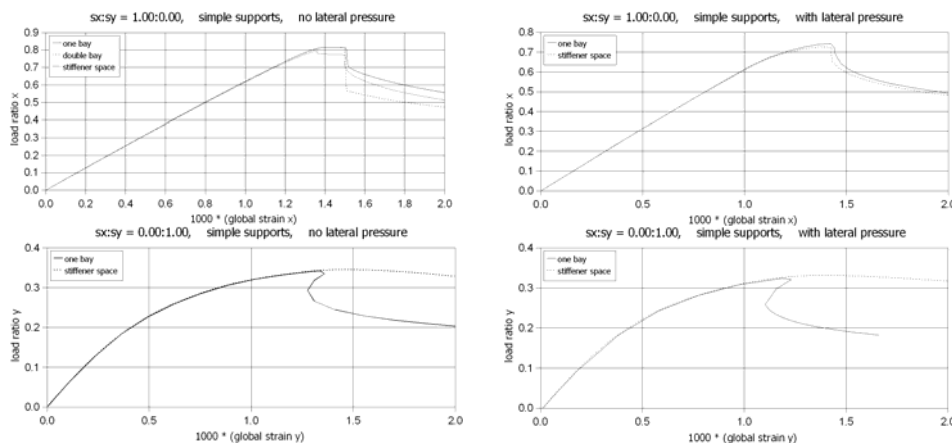| Load case		Ultimate strength (panel with simple supports on longitudinal edges)					
		One-bay model		Stiffener space model		Two-bay model	
$\sigma_x : \sigma_y$	Lateral pressure MPa	σ_{xu}/σ_Y	σ_{yu}/σ_Y	σ_{xu}/σ_Y	σ_{yu}/σ_Y	σ_{xu}/σ_Y	σ_{yu}/σ_Y
1.00 : 0.00	0.00	0.8166	0.0000	0.7952	0.0000	0.8169	0.0000
	0.16	0.7441	0.0000	0.7280	0.0000	-	-
0.00 : 1.00	0.00	0.0000	0.3424	0.0000	0.3456	-	-
	0.16	0.0000	0.3245	0.0000	0.3317	-	-

Figure 40: Relations between load ratio and global strain for cases with uniaxial compression and longitudinal edges simply supported (Results for models of different sizes are compared – the solid lines are the reference results for the one-bay model.)

8.3.5   Effect of Material Hardening

The influence of material hardening on the ultimate strength and behaviour of the stiffened panel was investigated by Cetena S.P.A. Three material models were used for comparison (see Figure 41):

- Without hardening (the same as in all other studies)
- With hardening and plastic modulus equal to 5% of Young's modulus, ultimate tensile stress $\sigma_T = \sigma_Y / 0.67$
- With hardening and plastic modulus equal to 10% of Young's modulus, ultimate tensile stress $\sigma_T = \sigma_Y / 0.67$
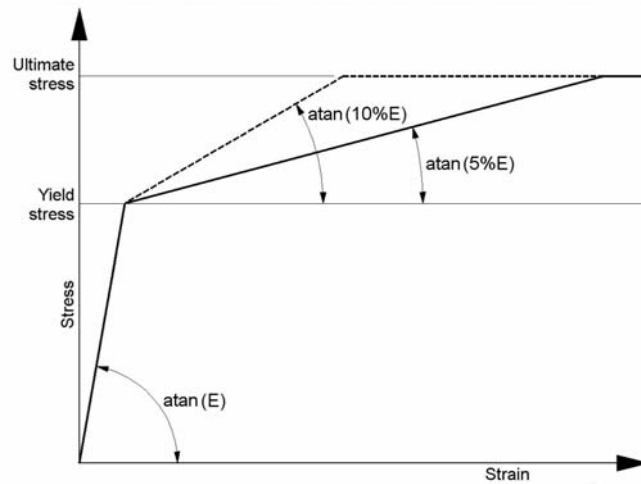

Figure 41: Material models used for investigation of hardening influence

The values of ultimate strength obtained for all three material models are presented in Figure 42, which reveals that material hardening had almost no influence on ultimate strength in cases where transverse compression (across stiffeners) was predominant. This occurred because loss of stability in these cases was due to buckling at relatively low stress levels, before any post-yielding hardening effects appeared. When a panel is compressed longitudinally, plastic hardening gives an increase of ultimate strength because the loss of stability is accompanied by high stress and the appearance of some plastic strains, and thus material hardening results in an increased stiffness and strength. Another conclusion is that material hardening has a positive impact on strength when lateral pressure acts on the panel surface. As material hardening appears only after yielding, it is rather obvious that it will most influence structural behaviour after buckling, when the structure undergoes large deformations and plastic strains appear. This is clearly illustrated in Figure 43.
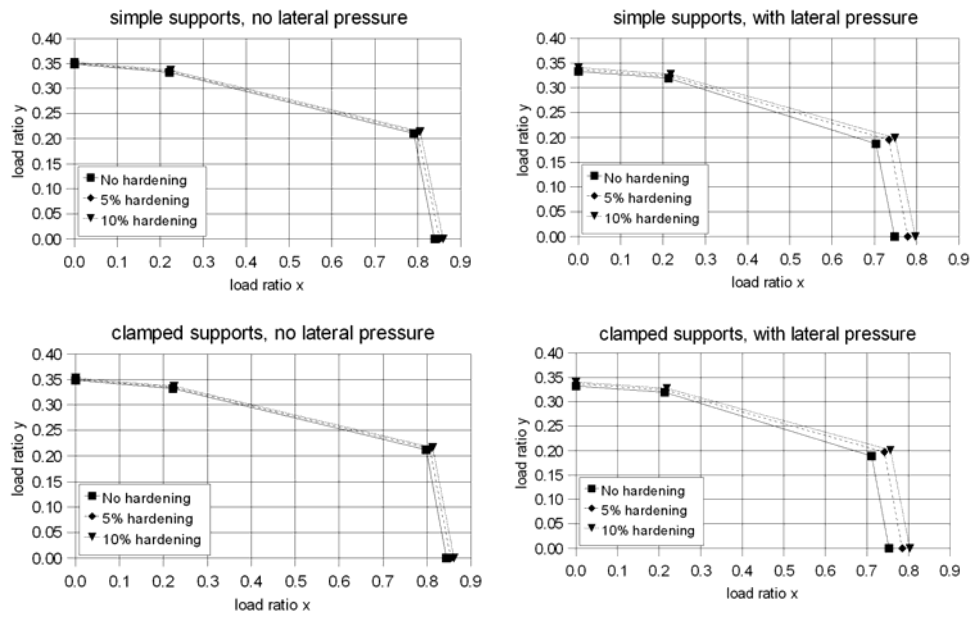
Figure 42: Interaction curves for material models with different hardening properties
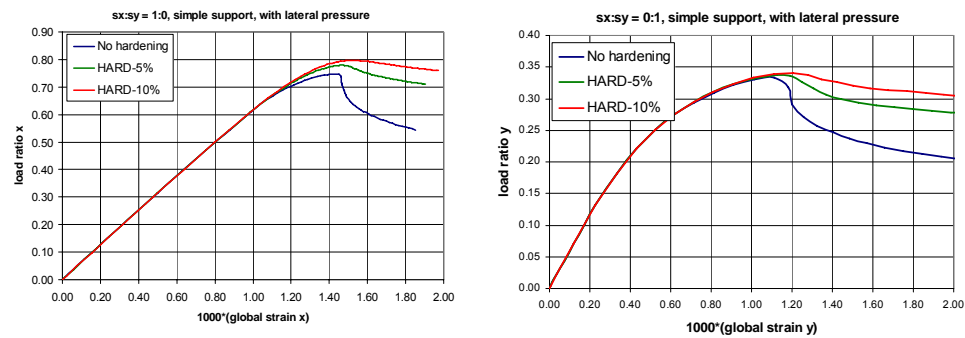

Figure 43: Equilibrium curves for cases with uniaxial compression and different material hardening

8.3.6 *Effect of Geometrical Imperfections with Buckling Modes*

Instituto Superior Tecnico performed a study to establish the influence of geometrical imperfections with buckling modes on the panel ultimate strength. The study was limited to one load case with uniaxial pressure and no lateral pressure, with the longitudinal edges simply supported. Four imperfection shapes, as shown in Figure 44, were considered. In the base case all imperfection modes were applied and ultimate strength (maximum load ratio) was set as a reference value. In subsequent analyses, one of the imperfections was removed so the influence of that particular imperfection on the ultimate strength and stiffness of the panel could be traced. The results for ultimate

strength are indicated in Table 15 and the equilibrium paths for the performed analyses are shown in Figure 45.

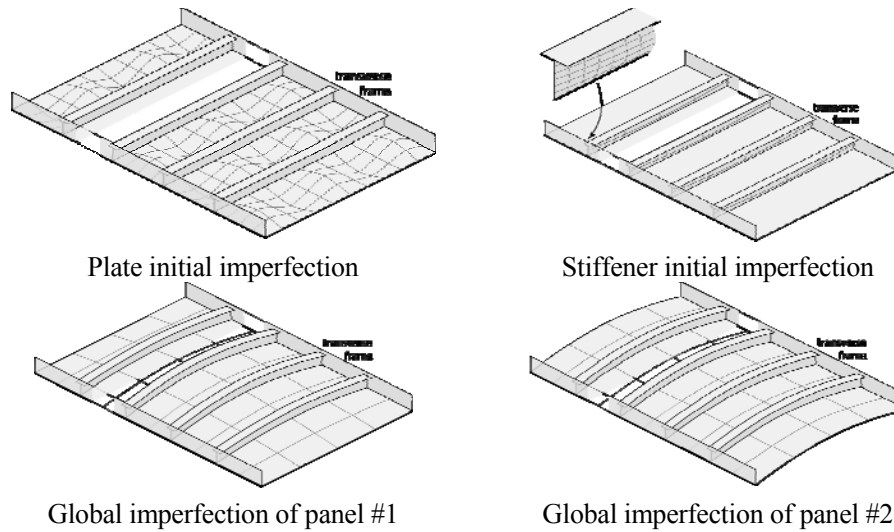| Plate initial imperfection | Stiffener initial imperfection |
| Global imperfection of panel #1 | Global imperfection of panel #2 |

Figure 44: Shapes of initial distortions considered in the benchmark study

The presented results show that in case of uniaxial compression along stiffeners, the plating imperfection has the determinant influence on panel stiffness and ultimate strength – if this initial distortion is absent, panel strength increases by 8.0%. The global imperfection has a secondary influence on panel behaviour. In case of its absence, strength increases by about 2% and the panel exhibits snap-back behaviour in the post-buckling phase. Initial deformations of stiffeners have negligible impact on strength characteristics of the panel, but greatly improve analysis convergence (see the thin solid line in Figure 45). One should remember that the influence of geometrical imperfection is inevitably conjugate with supports and loads applied to a structure, and thus the presented results cannot be generalised for all loading conditions.

Table 15
Ultimate strength results for different combinations of imperfections. (Applied imperfections are marked with a cross. The results correspond to uniaxial compression along stiffeners, absence of lateral pressure and simple supports on longitudinal edges.)

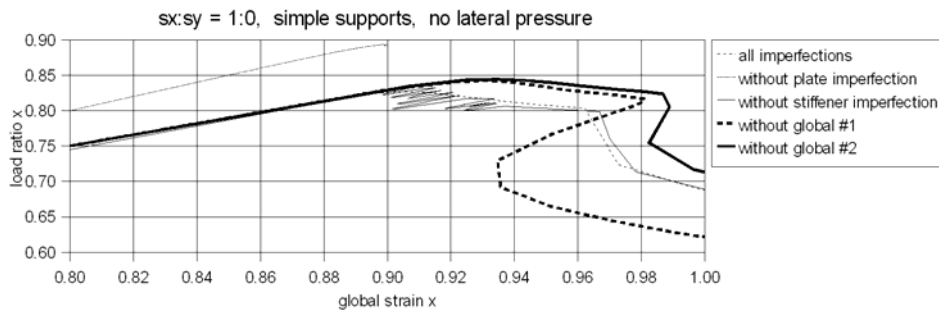| Imperfection				Ultimate strength	
Plating	Stiffeners	Global #1	Global #2	Load ratio	Difference
×	×	×	×	0.8274	–
	×	×	×	0.8939	+8.0%
×	√	×	×	0.8338	+0.8%
×	×	√	×	0.8420	+1.8%
×	×	×	√	0.8444	+2.1%

Figure 45: Relations between load ratio and global strain for different combinations of imperfections. (Figure presents behaviour of the panel in the region of collapse.)

8.3.7 Effect of Realistic Geometrical Imperfections

Nowatec AS investigated the influence of more realistic forms of geometrical imperfections on the ultimate strength of a stiffened panel. Imperfections with shapes similar to welding induced deformations were considered (see Figures 46 and 47) in comparison with buckling-mode imperfections. The magnitudes of initial deformations remained unchanged.
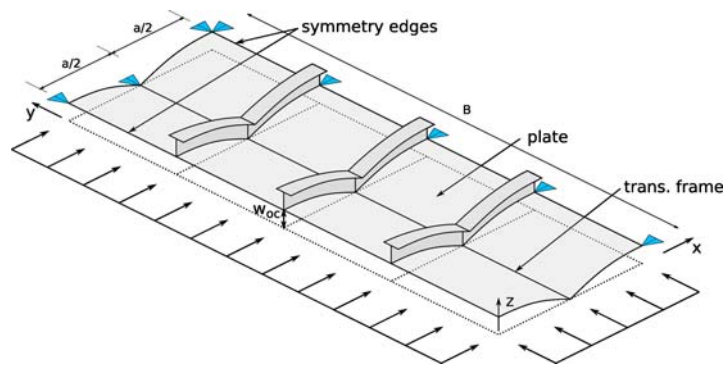

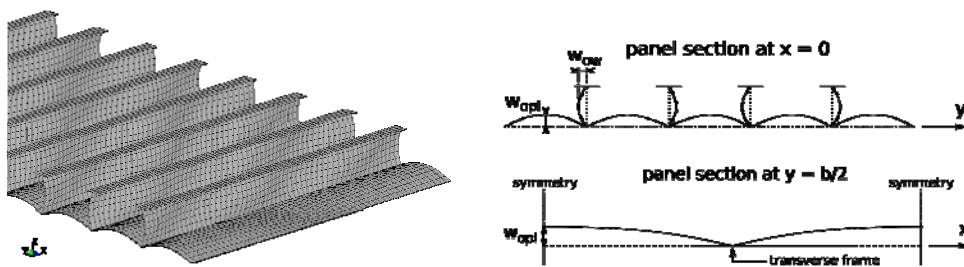Figure 46: Global mode of a realistic weld-induced geometrical imperfection

Figure 47: Local mode of welding-induced imperfections

The comparison of ultimate strength results for buckling-related and welding-related

imperfections is presented in Table 16 and Figure 48. It is noticeable that imperfections induced by welding result in a significant increase of panel stiffness and ultimate strength. The reason for this is that the shape of a panel at buckling is similar to the shape of buckling-related but not welding-related imperfections. Thus, the analysis of a panel with an imperfection mode as described in this chapter should include a transition from the initial deformation pattern to a buckling deformation pattern that gives extra stiffness and strength.

Table 16
Ultimate strength for models with different imperfection shapes

$\sigma_x : \sigma_y$	Pressure MPa	Buckling-related imperfections		Welding-related imperfections	
		σ_{xu}/σ_Y	σ_{yu}/σ_Y	σ_{xu}/σ_Y	σ_{yu}/σ_Y
1.00 : 0.00	0.00	0.8166	0	0.9805	0
1.00 : 0.00	0.16	0.7506	0	0.7961	0
0.00 : 1.00	0.00	0	0.3431	0	0.4012
0.00 : 1.00	0.16	0	0.3158	0	0.3230

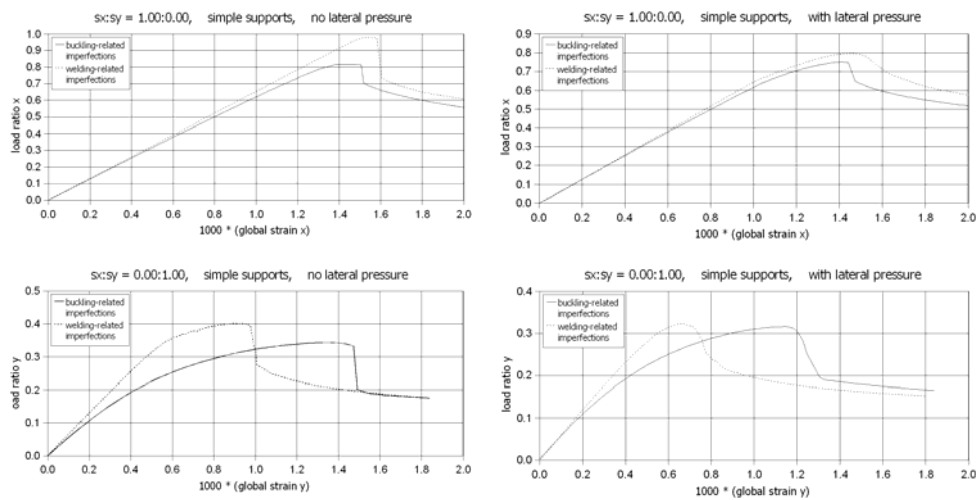Figure 48: Relations between load ratio and global strain for cases with uniaxial compression and longitudinal edges simply supported (Results for models with different imperfection shapes are compared – the solid lines are the reference results for buckling-related imperfections.)

8.3.8   Effect of Residual Stresses

Lloyd's Register and Nowatec carried out analyses to capture the influence of residual

stresses on panel ultimate strength. These stresses arise from the welding process when the area around the weld is first heated and then tends to shrink when cooling down. It is, however, connected to unheated parts of the structure, which prevent free shrinkage. Thus, tensile stress arises around welds and compressive stress arises in other parts of the structure. Nowatec and Lloyd's Register modelled residual stress in the panel in two different ways. In Nowatec's approach, a high initial temperature was prescribed around the connection of plate and stiffener and residual stress arose during cooling down. In the Lloyd's Register simulation, the initial stress state was directly prescribed to the desired elements.

8.3.8.1   Residual Stresses Resulting from Temperature Differences

Residual stresses in plates are compressive between stiffeners and rapidly change the tensile stress in the area around stiffeners, thus rendering gradients of stress very large and requiring the use of small elements. To acquire good accuracy, a detailed model made of solid elements was developed. The extent of the model covers the middle stiffener and a half of the plate (between stiffeners) on both sides. The FE model of this extent gives correct results in both the pre- and post-buckling phases only in case with compression in the longitudinal (x) direction, thus only these cases are considered in the current study. A model made of solid elements was first verified by comparison with the shell element model, and it presented a satisfactory compliance with results obtained in previous benchmark studies. The results of that comparison are presented in Figure 49.

Two levels of residual stress were considered, as follows.

- A slight level – average compressive stress equal to 5% of yield stress
- An average level – average compressive stress equal to 15% of yield stress

The residual stresses were initiated in a thermal analysis – a temperature of 1200°C was applied around the connection of the plate and stiffener, followed by a long period of cooling down. The level of resultant residual stress was adjusted by the range of the heated zone. The distribution of residual stress (in the x direction) over the width of the plate between stiffeners is presented in Figure 50.
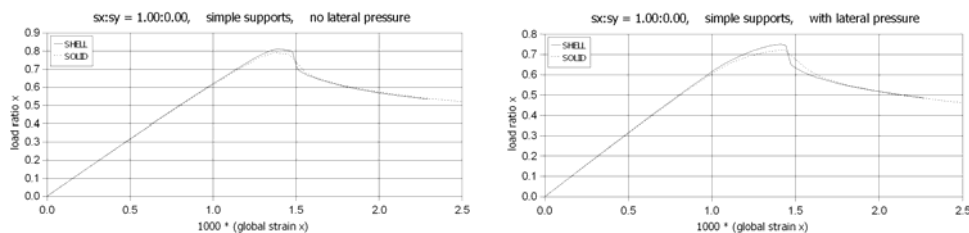

Figure 49: Equilibrium path for cases with uniaxial compression in the x direction with and without lateral pressure (Results for solid and shell models are compared.)

The results of simulations accounting for residual stresses are presented in Figure 51.

and Table 16. Residual stresses had a significant influence on ultimate strength of the panel and post buckling behaviour. The drop of strength was proportional to the magnitude of residual stress and reached 6% for the slight level and 15% for the average level of residual stresses. As the load approached ultimate strength, the pre-stressed panels exhibited ductile behaviour and a smooth transition to post-buckling response as opposed to panels without initial stress, which lose strength and stability suddenly. The obtained results also indicate that panels subjected to lateral pressure are less vulnerable to residual stresses.
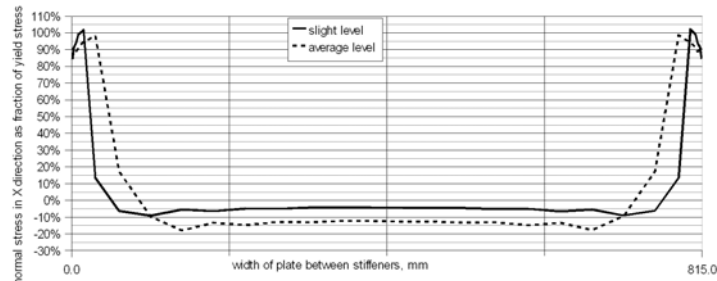
Figure 50: Distribution of residual stresses (σ_x) over width of the plate between stiffeners
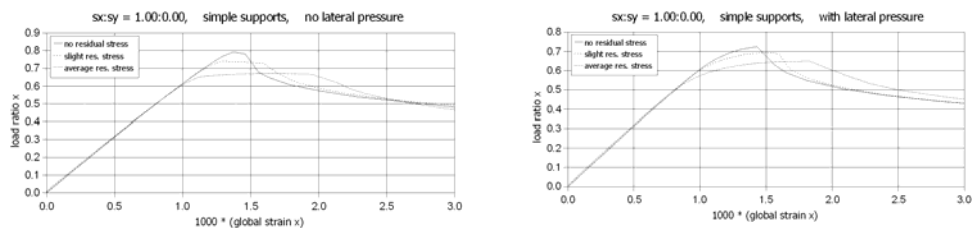
Figure 51: Equilibrium paths for cases with compression in the longitudinal direction with and without lateral pressure (Results for models with different levels of residual stresses are compared.)

Table 17
Results of ultimate strength for models with different levels of residual stresses

Load case		Ultimate strength				
$\sigma_x : \sigma_y$	Lateral pressure MPa	No residual stresses	Slight level of residual stresses (5%)		Average level of residual stresses (15%)	
		σ_{xu}/σ_Y	σ_{xu}/σ_Y	Difference	σ_{xu}/σ_Y	Difference
1.00 : 0.00	0.00	0.7922	0.7415	-6.4%	0.6719	-15.2%
	0.16	0.7255	0.6936	-4.4%	0.6490	-10.5%

8.3.8.2   Directly Prescribed Residual Stresses

To capture high gradient stress, a fine mesh is required. The model of the stiffened panel was evenly divided with 50 to 52 shell elements along the panel width (depending on the residual stress level). Desired residual stresses were acquired by

application of initial stress to elements of the plate (not the stiffener web or flange) as shown in Table 18.

The results of analyses are presented in Figure 52 and Table 19, with the ultimate strength of the panel dropping by 2.5% at the slight level, by 6.4% at the average level and by 12.3% at the severe level of residual stress. Pre-stressed panels exhibited non-linear behaviour before reaching the ultimate state and ductile collapse after buckling. Both effects became stronger with the increase of residual stress.

The conclusions that can be drawn from the present study are similar to those drawn from simulations performed by Nowatec AS (thermal induced residual stress), but in the latter the drop in ultimate strength was almost two times greater. The reason for this is that if high initial temperature is prescribed around the connection of the plate and stiffener, significant deformations arise during cooling. These deformations and the residual stress affect not only the plate but also the stiffeners. In contrast, when initial stress is explicitly prescribed to plate elements a balanced (or almost balanced if initial geometrical distortion are present) stress state is created, so no extra deformations arise and no extra stress is transferred from the plate to the stiffeners. Hence, in this case panel strength is higher.

Table 18
Assumed residual stresses

Level of residual stress	Residual stress		Number of finite elements		
	Compression block, σ_{rc}/σ_Y	Tension block σ_{rt}/σ_Y	Along panel breadth	Tension block	Compression block
No residual stress	0%	0%	52	0	52
Slight level	5%	60%	52	4	48
Average level	15%	80%	51	8	43
Severe level	25%	100%	50	10	40

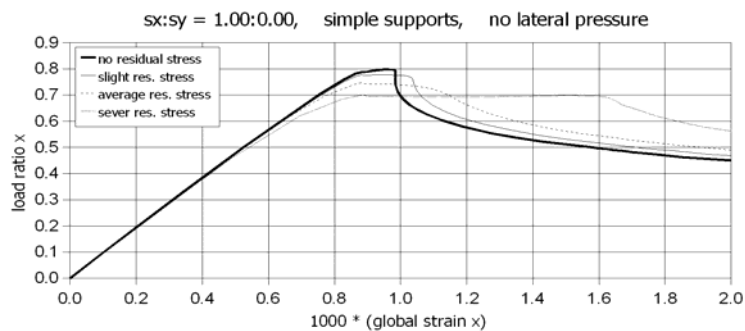Figure 52: Equilibrium path for different levels of residual stress

Table 19
Ultimate strength for models with different levels of residual stress

Load case		Level of residual stress	Ultimate strength	
$\sigma_x : \sigma_y$	Lateral pressure		σ_{xu}/σ_Y	Difference
1.00 : 0.00	0.0 MPa	No residual stress	0.7985	-
		Slight level (5%)	0.7785	-2.5%
		Average level (15%)	0.7470	-6.4%
		Severe level (25%)	0.7000	-12.3%

8.3.9   Effect of Fatigue Cracks

Bureau Veritas checked influence of fatigue cracks on ultimate strength of the panel. Two types of cracks were introduced (see Figure 53) – crack #1 at the junction of plate and transverse frame; and crack #2 including additional crack on stiffener web. Each of them was modelled in two variants – going through the whole span of plate (or web) and through 50% of span. Crack propagation was not taken into account.

Obtained results are presented in Figure 54 and Table 20. The table contains results only for cases with longitudinal edges simply supported, but change of boundary conditions has minor influence on the results. Conclusions from the study are:

- 50% crack #1 has small impact on ultimate strength and drop reaches at most 2.7% for cases with lateral pressure
- crack #1 (full) decreases strength by 5% to 9%. Decrease grows with domination of transverse compression and is almost independent on lateral pressure
- crack #2 in both variants (full and 50%) decreases strength by 6% to 55% and has a critical impact in combination with lateral pressure (primary factor) and transverse compression
- in general length of cracks in the plate affects strength of the panel
- cracks have particularly big effect in combination with lateral pressure
- under lateral pressure the area of buckling usually moves to the region where cracks are introduced
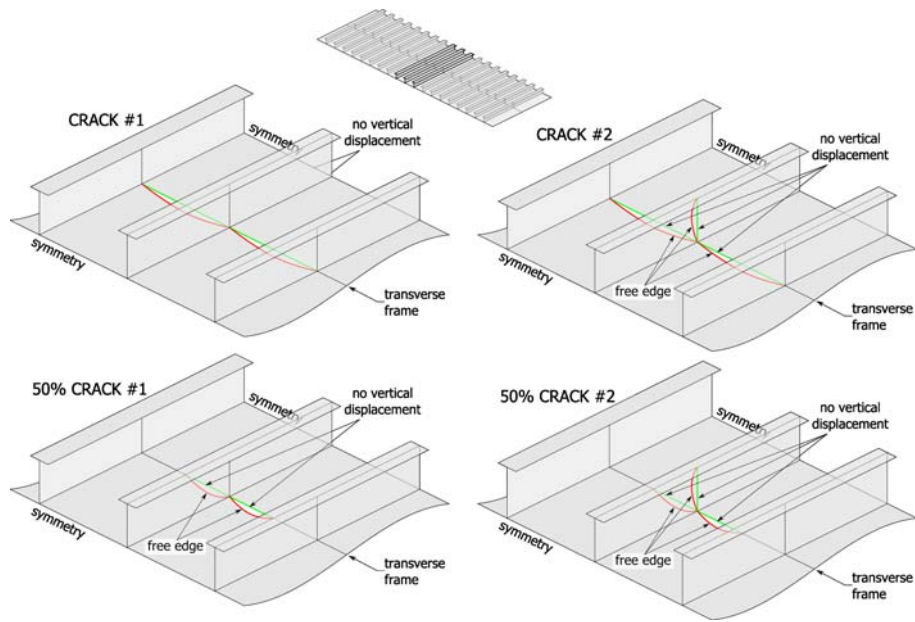
Figure 53: Different types of cracks applied

Table 20
Influence of different cracks on ultimate strength (simple supports)

Load case		No crack	Crack #1	50% crack #1	Crack #2	50% crack #2
$\sigma_x : \sigma_y$	Lateral pressure	$\sigma u/\sigma Y$	Difference	Difference	Difference	Difference
1.00 : 0.00	0.0MPa	0.83 (longi.)	-5.2%	-1.3%	-6.7%	-6.3%
	0.16MPa	0.76 (longi.)	-5.3%	-2.7%	-9.3%	-8.4%
0.79 : 0.21	0.0MPa	0.79 (longi.)	-4.5%	-1.0%	-6.0%	-5.7%
	0.16MPa	0.72 (longi.)	-4.5%	-2.6%	-26.9%	-24.0%
0.40 : 0.60	0.0MPa	0.33 (trans.)	-7.1%	-0.1%	-7.2%	-7.1%
	0.16MPa	0.31 (trans.)	-7.5%	-0.5%	-53.2%	-52.6%
0.00 : 1.00	0.0MPa	0.35 (trans.)	-9.2%	-0.8%	-10.4%	-10.2%
	0.16MPa	0.33 (trans.)	-9.0%	-0.3%	-54.9%	-54.3%

Figure 54: Interaction curves for different cracks under biaxial compression

9.   CONCLUSIONS AND RECOMMENDATIONS

Limit state based approaches are core methodologies for the design and safety assessment of newly-built structures, and also for the health monitoring of aging structu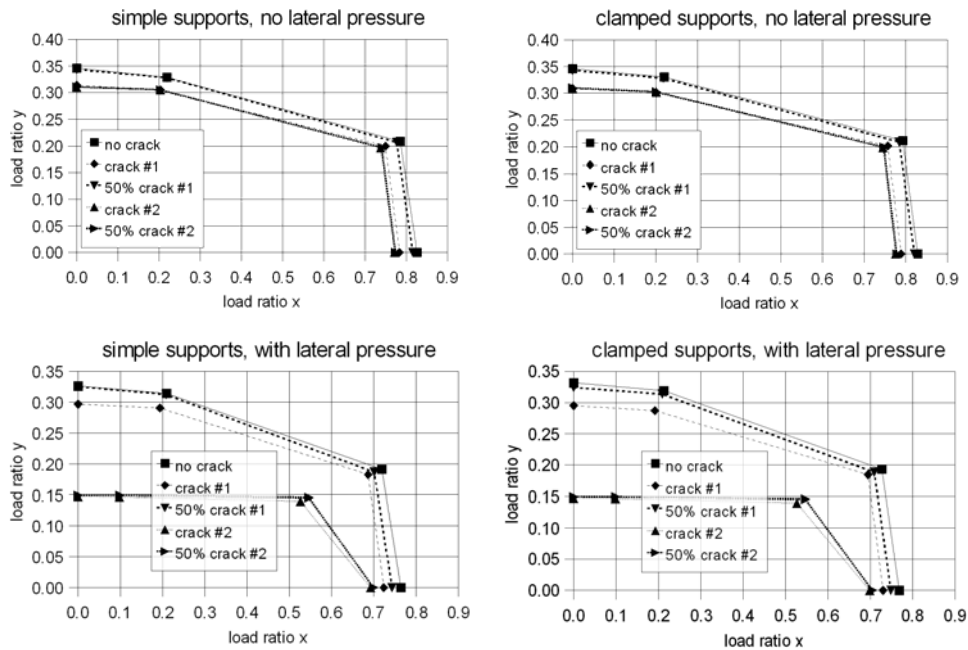res. While in service, structures are subjected to various phenomena arising from service requirements, ranging from routine to extreme or even accidental. As the environmental and operating conditions become harsher, structures are increasingly likely to be subjected to nonlinear structural consequences in conjunction with limit states, or the conditions under which they fail to perform their intended functions. It has been recognised that these limit states are a much better basis for structural design and strength assessment than allowable working stress because the true margin of structural safety is not determinable as long as limit states remain unknown.

As structures get older, they suffer various types of degradation, including corrosion and fatigue cracking damage. The health monitoring or condition assessment of aged structures is required to ensure their structural integrity and/or for structural longevity in association with relevant schemes of inspection and maintenance. Within the framework of health monitoring of aging structures, limit state based approaches play a key role.

In the three years since ISSC 2006, the maritime industry has used ultimate limit state design methods more extensively. The IACS CSR methods have been regularly applied

in the design and strength assessment of ship and offshore structures, and the ISO 18072-1 standard has been in effect since November 2007.

Various contributions to identifying the ultimate strength characteristics of structural components and system structures have been made in the last three years. However, there are still a lot of problem areas which are primarily due to the difficulty in determining the representative value of ultimate strength, i.e., C_k in Equation (1), and partial safety factor γ_C associated with uncertainties, while a variety of influencing parameters must be taken into account in ultimate strength computations.

The following are recommendations for future work in the area of ultimate strength in the maritime industry.

- Efforts are recommended to develop international standards that can be used to accurately and consistently compute the ultimate strength of ship structural components and hull girders, in association with various parameters of influence addressed in Chapter 1. Also, it is desirable to develop unified approaches of ultimate strength computations in association with the Common Structural Rules (CSR) of classification societies which currently differ depending on ship types.
- Today, nonlinear finite element methods are considered to be one of the most powerful approaches to computing ultimate strength. However, it is very important to realise that the nonlinear finite element method computations are significantly dependent on the structural modelling techniques applied. In this regard, the development of relevant nonlinear finite element method modelling techniques is highly desirable.
- Buckling collapse testing of large scale structural models and full scale ships is recommended to develop an experimental database which can be used to validate the analytical and numerical methods of ultimate strength computations.
- As the ocean environmental condition becomes harsher, the structure will be more likely subjected to dynamic or impact actions. Therefore, efforts are recommended to identify the buckling collapse characteristics of structural components and system structures under dynamic or impact actions.
- Efforts are recommended to determine the partial safety factors associated with the uncertainties indicated in Equation (1).
- Consideration of standardising ships in a similar fashion as aircraft is recommended so that structural designs can be thoroughly tested and proved, with more series of common designs instead of an ad-hoc approach that invariably introduces variation and hence the increased uncertainties and problems we face today.

REFERENCES

Abrate, S. (1991). Impact on laminated composite materials. *Applied Mechanical Review* 91:44, 155-190.

Adams, D.F. (2002). Tabbed versus untabbed compression specimens. *Composite Materials: Testing, Design, and Acceptance Criteria, ASTM STP 1416,* ed. A.T. Nettles, A. Zureick and W. Conshohocken, American Society of Testing Materials, PA, 1–14.

Adams, D.F. and Welsh, J.S. (1997). The Wyoming combined loading compression (CLC) test method. *Journal of Composite Technology Research* 19:3, 123–33.

Alinia, M.M., Hosseinzadeh, S.A.A. and Habashi, H.R. (2007). Numerical modelling for buckling analysis of cracked shear panels. *Thin-Walled Structures* 45, 1058–1067.

Alinia, M.M. and Moosavi, S.H. (2009). Stability of longitudinally stiffened web plates under interactive shear and bending forces. *Thin-Walled Structures* 47, 53-60.

Alsos, H.S. and Amdahl, J. (2007). On the resistance of tanker bottom structures during stranding. *Marine Structures* 20, 218-237.

Amlashi, H.K.K. and Moan, T. (2008). Ultimate strength analysis of a bulk carrier hull girder under alternate hold loading condition – A case study Part 1: Nonlinear finite element modelling and ultimate hull girder capacity. *Marine Structures* 21, 327-352.

API (1993). Recommended practice for planning – Designing and constructing fixed offshore platforms – working stress design, American Petroleum Institute.

Aquelet, N., Souli, M. and Olovsson, L. (2006). Euler-Lagrange coupling with damping effects: application to slamming problems. *Computer Methods in Applied Mechanics and Engineering* 195, 110–132.

Ashby, M.F. (1992). *Materials selection in mechanical design*. Pergamon, Oxford.

ASME V&V 10 (2006). Guide for verification and validation in computational solid mechanics, American Society of Mechanical Engineers, USA.

ASTM Standard D695-02a. (2002). Standard test method for compressive properties of rigid plastics. American Society of Testing Materials, West Conshohocken, PA, USA.

ASTM Standard D2344. (1995). Standard test method for apparent interlaminar shear strength of parallel fiber composites by short-beam method. American Society of Testing Materials, West Conshohocken, PA, USA.

ASTM Standard D3039–00. (2000). Standard test for tensile properties of polymer matrix composite materials. American Society of Testing Materials, West Conshohocken, PA, USA.

ASTM Standard D3410–95. (1995). Standard test method for compressive properties of polymer matrix composite materials with unsupported gage section by shear loading. American Society of Testing Materials, West Conshohocken, PA, USA.

ASTM Standard D3518. (2001). Standard test method for in-plane shear response of polymer matrix composite materials by tensile test of a ±45◦ laminate. American Society of Testing Materials, West Conshohocken, PA, USA.

ASTM Standard D3846. (1994). Standard test method for in-Plane shear strength of reinforced plastics. American Society of Testing Materials, West Conshohocken, PA, USA.

ASTM Standard D5379. (1998). Standard test method for shear properties of composite materials by the V-notched beam. American Society of Testing Materials, West Conshohocken, PA, USA.

Backman, M.E. and Goldsmith, W. (1978). The mechanics of penetration of projectiles into targets. *International Journal of Engineering Science* 16, 1-99.

Badran, S.F., Nassef, A.O. and Metwalli, S.M. (2007). Stability of Y stiffeners in ship plating under uniaxial compressive loads. *Ships and Offshore Structures* 2:1, 87-94.

Balden, V.H. and Nurick, G.N. (2005). Numerical simulation of the post-failure motion of

steel plates subjected to blast loading. *International Journal of Impact Engineering* 32, 14–34.

Bambach, M.R. Jama, H., X L Zhao, X.-L., and Grzebieta R.H.(2008). Hollow and concrete filled steel hollow sections under transverse impact loads. *Engineering Structures* 30:10, 2859-2870.

Belenkiy, L.M., Raskin, Y.N. and Vuillemin, J. (2007). Effective plating in elastic-plastic range of primary support members in double-skin ship structures. *Marine Structures* 20, 115-123.

Berggreen, C., Branner, K., Jensen, J. F. and Schultz, J. P. (2007). Application and analysis of sandwich elements in the primary structure of large wind turbine blades. *Journal of Sandwich Structures and Materials* 9, 525-552.

Blachut J. and Smith P. (2008). Buckling of multi-segment underwater pressure hull. *Ocean Engineering* 35, 247-260

Bollero, A., Casuscelli, F. and Rizzuto, E. (2002). Uncertainties in the evaluation of the longitudinal strength of ship. *Proc. International Shipbuilding Conference (ISC'2002)*, St. Petersburg.

Bolotin, V.V. (1996). Delaminations in composite structures: its origin, buckling, growth and stability. *Composites Part B*, 27B, 129–145.

Boon, B. (2007). A plea for large-scale testing. *Proc. MARSTRUCT 2007 Conference*, Glasgow.

Boutillier, V., Serror, M. and Parmentier, G. (2008). Simulation of the behaviour of fatigue cracks: A tool for inspection decision making on a ship's deck beam. *Proc. ASRANet Colloquium*, Athens, 25-27.

Branner, K. (2006). Modelling failure in cross-section of wind turbine blade. *Risø National Laboratory, NAFEMS-Seminar*, Denmark.

Branner, K., Jensen, F.M., Berring, P., Puri, A., Morris, A. and Dear, J. (2008). Effect of sandwich core properties on ultimate strength of a wind turbine blade. *Proc. 8th International Conference on Sandwich Structures*, University of Porto, Portugal.

Brazier, L.G. (1926). Late of the royal aircraft establishment. On the flexure of thin cylindrical shells and other 'thin' sections. *Reports and Memoranda* 1081:M.49, 1–30.

Bridgman, P. (1952). Studies in large plastic flow and fracture. *McGraw-Hill*, New York.

Brøndsted, P., Lilholt, H. and Lystrup, A. (2005). Composite materials for wind power turbine blades. *Annual Review of Materials Research* 35:38, 505.

Brubak, L. and Hellesland, J. (2008). Strength criteria in semi-analytical, large deflection analysis of stiffened plates in local and global bending. *Thin-Walled Structures* 46, 1382-1390.

Brubak, L., Hellesland, J. and Steen, E. (2007). Semi-analytical buckling strength analysis of plates with arbitrary stiffener arrangements. *Journal of Constructional Steel Research* 63, 532–543.

Cabezas, E. and Celentano, D. (2002). Experimental and numerical analysis of the tensile test using sheet specimens. *Mecánica Computacional* XXI, 854–873.

Chen, N. and Guedes Soares, C. (2008). Ultimate longitudinal strength of ship hulls of composite materials, *Journal of Ship Research* 52:3, 184–193.

Cho, S.R., Park, H.Z., Kim, H.S. and Seo, J.S. (2007). Experimental and numerical investigations on the ultimate strength of curved stiffened plates. *Proc. 10th International Symposium on Practical Design of Ships and Other Floating Structures*, Huston.

Choo, Y.S., Chen, Z., Wardenier, J. and Gronbech, J. (2007a). Static strength of simple and grouted tubular X-joints subjected to in-plane bending. *Proc. 5th International Conference on Advanced Steel Structures,* Singapore.

Choo, Y.S., Qian, X.D. and Wardenier, J. (2006). Effects of boundary conditions and chord stresses on static strength of thick-walled CHS K-joints. *Journal of Constructional*

Steel Research 62, 316-328.

Choo, Y. S., Shen, W. and Gronbech, J. (2007b). Hot spot stresses for as-welded and grouted tubular X-joints subjected to in-plane bending. *Proc. 11th International Conference on Jack-up Platform*, London.

Collette, M.D. (2007). The impact of fusion welds on the ultimate strength of aluminium structures. *Proc. ORADS 2007*, Houston.

Davies, G.A.O., Hitchings, D. and Ankersen, J. (2006). Predicting delamination and debonding in modern aerospace composite structures. *Composites Science and Technology* 66, 846–854.

De Smet, B.J. and Bach, P.W. (1994). Database FACT: Fatigue of composites for wind turbines. *Proc. 3rd IEA Symposium on Wind Turbine Fatigue, ECN, Petten*, 22–23, The Netherlands.

De Vries, W. E., van der Tempel, J., Carstens, H., Argyriadis, K., Passon, P., Camp, T. and Cutts, R. (2007). Assessment of bottom-mounted support structure types with conventional design stiffness and installation techniques for typical deep water sites. *Deliverable Report* D4.2.1, UpWind, EU.

DNV/Risø. (2002). Guidelines for design of wind Turbines. *2nd Edition, DNV/Risø publication*, Denmark.

Doege, E., Meyer-Nolkemper, H. and Saeed, I. (1986). Fliesskurvenatlas metallischer werkstoffe. *Carl Hanser Verlag*.

EN 1993-1-12.2007 (2007). *Eurocode 3: Design of steel structures* – Part 1.12: additional rules for the extension of EN 1993 up to steel grades S700.

Estefen, T.P., Werneck, D.S. and Estefen, S.F. (2007). Influence of the geometric imperfection on the buckling behavior of floating platform column under axial Load. *Proc. OMAE 2007*, San Diego, OMAE2007-29659.

Fleck, N.A. (1997). Compressive failure in fibre composites. *Advances in Applied Mechanics* 33, 43–117.

Fleischer, O., Herion, S. and Puthli, R. (2008). Numerical investigations on the static behaviour of CHS X-joints made of high strength steels. *Proc. 12th International Symposium on Tubular Structures*, Shanghai, China.

Fujikubo, M., Harada, S, Yao, T., Khedmati, M.R. and Yanagihara, D. (2005a). Estimation of ultimate strength of continuous stiffened panel under combined transverse thrust and lateral pressure, Part 2: Continuous stiffened panel. *Marine Structures* 18, 411–417.

Fujikubo, M., Yao, T., Khedmati, M.R., Harada, S. and Yanagihara, D. (2005b). Estimation of ultimate strength of continuous stiffened panel under combined transverse thrust and lateral pressure, Part 1: Continuous plate. *Marine Structures* 18, 383–410.

Gavrylenko, G.D. (2007). Transformed initial dent as a trigger of the post-buckling process. *Thin-Walled Structures* 45, 840–844.

Gho, W.M. and Yang, Y. (2008). Parametric equation for static strength of tubular circular hollow section joints with complete overlap of braces. *Journal of Structural Engineering* 134:3, 393-401.

Goldfeld, Y. (2009). An alternative formulation in linear bifurcation analysis of laminated shells. *Thin-Walled Structures* 47, 44-52.

Gong, S.W. and Lam, K.Y. (2006). On attenuation of floating structure response to underwater shock. *International Journal of Impact Engineering* 32, 1857–1877.

Gordo, J.M. (2008). Resistência de placas imperfeitas sob compressão axial (Ultimate strength of imperfect plates under axial compression). *XIV Congresso SOBENA 2008*, Rio de Janeiro, Brasil (in Portuguese).

Gordo, J. M. and Guedes Soares, C. (2004). Experimental evaluation of the ultimate bending moment of a box girder. *Marine Systems and Offshore Technology* 1:1, 33–

46.

Gordo, J.M. and Guedes Soares, C. (2007). Experimental evaluation of the behavior of a mild steel box girder under bending moment. *Proc. International Conference on Advancements in Marine Structures (MARSTRUCT 2007)*, Glasgow.

Gordo, J.M. and Guedes Soares, C. (2008a). Compressive tests on short continuous panels. *Marine Structures* 21, 113–137.

Gordo, J.M. and Guedes Soares, C. (2008b). Compressive tests on continuous long stiffened panels. *Proc. OMAE 2008*, OMAE2008-57873, Portugal.

Gordo, J.M. and Guedes Soares, C. (2008c). Experimental evaluation of the behaviour of a mild steel box girder under bending moment. *Ships and Offshore Structures* 3:4, 347-358.

Graham, D. (2007). Predicting the collapse of externally pressurised ring-stiffened cylinders using finite element analysis. *Marine Structures* 20, 202-217.

Gudze, M.T. and Melcher, R.E. (2006). Prediction of naval ship ballast tank corrosion using operational profiles. *International Journal of Maritime Engineering* 148:A3, 77-86.

Guedes Soares, C. (2007). Collapse behaviour of damaged panels with a dimple imperfection. *Proc. OMAE 2007*, OMAE2007-29777, Hamburg.

Guedes Soares, C.,Teixeiria, A.P., Luis, R.M., Quesnel, T., Nikolov, P.I., Steen, E., Khan, I.A., Toderan, C., Olaru, V.D., Bollero, A. and Taczlaca, M. (2005). Effect of the shape of localized imperfections on the collapse strength of plates. *Maritime Transportation and Exploitation of Ocean 2005*.

Guo, J., Wang, G., Ivanov, L. and Perakis, A.N. (2008). Time-varying ultimate strength of aging tanker deck plate considering corrosion effect. *Marine Structures* 21, 402-419.

Han, L.H., Lu, H., Yao G.H. & F Y Liao F.Y. (2006). Further study on the flexural behaviour of concrete-filled steel tubes. Journal of Constructional Steel Research 62, 554-565.

Han, L.H., Tao Z. and Yao G.H. (2007). Behaviors of concrete-filled steel tubular members subjected to combined loading. *Thin-Walled Structures* 45, 600-619.

Harada, M. and Shigemi, T. (2007). A method for estimating the uncertainties in ultimate longitudinal strength of cross section of a ship's hull based on nonlinear FEM. *Proc. PRADS 2007,* Houston.

Harada, M. and Fujikubo, M. (2005). Estimation of buckling and ultimate strength of a stiffened web plating with cutout. *Proc. ISOPE 2005 Conference* IV, 745–751.

Hong, L. and Amdahl, J. (2007). Plastic design of laterally patch loaded plates for ships. *Marine Structures* 20, 124–142.

Hong, L. and Amdahl, J. (2008a). Plastic mechanism analysis of the resistance of ship longitudinal girders in grounding and collision. *Ship and Offshore Structure*s 3:3, 159–171.

Hong, L. and Amdahl, J. (2008b). Crushing resistance of web girders in ship collision and grounding. *Marine Structures* 21, 374-401.

Horte, T., Wang, G. and White, N. (2007). Calibration of the hull girder ultimate capacity criterion for the double hull tanker. *Proc. PRADS 2007 Conference*, Houston.

Huilong, R., Chenfeng, L. and Guoqing, F. (2008). Calculation method of the residual capability of damaged warships. *Proc. OMAE 2008 Conference*, OMAE2008-57726, Portugal.

IIW (2008). Static design procedure for welded hollow section joints – recommendations. International Institute of Welding IIW Doc. XV-E-1281r1-08, IIW Annual Assembly, Graz, Austria.

Iosipescu, N. (1967). New accurate procedure for single shear testing of metals. *Journal of Materials* 2:3, 537–66.

Ishibashi, K., Fujikubo, M. and Yao, T. (2006). Development of ISUM element for rectangular plate with cutout. *Proc. 16th International Offshore and Polar*

Engineering Conference IV, 339–345.

ISO 527. (1997). Plastics – Determination of tensile properties. International Organization for Standardization, Geneva.

ISO/TR 11069 (1995). Aluminium structures – Materials and design – Ultimate limit state under static loading. International Organization for Standardization, Geneva.

ISO 14126. (1999). Fibre-reinforced plastic composites – Determination of the compression properties in the in-plane direction. International Organization for Standardization, Geneva.

ISO 14129. (1998). Fibre-reinforced plastic composites – Determination of the in-plane shear stress/shear strain response, including the in-plane shear-modulus, by the ±45° tension test method. International Organization for Standardization, Geneva.

ISO 16587 (2005). Mechanical vibration and shock – Performance parameters for condition monitoring of structures. International Organization for Standardization, Geneva.

ISO 18072-1 (2007). Ships and marine technology – Ship structures – Part 1: General requirements of their limit state assessment. International Organization for Standardization, Geneva.

ISO/Draft DIS 18072-2 (2009). Ships and marine technology – Ship structures – Part 2 – Requirements for their ultimate limit state assessment. International Organization for Standardization, Geneva.

ISO 19901 (2004). Petroleum and natural gas industries – Specific requirements for offshore structures – Part 2: Seismic design procedures and criteria. International Organization for Standardization, Geneva.

Ivanov, L. D. and Wang, G. (2007). An approximate analytical method for calculation of the still water bending moments, shear forces and the ship's trim in the early design stages. *International Journal of Maritime Engineering* 149:A2, 1–40.

Jensen, F.M. (2008). Ultimate strength of a large wind turbine blade. Risø National Laboratory for Sustainable Energy, Technical University of Denmark, Denmark.

Jensen, F.M., Falzon, B.G., Ankersen, J. and Stang, H. (2005). Structural testing and numerical simulation of a 34m composite wind turbine blade. *Composite Structures* 76, 52–61.

Jones, N. (2006). Some recent developments in the dynamic inelastic behaviour of structures. *Ships and Offshore Structures* 1:1, 37–44.

Karvinen, K.G. and Pegg, N.G. (2006). A simplified method for nonlinear failure analysis of stiffened plates. *Marine Structures* 19, 97–109.

Kensche, C.W., ed. (1996). Fatigue of Materials and Components for Wind Turbine Rotor Blades*, EUR 16684. Eur. Comm.*, Luxembourg.

Khan, I.A. and Das, P.K. (2008). Reliability analysis of intact and damaged ships considering combined vertical and horizontal bending moments. *Ships and Offshore Structures* 3:4, 371–384.

Khan, I.A., Das, P.K. and Parmentier, G. (2006). Ultimate strength and reliability analysis of a failed VLCC. *Proc. 3rd International ASRANet Colloquium*, Glasgow.

Khedmati, M.R. and Rastani, M. (2006). Nonlinear elastoplastic behaviour of intermittently welded stiffened plates under inplane compression. *Proc. OMAE 2006 Conference*, OMAE2006-92603, San Diego.

Kim, U.N, Choe, I.H. and Paik, J.K. (2008). On buckling and ultimate strength of perforated plate panels under axial compression: experimental and numerical investigations with design formulations. *Proc. SNAME Annual Meeting*, Houston.

Kippenes, J., Byklum, E. and Steen, J. (2007). Ultimate strength of open corrugated panels. *Proc. PRADS 2007 Conference*, Houston.

Kleiber, M., Kotula, W. and Saran, M. (1987). Numerical analysis of dynamic quasi-bifurcation. *Engineering Computations* 4, 48–52.

Kong, C., Bang, J. and Sugiyama, Y. (2005). Structural investigation of composite wind turbine blade considering various load cases and fatigue life. *Energy* 30, 2101–2114.

Kubiak, T. (2007). Criteria of dynamic buckling estimation of thin-walled structures. *Thin-Walled Structures* 45, 888–892.

Kühlmeier, L. (2007). Buckling of wind turbine rotor blades – Analysis, design and experimental validation. Ph.D. Thesis, Aalborg University, Denmark.

Kühlmeier, L., Thomsen, O.T. and Lund, E. (2005). Large scale buckling experiment and validation of predictive capabilities. *Proc. 15th International Conference on Composite Materials (ICCM-15)*, Durban, South Africa.

La Rosa, G., Mirone, G. and Risitano, A. (2003). Post necking elasto-plastic characterisation: degree of approximation in the Bridgman method and properties of the flow stress/true stress ratio. *Metallurgical and Materials Transactions* A34, 615–624.

Lai, W. (2007). Transient dynamic response of submerged sphere shell with an opening subjected to underwater explosion. *Ocean Engineering* 34, 653–664.

Lamothe, R.M. and Nunes, J. (1983). Evaluation of fixturing for compression testing of metal matrix and polymer/expoxy composites. *Compression Testing of Homogeneous Materials and Composites. ASTM STP 808*, Edited by R Chait, R Papino, W., American Society of Testing Materials, Conshohocken, PA, 241–253.

Liang, C. and Tai, Y. (2006). Shock responses of a surface ship subjected to noncontact underwater explosions. *Ocean Engineering* 33, 748–772.

LM Glasfiber (2004). LM Newsletter, May 2004. LM Glasfiber A/S. http://www.lmglasfiber.com/upload/lmnews_200405_uk.pdf.

Loskin, A.Z., Mishkevich, V.G. and Ivanov, L.D. (2008). Buckling of a simply supported beam on an elastic foundation supported within its span with elastic supports – Buckling of grillages. *Ships and Offshore Structures* 3:2, 99-104.

Luis, R., Guedes Soares, C. and Nikolov, P.I. (2008). Collapse strength of longitudinal plate assemblies with dimple imperfections. *Ships and Offshore Structures* 3:4, 359–370.

Luis, R., Witkowska, M. and Guedes Soares, C. (2006). Ultimate strength of transverse plate assemblies under uniaxial loads. *Proc. OMAE 2006 Conference*, San Diego, OMAE2006-92664.

Mandell, J.F. and Samborsky, D.D. (1997). DOE/MSU Composite materials fatigue database. Test Methods, materials, and analysis. *SAND97-3002, UC-1210, Sandia Natl. Lab.,* Albuquerque, NM.

Manevich, A.I. (2007). Effect of strain hardening on the buckling of structural members and design codes. *Thin-Walled Structures* 45, 810–815

Mansour, A.E. and Liu, D. (2008). Strength of ships and ocean structures. SNAME, Jersey City, NJ, USA.

Masaoka, K. and Mansour, A. (2008). Compressive strength of stiffened plates with imperfections: Simple design equations. *Journal of Ship Research* 52:3, 227–237.

Mayer, R.M., ed. (1996). Design of composite structures against fatigue. *Mechanical Engineering*, Suffolk, UK.

Mirone, G. (2004). Approximate model of the necking behaviour and application to the void growth prediction. *International Journal of Damage Mechanics* 13:3, 241–261.

Mittelstedt, C. (2008). Explicit analysis and design equations for buckling loads and minimum stiffener requirements of orthotropic and isotropic plates under compressive load braced by longitudinal stiffeners. *Thin-Walled Structures* 46, 1409–1429.

Moan, T. (2004). Marine structures for the future – a sea of opportunities, *Marine Systems and Offshore Technology* 1:1, 5–24.

Moan, T. (2007). Design of offshore structures and ships for damage tolerance. *Marine Systems and Offshore Technology* 3:1, 51-65.

Moan, T., Gao, Z. and Uraga, E. (2005). Uncertainty of wave induced repose of marine

structures due to long-term variation of extratropical wave conditions. *Marine Structures* 18:4, 359–382.

Moon, J., Yi, J.W., Choi, B.H. and Lee, H.E. (2009). Lateral-torsional buckling of I-girder with corrugated webs under uniform bending. *Thin-Walled Structures* 47, 21-30.

Mukherjee, K.S. and Yao, T. (2006). Buckling/elastoplastic collapse behavior and strength of continuous tee-bar stiffened plates. *Journal of Offshore Mechanics and Arctic Engineering* 128, 145–155.

Murphy, A., McCune, W., Quinn, D. and Price M. (2007). The characterisation of friction stir welding process effects on stiffened panel buckling performance. *Thin-Walled Structures* 45, 339–351.

Nakai, T., Matsushita, H. and Yamamoto, N. (2006). Effect of pitting corrosion on the ultimate strength of steel plates subjected to in-plane compression and bending. *Journal of Marine Science and Technology* 11, 52–64.

Nikolov, P.I. (2007). Collapse strength of damaged plating between stiffeners, maritime transportation and exploitation of ocean and coastal resources. Edited by C. Guedes Soares & P. Kolev, Taylor & Francis Group, 237–244, London.

Nikolov, P.I. (2008). Collapse strength of damaged plating, proceeding. *Proc. OMAE 2008 Conference*, OMAE2008-57119, Lisbon.

Nilsson, K.F., Asp, L.E., Alpman, J.E. and Nystedt, L. (2001). Delamination buckling and growth for delaminations at different depths in a slender composite panel. *International Journal of Solids and* Structures 38, 3039–3071.

Ok, D., Pu, Y. and Incecik, A. (2007a). Artificial neural networks and their application to assessment of ultimate strength of plates with pitting corrosion. *Ocean Engineering* 34, 2222–2230.

Ok, D., Pu, Y. and Incecik, A. (2007b). Computation of ultimate strength of locally corroded unstiffened plates under uniaxial compression. *Marine Structures* 20, 100-114.

Overgaard, L. and Lund, E. (2005). Structural design sensitivity analysis and optimization of vestas V52 wind turbine blade. *Proc. 6th World Congress on Structural and Multidisciplinary Optimization*, Rio de Janeiro, Brasil.

Overgaard, L. and Lund, E. (2007a). Damage analysis of a wind turbine blade. *Proceedings of the ECCOMAS thematic Conference on Mechanical Response of Composites*, Portugal.

Overgaard, L. and Lund, E. (2007b). Interdisciplinary damage and stability analysis of a wind turbine blade. *Proc. 16th International Conference on Composite Materials*, Tokyo.

Ozguc, O., Das, P.K. and Barltrop, N. (2006a). Analysis on the hull girder ultimate strength of a bulk carrier using simplified method based on an incremental – Iterative Approach. *Proc. OMAE 2006 Conference*, OMAE2006-92338, San Diego.

Ozguc, O., Das, P.K. and Barltrop, N. (2006b). A proposed method to evaluate hull girder ultimate strength. *Ships and Offshore Structures* 1:4, 335–345.

Packer, J.A., Sherman, D.R. and Lecce, M. (2008). Hollow structural section connections design guide. *American Institute of Steel Construction*, Chicago, USA.

Pahos, S.J., Das, P.K. and Dow, R. (2008). The structural response of a bulk carrier under internal impulsive loading from cargo auto-ignition. *Maritime Industry, Ocean Engineering and Coastal Resources*, 257–262.

Paik, J.K. (2004). Corrosion analysis of seawater ballast tank structure. *International*

Journal of Maritime Engineering 146:A1, 1–12.

Paik, J.K. (2005). Ultimate strength of dented steel plates under edge shear loads. *Thin-Walled Structures* 43, 1475–1492.

Paik, J.K. (2007a). Empirical formulations for predicting the ultimate compressive strength of welded aluminium stiffened panels. *Thin-Walled Structures* 45, 171–184.

Paik, J.K. (2007b). Characteristic of welding induced initial deflections in welded aluminium plates. *Thin-Walled Structures* 45, 493–501.

Paik, J.K. (2007c). Ultimate limit state performance of oil tanker structures designed by IACS common structural rules. *Thin-Walled Structures* 45, 1022–1034

Paik, J.K. (2007d). Practical techniques for finite element modelling to simulate structural crashworthiness in ship collisions and grounding (Part I: Theory). *Ships and Offshore Structures* 2:1, 69–80.

Paik, J.K. (2007e). Practical techniques for finite element modelling to simulate structural crashworthiness in ship collisions and grounding (Part II: Verification). *Ships and Offshore Structures* 2:1, 81–85.

Paik, J.K. (2007f). Ultimate strength of perforated steel plates under edge shear loading. *Thin-Walled Structures* 45, 301–306.

Paik, J.K. (2007g). The effective use of experimental and numerical data for validating simplified expressions of stiffened steel panel ultimate compressive strength. *Marine Technology* 44, 93-105.

Paik, J.K. (2008a). Ultimate strength of perforated steel plates under combined biaxial compression and edge shear loads. *Thin-Walled Structures* 46, 207–213.

Paik, J.K. (2008b). Some recent advances in the concepts of plate-effectiveness evaluation. *Thin-Walled Structures* 46, 1035–1046.

Paik, J.K. (2008c). Residual ultimate strength of steel plates with longitudinal cracks under axial compression – experiments. *Ocean Engineering* 35, 1775-1783.

Paik, J.K. (2009). Mechanical collapse testing of friction stir welded aluminium stiffened plate structures. SR-1454, Ship Structure Committee, Washington D.C., USA.

Paik, J.K., Andrieu, C. and Cojeen, H.P. (2008a). Mechanical collapse testing on aluminium stiffened plate structures for marine applications. *Marine Technology* 45:4, 228–240.

Paik, J.K. and Frieze, P.A. (2001). Ship structural safety and reliability. *Progress in Structural Engineering and Materials* 3:2, 198-210.

Paik, J.K., Hwang, S.W., Park, J.S. and Kim, M.S. (2008b). Ultimate limit state performance of 300k double hull oil tanker structures: Pre-CSR versus CSR designs. *Proc. ASRANet Colloquium*, 25-27 June, Athens, Greece.

Paik, J.K., Hughes, O.F., Hess, P.E. and Renaud, C. (2005a). Ultimate limit state design technology for aluminum multi hull ship structure. *Trans. SNAME* 113, 270–305.

Paik, J.K., Kim, J.Y., Jung, J.M. and Kim, M.S. (2008c). Ultimate limit state performance of 170k bulk carrier structures. *Proc. ASRANet Colloquium*, 25-27 June, Athens, Greece.

Paik, J.K., Kim, B.J. and Seo, J.K., (2007). Evaluation of IACS common structural rules in terms of ultimate limit state design and assessment of ship structures. *Proc. OMAE 2007 Conference*, OMAE2007-29187, Hamburg.

Paik, J.K., Kim, B.J. and Seo, K.J. (2008d). Methods for ultimate limit state assessment of ships and ship-shaped offshore structures: Part I – Unstiffened plates. *Ocean Engineering* 35, 261–270.

Paik, J.K., Kim, B.J. and Seo, J.K. (2008e). Methods for ultimate limit state assessment of

ships and ship-shaped offshore structures: Part II – Stiffened panels. *Ocean Engineering* 35, 271–280.

Paik, J.K., Kim, B.J. and Seo, J.K. (2008f). Methods for ultimate limit state assessment of ships and shipshaped offshore Structures: Part III – Hull girders. *Ocean Engineering* 35, 281-286.

Paik, J.K. and Kumar, Y.V. (2006). Ultimate strength of stiffened panels with cracking damage under axial compression or tension. *Journal of Ship Research* 50, 231-238.

Paik, J.K., Kumar, Y.V. and Lee, J.M. (2005b). Ultimate strength of cracked plate elements under axial compression or tension. *Thin-Walled Structures* 43, 237–272.

Paik, J.K., Lee, J.M., Hwang, J.S. and Park, Y.I. (2003a). A time-dependent corrosion wastage model for the structures of single- and double-hull tankers and FSOs and FPSOs. *Marine Technology* 40:3, 201–217.

Paik, J.K., Lee, J.M. and Ko, M.J. (2004). Ultimate shear strength of plate elements with pit corrosion wastage. *Thin Walled Structures* 42, 1161–1176.

Paik, J.K. and Melchers, R.E. (2008). Condition assessment of aged structures. CRC Press, New York.

Paik, J.K. and Seo, J.K. (2007). A method for progressive structural crashworthiness analysis under collision and grounding. *Proc. M ARSTRUCT 2007 Conference*, Glasgow.

Paik, J.K., Seo, J.K. and Kim, B.J. (2008g). Ultimate limit state assessment of the M.V. Derbyshire hull structure. *Journal of Offshore Mechanics and Arctic Engineering* 130, 021002-1-9.

Paik, J.K., Seo, J. K., Lee, J.M. and Park, J.H. (2006). Ultimate limit state assessment of the M.V. Derbyshire hull structure. *Proc. OMAE 2006 Conference*, San Diego, OMAE2006-92384.

Paik, J.K. and Shin, Y. S. (2006). Structural damage and strength criteria for ship stiffened panels under impact pressure actions arising from sloshing, slamming and green water loading. *Ships and Offshore Structures* 1:3, 249–256.

Paik, J.K. and Thayamballi, A.K. (2003). *Ultimate limit state design of steel-plated structures*. John Wiley & Sons, Chichester, UK.

Paik, J.K. and Thayamballi, A.K. (2007). *Ship-shaped offshore installations: Design, building, and operation*. Cambridge University Press, Cambridge, UK.

Paik, J.K., Thayamballi, A.K., Park, Y.I. and Hwang, J.S. (2003b). A time-dependent corrosion wastage model for bulk carrier structures. *International Journal of Maritime Engineering* 145:A2, 61–87.

Paik, J.K., Thayamballi, A.K., Ryu, J.Y., Jang, J.H., Seo, J.K., Park, S.W., Seo, S.K., Andrieu, C., Cojeen, H.P. and Kim, N.I. (2006). The statistics of weld induced initial imperfections in aluminum stiffened plate structures for marine application. *International Journal of Maritime Engineering* 148:A4, 19–63.

Paik, J.K. and Won, S.H. (2007). On deformation and perforation of ship structures under ballistic impacts. *Ships and Offshore Structures* 2:3, 217–226.

Park, B. and Cho, S. (2006). Simple design formulae for predicting the residual damage of unstiffened and stiffened plates under explosion loadings. *International Journal of Impact Engineering* 32, 1721–1736.

Parunov, J., Senjanovic, I. and Guedes Soares, C. (2007). Hull-girder reliability of new generation oil tankers. *Marine Structures* 20, 49-70.

Pavier, M.J. and Clarke, M.P. (1995). Experimental techniques for the investigation of the

effects of impact damage on carbon fibre composites. *Composites Science and Technology* 55, 157–169.

Peck, S.O. and Springer, G.S. (1991). The behaviour of delaminations in composite plates – analytical and experimental results. *Journal of Composite Materials* 25: 907–929.

Pecknold, D.A., Marshall, P.W. and Bucknell, J. (2007). New API RP2A tubular joint strength design provisions. *Journal of Energy Resources Technology* 129:3, 177-189.

Puskar F.J., Spong R.E., Ku A., Gilbert R.B. and Choi Y.J. (2006b). Assessment of fixed offshore platform performance in Hurricane Ivan. *Offshore Technology Conference*, OTC 18325, Houston.

Puskar F.J., Westlake H.S., P.E. O'Connor and Bucknell J. (2006a). The development of a recommended practice for structural integrity management (SIM) of fixed offshore platforms. *Offshore Technology Conference*, OTC 18332, Houston.

Puthli, R. (2008). High strength steels and cast steel nodes for tubular structures – investigations, applications and research results. ISTS Kurobane Lecture. *Proc. 12th International Symposium on Tubular Structures*, Shanghai, China.

Qi, E. and Cui, W. (2006a). Analytical method for ultimate strength calculations of intact and damaged ship hulls. *Ships and Offshore Structures* 1:2, 153–163.

Qi, E. and Cui, W. (2006b). Design-oriented methods of ultimate hull girder strength. *Proc. OMAE 2006 Conference*, OMAE2006-92506, San Diego.

Qian X.D., Choo, Y.S., Liew, J.Y.R. and Wardenier, J. (2007). Static Strength of Thick-Walled CHS X-joints Subjected to Brace Moment Loadings, *Journal of Structural Engineering* 133:9, 1278-1287.

Qian, X., Choo, Y.S., Vegte, G.J. van der, Wardenier, J. (2008). Evaluation of the new IIW CHS strength formulae for thick-walled joints. *Proc. 12th International Symposium on Tubular Structures*, Shanghai, China.

Qian, X., Wardenier, J. and Choo Y.S. (2007). A uniform approach for the design of 100% CHS overlap joints. *Proc. 5th International Conference on Advances in Steel Structures*, Singapore.

Qin, Z. and Batra, R.C. (2008). Local slamming impact of sandwich composite hulls. *International Journal of Solids and Structures*, in press.

Rabczuk, T., Samaniego, E., and Belytschko, T. (2007). Simplified model for predicting impulsive loads on submerged structures to account for fluid-structure interaction. *International Journal of Impact Engineering* 34, 163–177.

Rajendran, R., Kim, B. J. and Paik, J. K. (2006). Design of warship plates against underwater explosions. *Ships and Offshore Structures* 1:4, 347–356.

Rushton, N., Schleyer, G.K., Clayton, A.M. and Thompson, S. (2008). Internal explosive loading of steel pipes. *Thin-Walled Structures* 46, 870-877.

Samuelides, M.S., Daliakopoulos, D. and Paik, J.K. (2007). Simulation of response of steel plates under pressure pulses. *Proc. PRADS 2007 Conference*, Houston.

Satoh, K. and Toyoda, M. (1970). Static strength of welded plates including soft interlayer under Tension across a Weld Line. *Trans. of the Japan Welding Society* 1:2, 10–17.

Schleyer, G.K., Kewaisy, T.H., Wesevich, J.W. and Langdon, G.S. (2006). Validated finite element analysis model of blast wall panels under shock pressure loading. *Ships and Offshore Structures* 1:3, 257–271.

Schleyer, G.K., Langdon, G.S. (2005). Inelastic deformation and failure of profiled stainless steel blast wall panels. Part I: experimental investigations. *International Journal of Impact Engineering* 31, 341–369.

Schleyer, G.K. and Langdon, G.S. (2006). Deformation and failure of profiled stainless steel blast wall panels. Part III: finite element simulations and overall summary. *International Journal of Impact Engineering* 32, 988–1012.

Schleyer, G.K., Lowak, M.J., Polcyn, M.A. and Langdon, G. S. (2007). Experimental investigation of blast wall panels under shock pressure loading. *International Journal of Impact Engineering* 34, 1095–1118.

Short, G.J, Guild, F.J. and Pavier, M.J. (2001). The effect of delamination geometry on the compressive failure of composite laminates. *Composites Science and Technology* 61, 2075–2086.

Short, G.J., Guild, F.J. and Pavier, M.J. (2002). Delaminations in flat and curved composite laminates subjected to compressive load. *Composite Structures* 58, 249–258.

Shufrin, I., Rabinovitch, O. and Eisenberger, M. (2008). Buckling of laminated plates with general boundary conditions under combined compression, tension, and shear – A semi-analytical solution. *Thin-Walled Structures* 46, 925-938.

Sielski, R.A. (2007). Review of structural design of aluminium ships and crafts. *Trans. SNAME* 115, 1-30.

Sielski, R.A. (2008). Research needs in aluminium structure. *Ships and Offshore Structures* 3:1, 57–65.

Smith, M.J. and MacKay, J.R. (2005). Overall elasto-plastic collapse of ring stiffened cylinders with corrosion damage. *International Journal of Maritime Engineering* 147:A1, 54-62.

Smits, A., van Hemelrijck, D. and Philippidis, T. (2004a). The digital image correlation technique as full field strain technique on biaxial loaded composites using cruciform specimens. *Proc. 12th International Conference on Experimental Mechanics*, Politecnico di Bari.

Smits, A., van Hemelrijck, D., Philippidis, T., van Wingerde, A.M. and Cardon, A. (2004b). Optimisation of a cruciform test specimen for bi-axial loading of fibre reinforced material systems. *Proc. 11th European Conference on Composite Materials*, London.

Steen, E., Byklum, E. and Hellesland, J. (2008). Elastic postbuckling stiffness of biaxially compressed rectangular plates. *Engineering Structures* 30:10, 2631-2643.

Sun, H.H. and Spencer, J. (2005). Buckling strength assessment of corrugated panels in offshore structures. *Marine Structures* 18, 548–565.

Sun, H.H. and Wang, X. (2005a). Buckling and ultimate strength assessment of FPSO structures. *Trans. SNAME* 113, 634-656.

Sun, H.H. and Wang, X. (2005b). Procedure for calculating hull girder ultimate strength of ship structures. *Marine Systems and Offshore Technology* 1:3, 137–144.

Teixeira, A.P. and Guedes Soares, C. (2008). Simulation of inspections on ship plates with random corrosion patterns. *Journal of Ship Production* 24:3, 168–175.

Toderan, C., Richir, T., Caprace, J. and Rigo, P. (2006). Assessment of ultimate bending moment of ships from a reliability point of view, using independent perturbations method. *Proc. ASRANet 2006,* 62–85.

Ueda, Y. and Yao, T. (1985). The influence of complex initial deflection modes on the behaviour and ultimate strength of rectangular plates in compression. *Journal of Constructional Steel Research* 5:4, 265–302.

Van Wingerde, A.M., Nijssen, R.P.L., van Delft, D.R.V., Janssen, L.G.J., Brøndsted, P., et al. (2003). Introduction to the OPTIMAT BLADES project. *Proc. European Wind Energy Conference Exhibition*, Madrid.

Vegte, G.J. van der, Makino, Y. and Wardenier, J. (2007a). New ultimate strength formulation for axially loaded CHS K-joints. *Proc. 5th International Conference on Advances in Steel Structures*, Singapore.

Vegte, G.J. van der, Makino, Y. and Wardenier, J. (2007b). Effect of chord load on ultimate strength of CHS X-joints. *International Journal of Offshore and Polar Engineering* 17:4, 301-308.

Vegte, G.J. van der, Wardenier, J., Qian, X.D., Choo, Y.S. (2008a). Re-analysis of the moment capacity of CHS joints. *Proc. 12th International Symposium on Tubular Structures*, Shanghai, China.

Vegte, G.J. van der, Wardenier, J., Zhao, X.L. and Packer, J.A. (2008b). Evaluation of the new CHS strength formulae to design strengths. *Proc. 12th International Symposium on Tubular Structures*, Shanghai, China.

Vhanmane, S. and Bhattacharya, B. (2008). Estimation of the ultimate hull girder strength with initial imperfections. *Ships and Offshore Structures* 3:3, 149–158.

Wang, X. and Huang, J. (2009). Elastoplastic buckling analyses of rectangular plates under biaxial loadings by the differential qudrature method. *Thin-Walled Structures* 47, 14-20.

Wang, X., Sun, H.H., Yao, T., Fujikubo, M. and Basu R. (2008). Methodologies on hull girder ultimate strength assessment of FPSOs. *Proc. OMAE 2008 Conference*, OMAE2008-57899, Lisbon.

Wang, X.W., Pont-Lezica, I., Harris, J.M., Guild, F.J. and Pavier, M.J. (2005). Compressive failure of composite laminates containing multiple delaminations. *Composites Science and Technology* 65, 191–200.

Wardenier, J. (2007). A uniform effective width approach for the design of CHS overlap joints. *Proc. 5th International Conference on Advances in Steel Structures*, Singapore.

Wardenier J. and Choo Y.S. (2006). Recent developments in welded hollow section joint recommendations. *Advanced Steel Construction* 2, 109-127.

Wardenier, J., Kurobane, Y., Packer, J.A., Vegte, G.J. van der and Zhao, X-L. (2008b). Design guide for circular hollow section (CHS) joints under predominantly static loading. CIDECT Series "Construction with Hollow Steel Sections", Serial No. 1, 2nd Edition, TÜV-Verlag, Köln, Germany.

Wardenier, J., Vegte, G.J. van der, Makino, Y. and Marshall, P.W. (2008a). Comparison of the new IIW (2008) CHS joint strength formulae with those of the previous IIW (1989) and the new API (2007). *Proc. 12th International Symposium on Tubular Structures*, Shanghai, China.

Witkowska, M. and Guedes Soares, C. (2008). Collapse strength of stiffened panels with local dent damage. *Proc. OMAE 2008 Conference*, OMAE2008-57950, Lisbon.

Yamada, Y. and Pedersen, P.T. (2008). A benchmark study of procedures for analysis of axial crushing of bulbous bows. *Marine Structures* 21, 257-293.

Yu, Q., Tao Z. and Wu Y.X. (2008). Experimental behaviour of high performance concrete-filled steel tubular columns. *Thin-Walled Structures* 46, 362-370

Zhang, S. and Kumar, P. (2007). Formulation for ultimate shear strength of ship structure. *Proc. MARSTRUCT 2007 Conference*, Glasgow.

Zhang, S., Kumar, P. and Rutherford, S.E. (2008). Ultimate shear strength of plates and stiffened panels. *Ships and Offshore Structures* 3:2, 105–112.

Zhang, A. and Suzuki, K. (2006). Dynamic FE simulations of the effect of selected parameters on grounding test results of bottom structures. *Ships and Offshore*

Structures 1:2, 117–125.

Zhang, A. and Suzuki, K. (2007). A comparative study of numerical simulations for fluid–structure interaction of liquid-filled tank during ship collision. *Ocean Engineering* 34, 645–652.

Zhao, X.L., Wardenier, J., Packer, J.A. and Vegte, G.J. van der (2008). New IIW static design recommendations for hollow section joints. *Proc. 12th International Symposium on Tubular Structures*, Shanghai, China.

Zheng, Y., Aksu, S., Vassalos, D. and Tuzcu, C. (2007). Study on side structure resistance to ship-ship collisions. *Ships and Offshore Structures* 2:3, 273–293.